Holocene climate variability based on two lacustrine sediment sequences from Cádiz, southern Spain.

I n a u g u r a l - D i s s e r t a t i o n

zur

Erlangung des Doktorgrades

der Mathematisch-Naturwissenschaftlichen Fakultät

der Universität zu Köln

Köln, 2017

Vorgelegt von:

Jasmijn van ´t Hoff
aus Leidschendam

Berichterstatter: **Prof. Dr. Martin Melles**
(Gutachter)

Prof. Dr. Klaus Reicherter

Prof. Dr. Juan Ignacio Santisteban Navarro

Tag der mündlichen Prüfung: 07.07.2017; 10.00 Uhr

Laguna de Medina on a cloudy day
Picture by Florian Steiniger

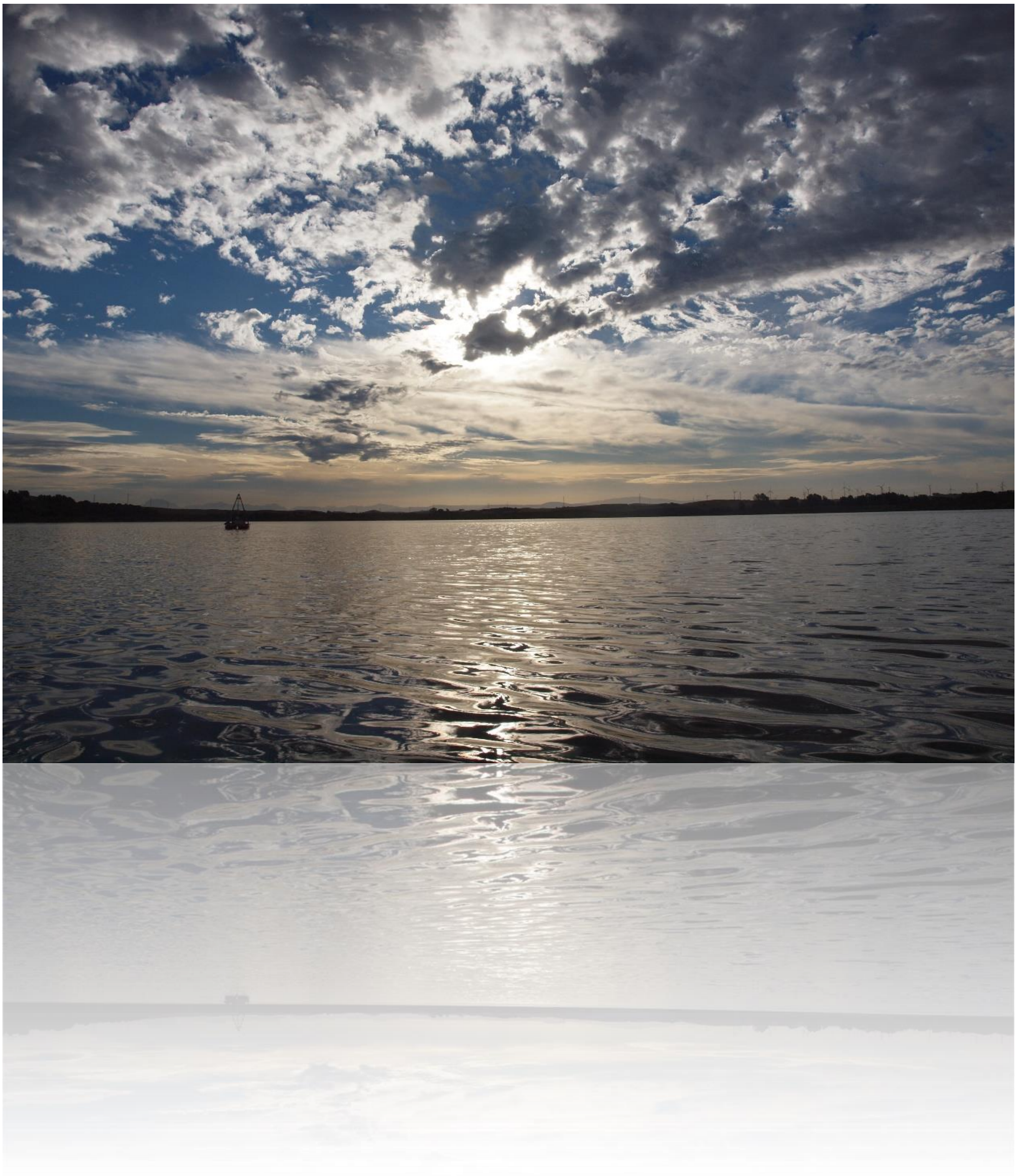

I

Abstract, Kurzfassung

Abstract

Iberia, and especially southern Spain, has been the focus of only limited palaeoclimatological research. The scarcity of palaeoclimate archives has led to an interpolation of archives from distant sites. The palaeoclimate reconstruction of southern Spain is therefore mainly based on the interpolation of marine records from the Alboran Sea, the Gulf of Cádiz and the North Atlantic Ocean. The understanding of the impact and effects of Holocene changes is relatively poor. The execution of palaeoclimatological research in southern Spain has been hampered by the lack of suitable sites. This thesis contributes to the understanding of the Holocene climate change in southern Spain with two new cores drilled in shallow saline lakes. The arid southern Spain is a region without deep natural lakes, these ´*salinas*´ represent a promising alternative for palaeoclimate research.

In this thesis, the methods and results of sedimentary and palaeoclimatological analyses of the modern lake sediment and soil catchment samples of Laguna de Medina, and the sediment sequences of Laguna de Medina and Laguna Salada are presented. The methods include XRF scanning, MSCL logging, particle-size analysis, total (in)organic carbonate analysis, determination of total sulphur, and total nitrogen, and XRD analysis, reinforced with the statistical method principal component analysis. The results are used to characterize the sediments and to interpret the changing climatological and environmental settings during the Holocene. The modern sediments of Laguna de Medina were studied with the same methods, to obtain a modern analogue for the long record.

The primary objective of this thesis was to disentangle the Holocene climate of southern Spain, based on the lacustrine archives Laguna de Medina and Laguna Salada using 25.65 and 12 m long cores, respectively.

Shifts in sedimentary deposition and geochemical proxies identify that southern Spain is highly vulnerable and responsive to climate change. Sedimentological, geochemical, mineralogical and granulometric analysis of the lacustrine sediment sequences provide a detailed palaeoclimatological and –hydrological reconstruction of the changes for the last 9,600 cal yr BP (Laguna de Medina) and 8,500 cal yr BP (Laguna Salada).

Based on these two new lacustrine archives, this thesis provides the first high-resolution palaeoclimate reconstruction for southern Spain and a new archive for the Holocene from a shallow desiccated lake. The two cores provide insight in the Holocene climate evolution, which is divided into three stages in southern Spain: 1) the warm and arid Early Holocene, 2) the humid climatic optimum in the Middle Holocene, and 3) the progressive aridification trend in the Late Holocene. The high-resolution record of Laguna de Medina gives insight in the timing and duration of rapid climate changes (RCC´s) during the Holocene. Five arid periods 9,160-7,870, 5,780-4,800, 3,150-2,420, 1,950-1,450, and 1,264-550 cal yr BP and one humid period 550-170 cal yr BP could be identified and related to RCC in the Holocene. The sequence of Laguna de Medina reinforces the connection between global changes in the hydrological regime, rapid climate change and North Atlantic Oscillation dynamics.

Kurzfassung

Iberia, und im Besonderen Südspanien, waren bisher nur wenig im Fokus der paläoklimatologischen Forschung. Der Mangel paläoklimatologischer Archive führte zu einer Interpolation weitentfernter Archive. Die paläoklimatologische Rekonstruktion Südspaniens basiert daher hauptsächlich auf der Interpolation von marinen Records des Alborischen Meer, des Golfs von Cádiz, und des Nordatlantischen Ozeans. Das Verständnis der Auswirkungen und Effekte der holozänen Veränderungen ist relativ schlecht. Die Durchführung paläoklimatologischer Forschung würde durch den Mangel an geeigneten Lokationen behindert. Diese Dissertation trägt zum Verständnis der holozänen Klimaveränderungen in Südspanien, anhand zweier, neu gebohrter Kerne aus flach salzigen Seen, bei. Das aride Südspanien ist eine Region ohne natürlich tiefe Seen, aber dafür sind die *´salinas´* eine vielversprechende Alternative für die paläoklimatologische Forschung.

In dieser These werden die Methoden und Resultate der sedimentologischen und paläoklimatologischen Analysen der modernen Seesedimente und Bodenproben des Einzugsgebietes der Laguna de Medina, und die Sedimentsequenzen der Laguna de Medina und der Laguna Salada präsentiert. Die Methoden umfassen Röntgenfluoreszenzmessungen (XRF), Multisensorkernlogging (MSCL), Korngrößenanalyse, die Analyse des gesamten (in-) organischem Karbonates, die Bestimmung des gesamten Schwefel und gesamten Stickstoff, und Röntgendiffraktionsanalyse (XRD), kombiniert mit der statistischen Methode der Hauptkomponentenanalyse. Die Resultate werden benutzt, um die Sedimente zu charakterisieren, und um die veränderten Klima- und Umweltbedingungen während des Holozäns zu interpretieren. Die modernen Sedimenten der Laguna de Medina sind mit den gleichen Methoden analysiert worden, sodass ein modernes Analog für den langen Kern entstand.

Das Hauptziel dieser These war es das holozäne Klima Südspaniens zu rekonstruieren, basierend auf den lakustrinen Archiven der Laguna de Medina und der Laguna Salada, unter Benutzung der 25,65 m und 12 m langen Kerne.
Änderungen der sedimentologischen Ablagerung und der geochemischen Proxies zeigen, dass Südspanien sehr anfällig für Klimaänderungen ist und darauf reagiert. Sedimentologische, geochemische, mineralogische und granulometrische Analysen der lakustrinen Sedimentkernen liefern eine detaillierte paläoklimatologische und hydrologische Rekonstruktion der Veränderungen der letzten 9.600 Kalender Jahre vor heute (Laguna de Medina) und 8.500 Kalender Jahre vor heute (Laguna Salada).
Basierend auf diesen zwei neuen, lakustrinen Archiven, stellt diese These die erste hochaufgelöste, paläoklimatologische Rekonstruktion für Südspanien dar, und umfasst ein neues holozänes Archiv aus einem flachen, teilweise ausgetrockneten See.
Die zwei neuen Kerne geben Einblick in die holozäne Klimaevolution, die sich in Südspanien in drei Stufen gliedert: 1) das warme und trockene Frühe Holozän, 2) das feuchte Klimaoptimum während des Mittleren Holozäns, und 3) die progressive Aridifizierung des Späten Holozäns. Der hochaufgelöste Kern der Laguna de Medina gibt Einblicke in die Zeit und Dauer der rapiden Klimaveränderungen (RCC) während des Holozäns. Fünf trockne Perioden wurden mit den RCCs im Holozän verbunden 9.160-7.870, 5.780-4.800, 3.150-2.420, 1.950-1.450 und 1.264-550 Kalender Jahre vor heute und eine feuchte Periode zwischen 550-170 Kalender Jahre BP. Die Sequenz der Laguna de Medina verstärkt die Verbindung zwischen globalen Änderungen im hydrologischen Regime, dem RCC und der Dynamik der Nordatlantische Oszillation.

Coring team on the platform
Picture by Helmut Brückner

II

Acknowledgments

Acknowledgments

My first acknowledgment goes to the Deutsche Forschungsgemeinschaft for financially supporting the project CRC 806 ‘Our Way to Europe´ for what I am writing my thesis. Their support also gave me the opportunity to attend some international conferences, and networking with other scientists working in Spain. I also want to thank the GSGS graduate school of Cologne, for financially supporting the last six months of my thesis with the Fellowship Grant No. GSGS-2017A-F01 of the Graduate School of Geosciences. It was due to this support, I had the change to finish my thesis.
The results of this thesis improved a lot by the contribution and discussions with numerous colleagues. My special thank goes to my supervisors Martin Melles and Klaus Reichterter. They introduced me into the field on palaeolimnology, and gave me advice and support the last three years. Martin Melles discussed with me about the data and helped me a lot improving my writing skills. Klaus Reichterter knows all the good coring spots in Spain, and helped a lot during the field campaigns. Furthermore, I want to thank Helmut Brückner, who kindly provided the platform coring equipment for our field campaigns in September 2014 and March 2015.
I want to thank Tabea Schröber, my colleague from Aachen with whom I work closely together on the cores. It was inspiring, discussing the data and really fun measuring everything together, and exploring the university by night.
Rosa Mediavilla, working in the geological department Madrid (IGME) and Santi Estaban, working in the University of Madrid, were of great help during the core description and the interpretation of the different facies. They taught me a lot about the Spanish processes, wherefore my greatest thank.
Furthermore, I thank Finn Viehberg for his cooperation in Laguna de Medina by counting the ostracods, which helped me a lot by the palaeoenvironmental reconstructions.
Janna Just is thanked for her motivational speeches, discussions, structural adjustments, and proofreading parts of my thesis. Alexander Francke is thanked for introducing me the age model software, and Ascelina Hasberg is thanked for her great translating skills.
I really want to thank all the other colleagues for the nice working atmosphere the last three years!
Dorothea Klinghardt and Nicole Mantkeare from the laboraties of Cologne, and my student assistants Christian Steffens and Anne-Sophie Mreyen, are greatly acknowledged for their enduring help in the laboratory and with the ArcGIS database.

I want to thank all the students and colleagues who helped during the two field campaigns: Martin Melles, Klaus Reicherter, Helmut Brückner, Tabea Schröder, Florian Steiniger, Janna Just, Raphael Gromig, Matthias Thienemann, Sandra Jivcov, Ascelina Hasberg, Matthias Lenz, Franz Hartung, Jan von Harten, Christian Steffens, Christian Scharrenberg, Daniel Kayser, Simon Washausen, and Marcel Baum. It was not only the physical strength, but also the cooking, barbequing, playing flunky ball, and drinking, what made the field campaigns a great successful time.
Special thanks goes to the guards of the Laguna de Medina and Laguna Salada, the Junta de Andalucía for their permission to core in the nature reserves, and their hospitality and cooperation at the lakes.
I want to thank the bachelor students who wrote their Bachelor thesis on one of the lakes: Raphael Petri, Sebastian Fuhr, Sandra Blanke, Patrick Braun, Tim Stanski, Gabriele Schmidt, and Jennifer Kösling. This really helped me a lot, and it was fun discussing with you, and reduced the laboratory work significantly.

I would like to thank my family, especially my parents Rosemarie Ritzema and Jan van ´t Hoff, as well as my brother Jasper van ´t Hoff and my sister Fleur van ´t Hoff for their support in everything I do. I would also like to thank my lovely zwijnenvriendinnetjes, who gave me distraction and support whenever I needed it.
Last, but not least, I would like to thank my beloved Thomas Schlink, for his patience in the last writing phase, as well as taking care if was eating and drinking enough, and just for being there!

Additionally, I would like to thank Prof. Dr. Frank Schäbitz for taking the chair of the examination committee as well as Dr. Finn Viehberg for acting as assessor at my defence.

Laguna de Medina on a cloudy day
Picture by Franz Hartung

III

Contents

Contents

Laguna de Medina and the platform
Picture by Helmut Brückner

Chapter 1

Introduction

1.1 Motivation

Since 1950, the climate is changing in a more rapid way as has been seen before. The atmosphere and ocean are warming, snow and ice are melting and the sea level is rising (IPCC, 2014). The ongoing climate change is affecting areas in different ways. Polar regions are getting warmer resulting in ice and glacier melting, and the rise of the sea level. Humid regions are getting more humid and arid regions are getting more arid (IPPC, 2014).

The arid southern Spain is very vulnerable for climatic changes (Giorgi and Lionello, 2008). The ongoing climate change leads to an increase in air temperatures, a decrease and more irregularity in precipitation (Bolle, 2003; de Castro et al., 2004; Met Office, 2011), and thus, to reduced water availability for surface and aquifer systems (Álvarez-Cobelas et al., 2005a). Aquifers, which are already overexploited, will experience problems with salinization (Puigdefábregas and Mendizabal, 1998). The changes in precipitation and evapotranspiration will not only affect the environment, but also the economy of Spain. Tourism and agriculture, two highly water-consuming sectors, will become more important in a socio-economic way (Gleick, 1993). Currently, tourism is the national work force for 13 % of the population, but it will be hard to justify and maintain the enormous water use for tourists when the population suffers from water stress (Hein et al., 2009).

From the ecological point of view, the ongoing climate change will have devastating effects on limnological systems. Spain has the greatest diversity of inland aquatic systems of Europe, containing unique flora and fauna, mainly triggered by the differences in climate, geology and the hydrological characteristics (Álvarez-Cobelas, 2005a). 49 Spanish wetlands are protected by the Ramsar Convention on Wetland of International Importance (Ramsar, Iran, 1971), including Laguna de Medina and Laguna Salada, the two lakes described in this thesis.

Not only for the future of the Spanish lakes, climate predictions and the understanding of the Mediterranean limnology is important. It is very likely that in the course of climate changes the cold temperate limnological systems become more similar to the current Mediterranean limnological systems, so it is good to have references to the new stage of these systems (Arnell et al., 1996; Álvarez-Cobelas et al., 2005b).
Álvarez-Cobelas et al. (2005b) listed the three most important questions about the Spanish limnological ecosystems:

- Will they still exist at the end of the century?
- Are they still permanent or did they become temporary?
- Will the biochemistry or biota change?

It is hard to answer these questions for the Spanish limnological systems at this point. Firstly, because only a few long-term studies exist and more research about Spanish limnological systems is needed. Secondly, the human influence on these systems cannot be predicted exactly. Álvarez-Cobelas et al. (2005b) wrote: *´Many endangered Mediterranean limnosystems will survive if, and only if, Mediterranean societies appreciate them (which is not the case right now)´*. In addition, regional climate models are at this stage not precise enough to predict the impact of global climate change in a regional scale.

The current atmospheric concentrations of the greenhouse gasses (GHG) CO_2, CH_4, and N_2O exceed the highest concentrations recorded in the ice cores during the last 800,000 years (IPCC, 2013b). Since 1750, the concentration of CO_2, CH_4, and N_2O increased by 40, 150, and 20 %, respectively (IPCC, 2013b). Without analogue GHG conditions in the last 800,000 years, it is hard for climate modellers to develop a reliable model. Although climate modellers continued to develop climate models, climate fluctuations can still not be predicted precisely, not even until the end of this century. To predict the future climate changes, it is important to concentrate on the more recent past, the Holocene, where the boundary conditions are relatively similar as today. Especially, compared with the large changes

between glacial and interglacial periods (Wanner et al., 2008). During the Holocene, most of the terrestrial environments developed that are still persisting today (Wanner et al., 2008).
For this purpose, it is important to have reliable palaeoclimate and -environmental archives in different regions.

Relatively little is known about climate variations of southern Spain. Records, which continuously cover the last glacial-interglacial cycle, are mainly found in marine archives from the Alboran Sea (e.g. MD95-2043; Cacho et al., 1999), the Gulf of Cádiz (e.g. MD99-2339; Voelker and de Abreu, 2011), and the North Atlantic off Portugal (e.g. MD95-2042; (Sánchez Goñi et al., 1999)) (Fig. 1.1). Although these records cover a long temporal range, the resolution, especially for the Holocene, is insufficient to reconstruct centennial-scale climatic changes throughout the Holocene.
Terrestrial archives are sparse, especially in southern Spain, and often only covering (partly) the Holocene (Fig. 1.1). Therefore, the palaeoclimate of southern Spain is mainly based on the interpolation of distal marine records. The distance between the terrestrial archives is up to 600 km, crossing the climatic zones of the humid Atlantic IP (Portugal) to the arid Mediterranean IP (Schuck et al., 2013). Most of the terrestrial records do not have high-resolution data, or do not cover the entire Holocene. Extending this database with new archives will enhance the knowledge about the palaeoclimatic conditions and will help to tune the climate models for better climate predictions, especially for the tip of southern Spain.

Lakes are promising archives for continental palaeoclimate and –environmental reconstruction (Cohen, 2003), because lacustrine sedimentary sequences can provide continuous high-resolution records (Moreno et al., 2012).
In the scope of the extension of lacustrine records, two lakes from the southern tip of Spain were cored during two field campaigns in September 2014 and March 2015, Laguna de Medina and Laguna Salada (Cádiz). The palaeoclimatological and -environmental conditions reconstructed from these retrieved sediments are the focus of this thesis.

Fig. 1.1: Location of selected continental (orange dots), and marine archives (blue dots), as well as the locations of the studies lakes Laguna Salada and Laguna de Medina (red stars).

1.2 CRC 806

This PhD thesis was conducted within the Collaborative Research Centre 806 (CRC 806) ´Our Way to Europe – Culture-Environment Interaction and Human Mobility in the Late Quaternary´. This is a DFG (Deutsche Forschungsgemeinschaft; German Science Foundation) funded interdisciplinary research project within the Universities of Aachen, Bonn and Cologne since 2009. Around 80 researchers from the institutes of geology, geography, archaeology and anthropology are working closely together.

1.2.1 The origin of hominids

Already 160 years ago, anthropologists and archaeologists began to investigate the origin of mankind. With the participation of the genetics into this discussion, the origin of the Anatomically Modern Human (AMH) or *Homo sapiens sapiens,* was found around 190,000 years ago (Richter et al., 2012).
Most of the scientists agree the genus *Homo* originated in East Africa about 2.4 million years ago (Streit, 1995). One group scientists denies this hypothesis, they state the genus *Homo* originated from Asia. Their argument is, if we cannot demonstrate the probable absence of a hominin in a region, we should reserve judgement as to when it first appeared there (Dennell and Roebroeks, 2005).

The first dispersion of the predecessor of the AMH, the *Homo erectus*, was around 1.7-1.9 million years ago (Ron and Levi, 2001; Dennell and Roebroeks, 2005). This is the generally accepted ´Out of Africa I´ theory (Lahr, 2010). The further evolution and dispersal of the AMH is still heavily discussed. Two main hypotheses divide the scientists into two groups (Richter, 1996):

- The AMH originated from the regional tribes of the *Homo erectus* (i.e. the current European from the European *Homo erectus,* and the current Asian from the Asian *Homo erectus)*. The close genetic relation between the current human population is the result of multiple contacts and mixing of the population.
- The high genetic relation between the current human population occurred, because mankind originated from one ´root´ during a relative short time frame. This ´root´ has to be the *Homo sapiens sapiens* population in East Africa before it started to disperse. This is the ´Out of Africa II´ theory.

The research focus of the CRC 806 is mainly based on the ´Out of Africa II´ theory, assuming the AMH originated from East Africa 190,000 years ago and started to migrate in several directions until they settled in Central Europe 40,000 years ago (Mellars and Stringer, 1990; Richter, 1996). There are two important routes to enter Europe (Fig. 1.2). The eastern trajectory, from East and North Africa via the Levante to Central Europe, is already proven. The western trajectory, from East Africa via Morocco, the Strait of Gibraltar to the Iberian Peninsula and Central Europe, is highly debated, and the key question for further research (Richter et al., 2012). More about the western trajectory in Chapter 1.2.2.
The CRC 806 investigates the relation between the climatological and environmental forces on the development of the cultural system, and is established to capture the complexity of chronology, regional structure, climatic, environmental, and socio-cultural contexts of major intercontinental and transcontinental events of dispersal of the AHM from East Africa to Central Europe (Richter et al., 2012). The time span of the CRC 806 covers the last 190,000 years with tree essential themes (Richter et al., 2012):

1. *The climatic, environmental and cultural context of the first expansion of the AMH´s dispersal from East Africa 190,000 years ago to its occupation in Central Europe 40,000 years ago.*
2. *Secondary occurrences of expansion and retreat of the AMH, induced by climatic, environmental or cultural changes, for instance reoccupation after the glacials.*
3. *Population changes, mobility and migration in coupled cultural and environmental systems, mainly due to the growing impact on the environment.*

The major events in the history of the AMH are a result of several dispersal processes, which were initiated by human agency, climate and environment (Richter et al., 2012). The eastern and western route cover the most interesting areas for the research of the CRC 806 to investigate the trajectories of human migration (Fig. 1.2):

- **The eastern trajectory**: The already proven principal eastern trajectory from East and North Africa via the Levante to Central Europe

- **The western trajectory:** The highly debated western trajectory from East Africa via Morocco, the Strait of Gibraltar to the Iberian Peninsula and Central Europe.

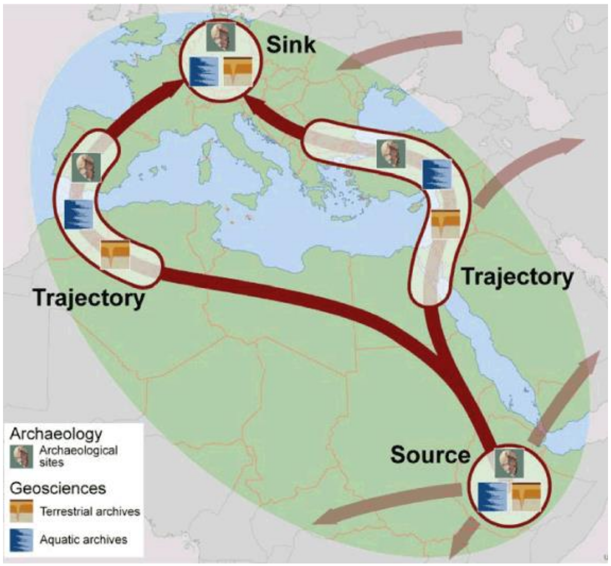

Fig. 1.2: CRC 806 ´Our Way to Europe´. The origin (source) of the AMH, the two different pathways (trajectories) and the settlement (sink) after Richter et al. (2012).

Following these supposed trajectories, the CRC 806 is divided into four regional clusters, covering the research in East Africa (A), the Levante and Balkans (B), Morocco and the Iberian Peninsula (C) and Central Europe (D). Two integrative and methodological clusters support the regional clusters by computational modelling (E) and chronological techniques (F). The last cluster (Z) covers the centralized tasks as the database and educational purposes.

1.2.2 The C Cluster: The Western Mediterranean – Bridge or Barrier?

Within the context of the western trajectory, the C Cluster focusses on climatological, environmental and cultural changes in Morocco and the Iberian Peninsula (IP). Because of its diversity, the IP and Morocco are ideal areas to study the climatological and environmental forcing on cultural change and human adaptation. Especially the semiarid regions in southern Spain and the deserts in Morocco are very sensitive for even minor climatological changes (Giorgi and Lionello, 2008).
The C cluster was established to investigate the possibility for the Strait of Gibraltar to function as a bridge or a barrier. The Strait of Gibraltar is an essential area in the settlement of the AMH, because it can be a possible connection between Africa and Europe (Currat et al., 2010). During the Last Glacial Maximum (LGM), the sea level was about 125±5 m lower (Fleming et al., 1998), reducing the width of the Strait of Gibraltar from 14 km to only 5 km (Richter et al., 2012).

To investigate the possibility for the Strait of Gibraltar to function as a bridge, the cluster C is divided into three projects. Within project C1, more than 100 archaeological sites in Spain were reanalysed to test the cultural patterning of Late Neanderthals and AMH in their environmental setting based on stratigraphical data (Schuck et al., 2013). Project C2 investigates the contact between humans in Africa and Europe. To fulfil this project, the climatic and environmental conditions in Morocco and the cultural development of the Epipalaeolithic-Neolithic transition were studied. Moreover, intercontinental networks, and the impact of African development on the processes on the IP are under investigation (Schuck et al., 2013).
The C3 Project is established to close the gap between the marine and terrestrial archives in southern Spain, mainly using lacustrine archives. Now, the distance between the existing palaeoclimate archives is up to 600 km, ranging from humid to arid climatological zones (Schuck et al., 2013). The focus of the C3 project is on MIS 3 to MIS 1, or in archaeological terms, the technocomplexes Late Middle

Palaeolithic - Early Upper Palaeolithic, Gravettian, Solutrean and Magdalenian. These technocomplexes are under investigation in the C1 project. The palaeoclimatological and -environmental data will be compared with the cultural changes and the results from the C1 project.

Although the strait of Gibraltar could potentially have been a bridge for the western trajectory between Morocco and the IP, it was very likely never used (Richter et al., 2012). The present state of research argues that the AMH did reach the IP, but came from Central Europe. The AMH never penetrated the IP further south than the Ebro river valley (Zilhão, 2000). A possible reason for this frontier is the hyper aridity of southern Spain during MIS 3 (Vegas et al., 2010). Therefore, the impact of climatic and environmental changes is becoming more important in this discussion.
Without the presence of the AMH, the southern IP turned into a refugium for the Neanderthals, where they survived longer than elsewhere in Europe (Finlayson et al., 2006; Finlayson and Carrión, 2007). In Europe, the replacement of the Neanderthals by the AMH took place around 40,000-30,000 cal yr BP (Mellars, 2004), while Neanderthals were found until 28,000 years ago at the southern tip of the IP (Finlayson et al., 2006). On the other side of the Strait of Gibraltar, in Morocco, the AMH was found, whereas Neanderthals never occurred (Richter et al., 2012).

The impact of climatic and environmental changes is becoming more important in the archaeology. Therefore, a close cooperation between the different projects in the C cluster is important. The Spanish archaeological sites of Solutrean and Magdalenian technocomplexes (about 24,000 to 17,0000 cal BP) are clustered close to the shores in the north, east and south of the IP and close to the Tagus River in Portugal (Fig. 1.3).

For a close collaboration between archaeologists and geologist, two lakes were selected closely situated to a cluster of Solutrean sites in the southern part of Spain. Laguna de Medina and Laguna Salada are both situated in the province of Cádiz, southern Spain (Fig. 1.3).
Laguna de Medina was already researched by Reed et al. (2001). This study shows the data of a 10.31 m long core, spanning the last 9,000 years. This record reflects the regional environmental and ecological changes, based on diatom data, supplemented with ostracods and pollen data. Extending this promising record would enhance the knowledge of the palaeoclimatic conditions of the Holocene.

Comparing the lacustrine data and combining these with the cultural data from the Solutrean sites gives insight in the impact of climatological and environmental forcing on the behaviour and dispersal processes.

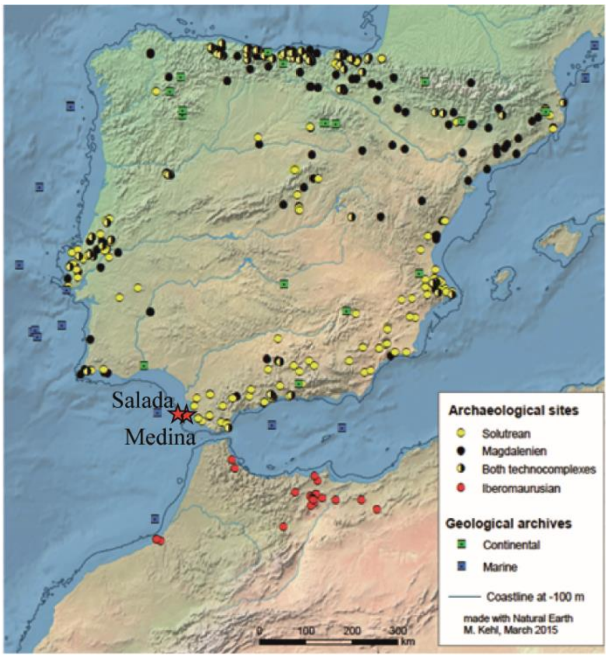

Fig. 1.3: Distribution of the archaeological sites, geological archives, and the location of Laguna de Medina and Laguna Salada (red stars) on the Iberian Peninsula and Morocco. Shorelines are 100 m lower than today, matching the situation during the last glacial. After Kehl (2015)

1.3 Terrestrial palaeorecords in southern Spain

As has been shown before, the terrestrial conditions on the IP are important to refine climate models and to understand the context of human adaptation and climate. In the following chapter, the state of the art of the Holocene archives of palaeoclimate conditions is briefly summarized.

1.3.1 Lacustrine environments in Spain

Already in 1948, a total of 2,474 lakes were listed in Spain. About 3.2 % of these lakes are inland salt lakes (Pardo, 1948), occurring in the semiarid and arid zones (Comín and Alonso, 1988). The Guadalquivir region in southern Spain is one of the four main districts with saline lakes (Comín and Alonso, 1988). The establishment of the endorheic character in southern Spain can be dated back to the Miocene (Plans, 1969). Most of the depressions, situated in a karstic and evaporitic catchment, were established during the Late Pleistocene due to karstic processes as dissolution and collapse (Ibañez, 1973; 1975; Valero-Garcés et al., 2014).

In assessment of the lakes in southern Spain, during the 1940´s, the presence of 140 lakes was revealed, 17 of which are endorheic salt lakes (Dantín Cereceda, 1940). These lakes are mainly semi-permanent or temporary. Natural fluctuations result to desiccation in very arid years, or annual desiccation during summer (Alonso, 1998).
Now, almost 80 years later, several of these lakes are completely desiccated. The ongoing climate change extends the desiccated period, groundwater extraction results in complete desiccation, heavy use of agriculture increases soil erosion and silting up, and several lakes are even completely drained for agricultural purposes (Luque et al., 1999; García-Ruiz, 2010; IPCC, 2013a; Díaz-Paniagua and Aragonés, 2015). One of the most excessive examples is the drainage of Laguna de la Janda, in southern Spain. This lake, which had a surface area of around 87 km^2, was drained in the 1930´s, and is now one of the biggest export areas for cotton and corn (Dantín Cereceda, 1940).

Deep lakes are suitable for reconstruction of the climate history by reflecting the past climatic, environmental and hydrological changes (Cohen, 2003). In Spain, and particularly in southern Spain, natural deep lakes do not frequently occur. However, small endorheic salt lakes (in Spanish: *Lagunas*) are common and present an alternative for deep lakes. These lakes are semi-permanent or temporal, with annual summer desiccation (Fig. 1.4). An advantage is, these lakes are highly sensitive to even small climate changes. The coring procedure on a desiccated lake is much easier than on a permanent lake, because of the accessibility. On the other hand, it can be a challenge to establish a good chronological control (Höbig et al., 2016) since desiccation events may result in hiatuses or the lack of organic matter (Chapter 3: Laguna Salada; Schröder et al., 2017).

The two lakes focused on in this thesis, Laguna de Medina and Laguna Salada, both in the province of Andalucía, show the differences between a semi-permanent lake (Laguna de Medina winter water depth: 3.2 m), which only dries out during very arid years, and a temporary lake (Laguna Salada winter water depth: 0.50 m) with annual summer desiccation.

Fig. 1.4: Example of a lake during an arid summer period. Picture is Laguna Salada (close to Cádiz, southern Spain) in September 2016)

1.3.2 Holocene palaeoclimate archives in (southern) Spain

The Holocene started about 11,700 cal years BP (Walker et al., 2009), and has been seen as a stable period for a long time. However, with the discovery of ice-rafted debris (IRD) in marine records (Bond et al., 1997), and in general the increase of high-resolution studies, short-term climate fluctuation became evident. It turned out, the Holocene climate is very dynamic, temperature and precipitation oscillations occurred mainly in southern Spain (Tarroso et al., 2016). The term rapid climate change (RCC) was introduced by Mayewski et al. (2004) for Holocene intervals with widespread evidence for climate change. The RCC´s are mainly based on the work of Denton and Karlén, (1973). Six periods of RCC are found during the Holocene: 9,000–8,000, 6,000–5,000, 4,200–3,800, 3,500–2,500, 1,200–1,000, and 600–150 (Little Ice Age; LIA) yr cal BP. The RCC were all initiated by major changes in atmospheric circulation, polar cooling, and arid tropics, except for the LIA, which is reflected by polar cooling and humid tropics (Mayewski et al., 2004). Although the Holocene has a lot of RCC´s which are not fully understood, it is still often neglected in climate archives.

Southern Spain is very vulnerable to global climatic changes on centennial to millennial timescale (Giralt et al., 1999), and responds to the changes in global atmospheric patterns (Martín-Puertas et al., 2008). Numerous millennial-scale oscillations correlate with the Bond cycles, of which the onset, and end is linked to feedback fluctuations in oceanic, and atmospheric circulation, insolation, and vegetation cover (Bond et al., 1997; Gasse, 2000). The current moisture patterns are closely linked to the North Atlantic Oscillation index (NAO), which is calculated as the pressure differences between the Azores High and Icelandic Low (Hurrell, 1995). Research of a high-resolution record from SW Greenland recovered the NAO controlled the climate oscillations at least the last 5,200 years (Olsen et al., 2012). Positive (negative) NAO values coincide with more arid (humid) conditions on the IP, and with cold (warm) temperatures over Greenland (Sánchez Goñi et al., 2002).

On the IP, several palaeoclimate studies were done in the last 50 years. Most of the terrestrial archives cover (partly) the Holocene, only a few penetrate into older sediments.
On the southern part of the IP, only a few terrestrial archives include the last glacial-interglacial cycle (Fig. 1.1). The Padul peat bog covers the last >54,000 years (Florschütz et al., 1971; Pons and Reille, 1988). This was the first record covering the complete postglacial vegetation history in a semi-arid region. The climatic fluctuations of the Holocene are of small amplitude. The Salines playa-lake focusses on the water availability of the last 70,000 years (Giralt et al., 1999). Both of the records have a poor age control for the Holocene. Comparison between the Padul peat bog and Salines playa lake resulted in a good correlation of the general trends in the Holocene. The Holocene is described as a humid period with some aridity crises at the beginning of the Holocene, the 8.2 ka event, and the middle Holocene, but the timing of the onset is questionable (Giralt and Juliá, 2003). The record from the Fuentillejo Maar includes the last 50,000 years. Some short cold and arid phases were found during the Holocene at 9,200-8,600, 7,500-7,000, and 5,500-5,000 cal yr BP, although the timing should be used with caution, because the age model of the Holocene is only based on two radiocarbon dates (Vegas et al., 2010). Laguna de Fuente de Piedra covers the last 28,000 years cal BP, and reflect the changes in facies in relation with climatological changes very well. However, this lake also deals with problems concerning the age model, the Holocene is only based on one radiocarbon date (Höbig et al., 2016).
The insufficient temporal resolution of the long palaeorecords disables comparison of RCC variability.

The age control of most of the short records for the Holocene is considerably better. Changes in palaeoclimate are reflected by vegetation dynamics, and lake level changes. The Holocene is divided into three periods.

The Early Holocene (prior to 8,000 cal yr BP) is characterized by a warm, dry and continental climate, reflected by low lake levels, and a transition towards steppe vegetation. In the lacustrine archives, this period is characterized by low lake levels or hypersaline conditions. Low lake levels are reconstructed in Lake Salines, SE Spain (Roca and Julià, 1997), Gallocanta Lake, NE Spain (Luzón et al., 2007), Portalet Lake, N Spain (González-Sampériz et al., 2006), Lake Siles, S Spain, (Carrion, 2002). In the La Mancha Plain, Central Spain, a transition towards more palustrine conditions coincides with a falling lake level (Dorado-Valiño et al., 2002) (Fig. 1.1).
From the palynological point of view, warm and dry conditions are found in the Guadiana Basin, S-Portugal, by the expansion of scrub and open-ground taxa (Fletcher et al., 2007). The same trend in visible in other Iberian pollen records, with the increase of xerophytes in the Segura Mountains, SE Spain (Carrion, 2002), steppe vegetation at San Rafael, SE Spain until 7,000 cal yr BP, (Pantaléon-Cano et al., 2003), a setback of arboreal vegetation and an increase in steppe vegetation in the La Mancha Plain, Central Spain, until 8,000 cal yr BP. In Villaverde, Central Spain, fire regime increases, (Carrión et al., 2001a), and in the Sierra de Estrela, Central Portugal, steppe to xerothermic forests occur until 8,700 cal yr BP (van der Knaap and van Leeuwen, 1995).

The Middle Holocene (roughly between 8,000-5,500 cal yr BP) represents the humid maximum, with a warm and moist oceanic climate, coinciding with the humid phase in the ´green´ Saharan desert (Gasse et al., 1990). This period is reflected by maximum lake levels, an expansion in vegetation cover and low fire activity (Carrión et al., 2010).
High lake levels are reconstructed in Gallocanta Lake around 8,100 (Luzón et al., 2007), Laguna de Medina between 6,320-4,800 cal yr BP based on diatoms (Reed et al., 2001), or between 8,000-6,700 cal yr BP based on stable isotopes (Roberts et al., 2008), and in Lake Siles between 7,400-5,300 cal yr BP (Carrion, 2002) (Fig. 1.1).
An increase in vegetation cover is found in San Rafael between 7,000-4,500 cal yr BP (Pantaléon-Cano et al., 2003), an increase in deciduous taxa and taxanomical diversity at the La Mancha Plain between 8,000-6,100 cal yr BP (Dorado-Valiño et al., 2002), a change from a xerothermic to mesothermic forest in the Sierra de Estrela, between 8,700-5,670 cal yr BP (van der Knaap and van Leeuwen, 1995). Forest expansion was observed in the Guadiana Basin between 9,130-4,920 cal yr BP (Fletcher et al., 2007), and an increase of *Quercus* in Villaverde between 7,350-5,900 cal yr BP (Carrión et al., 2001a).

The **Late Holocene** (onset between 5,500-4,500 cal yr BP) is a period of progressive aridification, although most of the archives show a complex evolution of several arid and humid intervals (Morellón et al., 2008). The onset of this arid period coincides with a change towards more positive NAO values (Sánchez Goñi et al., 2002; Moreno et al., 2012; Olsen et al., 2012).
Low lakelevels or periods of desiccation are found in Laguna de Medina (Reed et al., 2001), Gallocanta Lake (Luzón et al., 2007), Lake Estanya (Morellón et al., 2008), Lake Siles (Carrion, 2002), and Lake Zoñar, S Spain (Martín-Puertas et al., 2008) (Fig. 1.1).
Aridity trends are observed in pollen sequences in the Guadiana Basin by an expansion of shrublands (Fletcher et al., 2007), a transition towards steppe vegetation, and an increase in erosion in San Rafael (Pantaléon-Cano et al., 2003), an increase in steppe, and xerophytes in Villaverde, Sierra de Gádor and Sierra de Baza (Carrión et al., 2001a; 2003; 2007), a decline of arboreal vegetation at the La Mancha Plain (Dorado-Valiño et al., 2002), and an increase in steppe vegetation at the Padul peat bog (Pons and Reille, 1988).

1.4 Study sites

In the focus of the C3 project, two lakes were selected for palaeoclimate and -environmental reconstruction: Laguna de Medina and Laguna Salada, both in the province of Andalucía, southern Spain (Fig. 1.5).
The two lakes are a nature reserve since 1989, and protected by the Ramsar Convention on Wetland of International Importance (Ramsar, Iran, 1971), mainly because of their importance for nesting and overwintering water birds (Amat, 1984; Fernández-Palacios, 1990).
The province of Andalucía is influenced by a Mediterranean climate, characterized by moderate and relatively humid winters, controlled by the dominance of westerlies, bringing precipitation to the area. The hot and arid summers are strongly controlled by the decreasing branch of the Hadley circulation, resulting in a rainfall minimum (Rodwell and Hoskins, 1996; 2001; Peel et al., 2007). The summer months have a five months water deficit (Paéz, 1991), significantly influencing the water table in the lakes, resulting in desiccation during (very) arid summers.

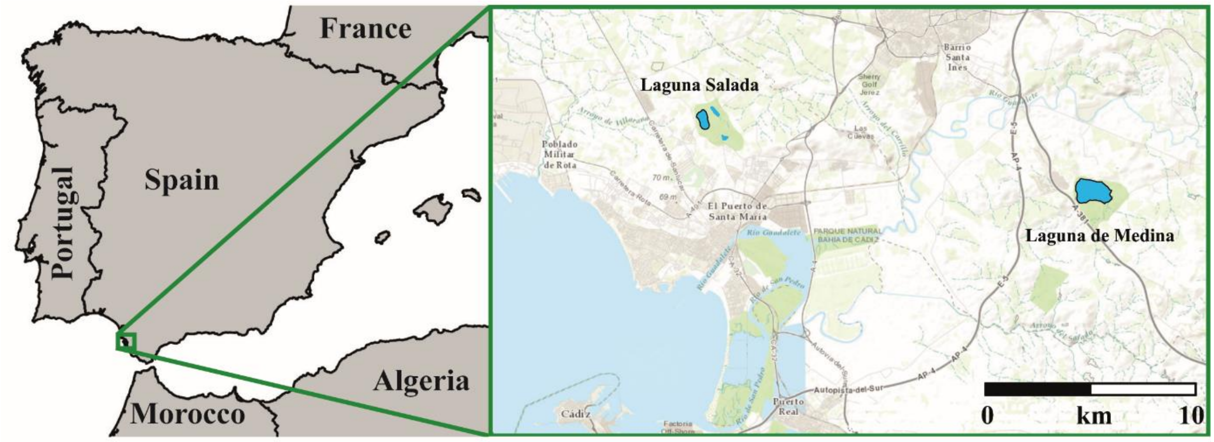

Fig. 1.5: Overview of the Iberian Peninsula and the locations of Laguna Salada and Laguna de Medina

Laguna de Medina is a small endorheic lake with a maximum water depth of 3.5 m. Two parallel cores were retrieved in the deepest part of the lake from a floating platform during two field campaigns in September 2014 and March 2015. It resulted in a composite record of 25.65 m.
Laguna Salada is the biggest lake of the Complejo Endorreico del Puerto de Santa María, which consists furthermore of Laguna Chica and Laguna Juncosa. It is a semi-permanent endorheic lake with a maximum water level of 0.5 m. During the field campaign in September 2014, the lake was desiccated. Two parallel cores were retrieved from the middle of the lake with a Cobra drill hammer. It resulted in a composite record of 12 m.
More detailed information about Laguna de Medina can be found in Chapters 2 and 3, and for Laguna Salada in Chapter 4.

The two selected lakes are only 20 km apart from each other. This gives the opportunity to compare the climatic signal of the two sites. This gives also insight whether the sedimentological units and the lithofacies are a climatic signal, or mainly influenced by the surrounding geology.
These lakes were selected, because they are situated close to the archaeological sites from the C cluster. Next to that, the southern tip of Spain is not researched jet, except for one study by Reed et al. (2001). Extending this study, will enhance the knowledge of the palaeoclimate of southern Spain.

1.5 Objectives

The research results presented in this thesis comprise two lacustrine sediment cores from southern Spain, Laguna de Medina and Laguna Salada, and the lake surface sediment, and soil catchment samples of Laguna de Medina. The aim of this thesis is to reconstruct the palaeoclimatological and –environmental settings for the Holocene.

Questions that arose during the three years of the Ph.D. are:

- How do the modern processes help to unravel the palaeoprocesses?
- How can we obtain a reliable age model?
- What are good proxies for such saline environments?
- Are the Holocene climate events synchronous in the two records, and how about the entire Iberian Peninsula?

This thesis includes the following manuscripts to address these questions:

Chapter 2: Modern sedimentation processes in Laguna de Medina, southern Spain, derived from lake surface sediment and catchment soil samples

This chapter comprises my first paper, which is already published in the Journal of Limnology. In this study, results from the lake surface sediment and soil catchment samples from Laguna de Medina are discussed. For a better understanding of past processes, it is important to distinguish how the modern processes function. For this purpose, 46 lake surface and 32 soil catchment samples were analysed with the same methods as for the long sediment sequence. Based on statistical analysis, mineralogical, geochemical, elemental, and granulometric compositions of the samples, the lake surface sediments can be divided into six provinces of individual composition and depositional processes, mainly based on the surrounding geology.

Chapter 3: A high-resolution Holocene palaeoclimate record from the Laguna de Medina, Cádiz, southern Spain

The palaeoclimatological results from the 25.65 m long record of Laguna de Medina are presented in Chapter 3. The multi-proxy approach provided a high-resolution record for the last 9,600 years. Based on the sedimentological, geochemical, mineralogical, and ecological (ostracods) data, reinforced with a statistical tool, the long-term palaeoclimatological and –hydrological evolution of the lake was reconstructed. The Early Holocene (9,600-7,870 cal yr BP) was an arid period, followed by a humid period, characterized by the maximum lake level between 7,870-5,780 cal yr BP. After this period, the prolonged aridification (5,780-3,750 cal yr BP) led to a decrease in lake level, although the lake level remains relatively high. The last ongoing aridification trend (from 3,750 cal yr BP on) results in a drastic decrease in the lake level with several desiccation periods.
Over this long-term trend, several periods of rapid climate change (RCC) resulted in short periods of aridification. Arid periods occurred between 9,160-7,870, 5,780-4,800, 3,150-2,420, 1,950-1,450 (corresponding to the RWP), and 1,264-550 (corresponding to the MCA) cal yr BP. The last RCC is a humid period, reflecting the Little Ice Age (550-170 cal yr BP).
The sequence of Laguna de Medina reinforces the connection between global changes in the hydrological regime, rapid climate change and NAO dynamics.

Chapter 4: A Holocene palaeoclimate record from the Laguna Salada, Cádiz, southern Spain

In this manuscript, the results from the 12 m long record from Laguna Salada are discussed. The multi-proxy study of this record represent the entire limnological history of the lake during the last 8,500 years. Based on the geochemical, and granulometric data, three humid phases were recognized. The Mid-Holocene Optimum 8,500-5,900 cal yr BP, the Iberian Roman Humid Period (2,500-1,100 cal yr BP) and the Little Ice Age (750-250 cal yr BP). Three arid periods occurred, the Late Holocene aridification (5,900-2,500 cal yr BP), the Medieval Climate Anomaly (1,100-750 cal yr BP) and the modern period after the Little Ice Age (250 cal yr BP-now).

Chapter 5: Synthesis

The last chapter includes the synthesis based on the three manuscripts. The questions that arose during this thesis are answered and discussed.

Laguna de Medina by sunset
Picture by Ascelina Hasberg

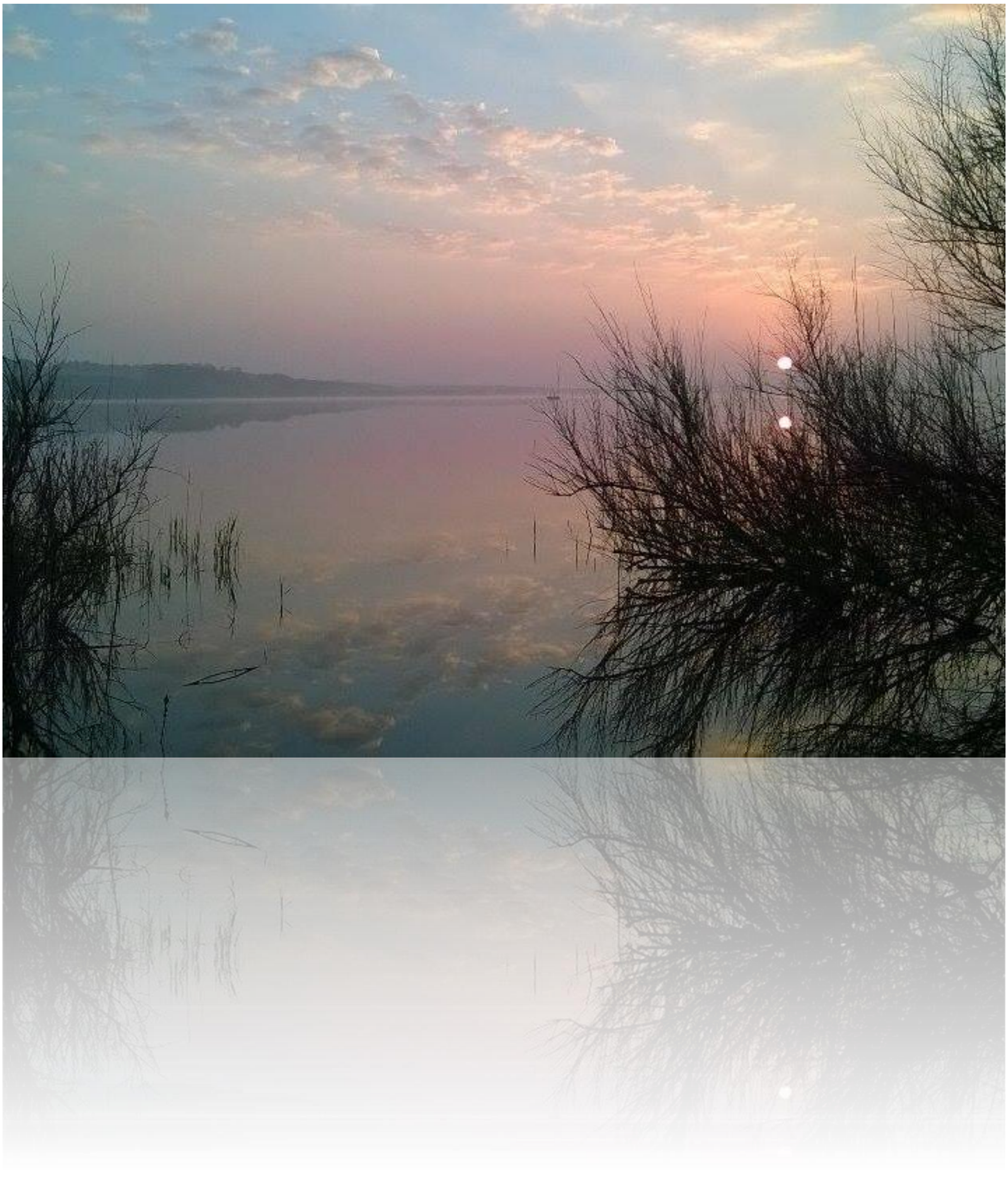

Chapter 2

Modern sedimentation processes in Laguna de Medina, southern Spain, derived from lake surface and soil catchment samples

2 Modern sedimentation processes in Laguna de Medina, southern Spain, derived from lake surface sediment and catchment soil samples

Jasmijn van ´t Hoff[a], Tabea Schröder[b], Peter Held[a], Stephan Opitz[c], Bernd Wagner[a], Klaus Reicherter[b], Martin Melles[a]

[a] Institute of Geology and Mineralogy, University of Cologne, Zülpicher Str. 49a, 506745 Cologne, Germany
[b] Institute of Neotectonics and Natural Hazards, RWTH Aachen University, Lochnerstr. 4-20, 52056 Aachen, Germany
[c] Institute of Geography, University of Cologne, Albertus Magnus Platz, 50923 Cologne, Germany

Corresponding author: Jasmijn van ´t Hoff: jvanthof@uni-koeln.de
Institute of Geology and Mineralogy
University of Cologne
Zülpicher Straße 49a
50674 Cologne, Germany

Key words: limnology, modern sedimentation patterns, Laguna de Medina, southern Spain,

Journal article (published), slightly changed

van 't Hoff, J., Schröder, T., Held, P., Opitz, S., Wagner, B., Reicherter, K., and Melles, M. (2017). Modern sedimentation processes in Laguna de Medina, southern Spain, derived from lake surface sediment and catchment soil samples. *Journal of Limnology*, *76*(1), 103–115. http://doi.org/10.4081/jlimnol.2016.1499

2.1 Abstract

Modern processes influencing sediment composition in the endorheic lake Laguna de Medina, southern Spain, are disentangled by the analysis of 46 lake surface sediment and 32 catchment soil samples. Based on statistical analysis of the mineralogical, geochemical, elemental, and granulometric compositions of all samples, the lake surface sediments can be divided into six provinces of individual composition and depositional processes.

High quartz contents and coarse grain sizes, reflecting input from ancient terraces of the Guadalete River that are exposed in the adjacent hinterland, characterize the lake sedimentation close to the northern shore. At the southeastern shore, sedimentation is characterized by terrestrial input of the Triassic Keuper facies via the most important inlet, the Arroyo Fuente Bermeja, as reflected by high relative intensities of Ti, K, Al, Fe, Mg, and Rb. Sediments close to the southern shore are characterized by high calcite contents, reflecting predominant sediment supply from the adjacent Cretaceous ´capas rojas´, a series of Subbetic deep-water marlstones and limestones. Close to the western shore, relatively high gypsum contents presumably are due to precipitation from upwelling ground water. Anthropogenic influence is only indicated in the northwestern and central eastern parts of the lake, where the surface sediments are significantly enriched in TOC and TN, reflecting enhanced primary production due to terrestrial organic matter supply from anthropogenic areas in the respective catchment. The central part of the lake is characterized by distal hemipelagic sedimentation, with high concentrations of clay and silt and a chemical and mineralogical composition that reflects a mixture of the sediment sources characterizing individual parts of the lake shores.

The results of this study shed new light on the depositional processes and their potential spatial heterogeneity in small endorheic lakes. Furthermore, they will provide important information concerning the interpretation of the climate-controlled sedimentary processes through time, which are reflected in a 25.65 m long sediment record (Co1313) that was recovered in the lake centre in 2014 and 2015.

2.2 Introduction

Spain, especially the arid southern Spain, is very vulnerable to the ongoing climate change. For instance, the average air temperature rose 2-3 °C since the 1970´s (de Castro et al., 2004). The annual rainfall is reduced and droughts are increased since 1960 (Met Office, 2011). According to climate simulations, temperature over the next 30 years may rise another 1.1-1.2 °C during winter and 1.8-2.0 °C during summer, and precipitation may decrease by 7 to 9 mm month-1, leading to water stress for 25-60 % of Spain's population (von Storch et al., 1993; Met Office, 2011; IPCC, 2013). Taking the more arid conditions of southern Spain, it can be expected that this region suffers more from water stress than the more humid northern Spain.

Comparatively little is known about the natural climatic variability in southern Spain on millennial timescales, beyond the range of meteorological measurements, and its impact on the regional environment. Such information is important to decipher the kind and rates of the spatial extend, magnitude, and temporal relationships of climatic forcing and environmental change. Most of the terrestrial archives only cover parts of the Holocene, have poor time resolution or age control, or are highly discontinuous (Reed et al., 2001; Fletcher et al., 2007; Martin-Puertas et al., 2008; Wolf and Faust, 2015). Only a few sediment cores, from the Padul peat bog and the Fuentillejo Maar, penetrate into sediments representing the Last Glacial Maximum (e.g., Pons and Reille, 1988; Vegas et al., 2010). Consequently, our current understanding of the Late Pleistocene history of southern Spain, including its vegetation history, is predominantly based on data from marine sediment records, specifically from the Atlantic margin off Portugal (Voelker and de Abreu, 2011), the Gulf of Cádiz (Toucanne et al., 2007), and the Alboran Sea (Martrat et al., 2014; Martinez-Ruiz et al., 2015). These records, however, integrate over large areas and thus lack sensitivity to detect the influence of climatic changes on regional scales.

One promising continental archive in southern Spain is the sediment record in the Laguna de Medina (Fig. 2.1). In this small endorheic lake, a 10 m sediment core was retrieved by Reed et al. (2001). According to chronostratigraphic, lithological information and palaeoenvironmental reconstructions, these sediments were continuously deposited during the past 9,000 years and reflect the regional environmental change with a high sensitivity. In order to extend the record in time, and to provide more material for further analyses also in the upper part, the record in the central part of the Laguna de Medina (site Co1313) was extended to 25.65 m during two coring campaigns in September 2014 and March 2015.

For a better understanding of the core composition and its significance for past environmental and climatic settings, 46 lake surface sediment and 32 catchment soil samples were taken, and analysed for their mineralogical, geochemical, elemental, and granulometric composition. Here, we present the data obtained from the surface samples, and discuss them in the light of the modern sedimentation processes, mainly controlled by the surrounding geology, post-depositional processes, and anthropogenic influences.

2.3 Study area

Laguna de Medina (36°37´04”N, 06°03´13”W) is an endorheic semi-permanent karst lake (Valero-Garcés et al., 2014) in southern Spain (Fig. 2.1), located roughly 12 km southeast of Jerez, 25 km northeast of Cádiz and about 3 km south of the river Rio Guadalete. This second largest inland salt lake of Andalucía is a nature reserve since 1987 (de Vicente et al., 2012). It is located 30 m above sea level (a.s.l.), the surface area amounts to 1.2 km^2, and the catchment area to 16 km^2 (Reed et al., 2001). At the southeastern shore, the most important inlet, the Arroyo Fuente Bermeja, enters the lake. This is a temporary inflow, which is dry during summer months (Reed et al., 2001). In September 2014 and March 2015, the maximum water depths were 1.7 m and 3.2 m, and the salinities 6.0 PSU and 2.2 PSU, respectively.

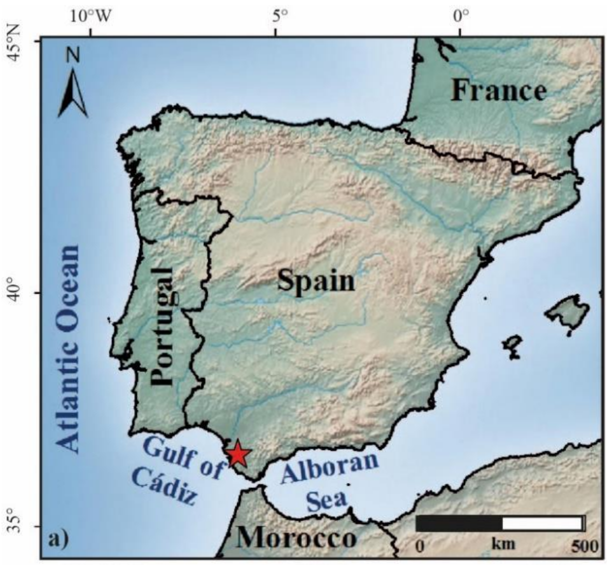

Figure 2.1: Overview of the Iberian Peninsula showing the location of Laguna de Medina (red star

The catchment of the Laguna de Medina (Fig. 2.2) is karstic and evaporitic (Durán Valsero et al., 2009), dominated by terrestrial Triassic claystones (Keuper facies), gypsum-rich evaporites, and marlstones (Paez, 1991). The inlet Arroyo de Fuente Bermejo predominantly drains the Triassic Keuper facies (claystones, sandstones, dolomites, and gypsum). Also the eastern area of the lake is dominated by Triassic units (IGME, 1984). In the north, remnants of alluvial terraces of Pleistocene sandstones and conglomerates of about 45 to 50 m a.s.l. demarcate the border of the lake. The southern area of the lake is characterized by the ´capas rojas´, a series of Subbetic deep-water marlstones and limestones (Vera and Molina, 1999). In the western catchment, Tertiary clays, marls, calcarenites, and biomicrites occur (IGME, 1984).

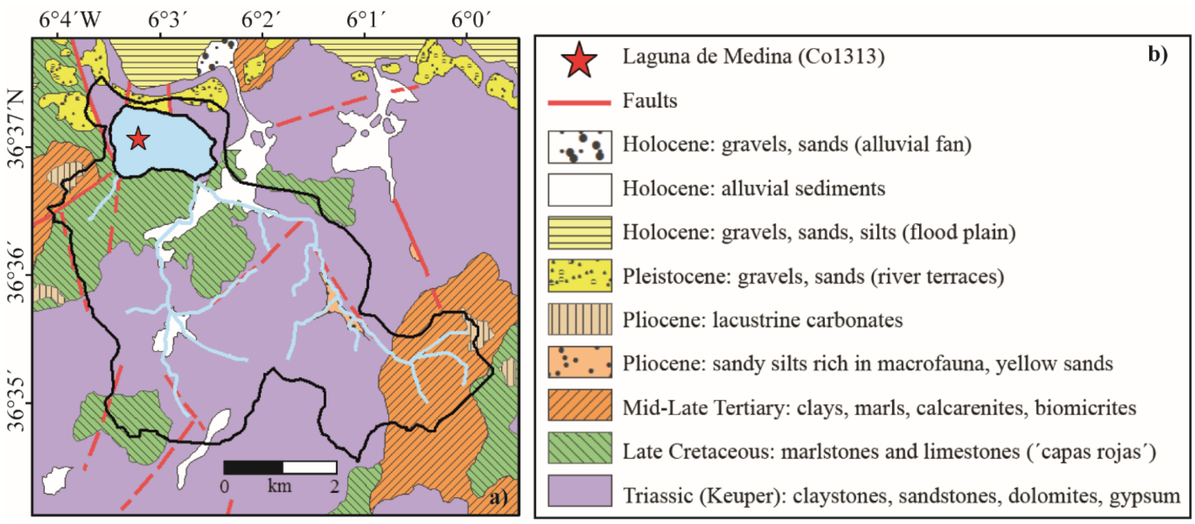

Figure 2.2: a) Geological map of the surroundings of Laguna de Medina, illustrating major stratigraphic units and fault systems (modified after IGME, 1984). The catchment area is encircled with a black line, the coring location of Co1313 is indicated by a red star. b) Legend for a).

The lake was formed as a result of 20 to 25 m diapiric uplift (Rodriguez Vidal et al., 1993), initiated by the high vulnerability of Triassic and Tertiary marls to halokinetic deformation (Wolf et al., 2014). The appearance of diapirs started in the Upper Miocene and has been related to extensional or compressional tectonics in the Gulf of Cádiz (Medialdea et al., 2009). In the Middle Pleistocene, the Rio Guadalete left the elevated areas and found its way in the valleys. The ground water dropped below the karst base level, resulting in sinkholes and the prolapse of old sinkholes. Laguna de Medina is an example of renewed karst sinking in Triassic gypsums, formed in the Upper Pleistocene (Rodriguez Vidal et al., 1993; Valero-Garcés et al., 2014). The modern configuration of the lake basin was probably established during the Late Pleistocene (Rodriguez Vidal et al., 1993).

Laguna de Medina today experiences a Mediterranean climate (Peel et al., 2007). During summer, average temperatures of 26°C occur and the precipitation is very low, with a five months period of water deficit. Meso-scale levanters, easterlies with velocities of 10-20 m/s, are frequent (Meteorological Office, 1962). The winters are characterized by an average temperature of 6°C and a relatively high precipitation of up to 90 mm per month (Paez, 1991). Both the levanters and the westerlies are weaker and less frequent than during summer (Dorman et al., 1995). The intensity and distribution of precipitation in the area is particularly influenced by the Azores High (Rodrigo et al., 2001) and by fluctuations of the North Atlantic Oscillation (Wolf et al., 2014). The mean annual precipitation is 525 mm, with a range of 250-975 mm (Paez, 1991).

The Laguna de Media is a shallow saline lake functioning as a hydrologically closed system (Fernández-Palacios, 1990). Nevertheless, there is a significant influence of ground-water inflow, which leads to the retention of water during summer times (Reed et al., 2001). The ground-water inflow is characterized by high salinities, due to dissolution of Triassic evaporites. This leads to a brine in the lake that consists of $Ca\text{-}Na\text{-}Mg\text{-}Cl\text{-}SO_4$, resulting in gypsum precipitation (Eugster and Hardie, 1978). However, the groundwater infiltration is very low, due to little permeable underground (Fernández-Palacios, 1990), which makes the lake very vulnerable to variations in precipitation and evaporation. Today, the lake level is highly affected by the seasonal precipitation changes, resulting in summer desiccation in very arid years. Long-term studies from Furest and Toja (1984), Marazanof (1967), and Reed et al. (2001), and also the results from the two coring campaigns show a connection between lake level and salinity changes, especially after irrigation since 1948 (Tello Ripa and López Bermúdez, 1988). On the other hand, the relation between lake level and salinity is complex, because of re-dissolution of precipitated salts and gypsum, leading to an increase in salinity with an increasing lake level (Reed et al., 2001).

In March 2015, 46 surface sediment samples were taken from the uppermost 2 cm of the lake bottom (Fig. 2.3). The samples were retrieved from a rubber boat using a gravity corer with a plastic liner of 63 mm diameter (UWITEC Corp., Austria). The sampling location was noted in the moment the gravity corer hit the lake bottom. Sampling partly failed close to the northern shore, where coarse sand and gravel dominate.

The lake sediment sample set is complemented by 25 soil samples from the uppermost 5-10 cm in the catchment and 7 sediment samples from the Arroyo Fuente Bermeja, the only significant inlet. These samples were collected in September 2014 and March 2015.

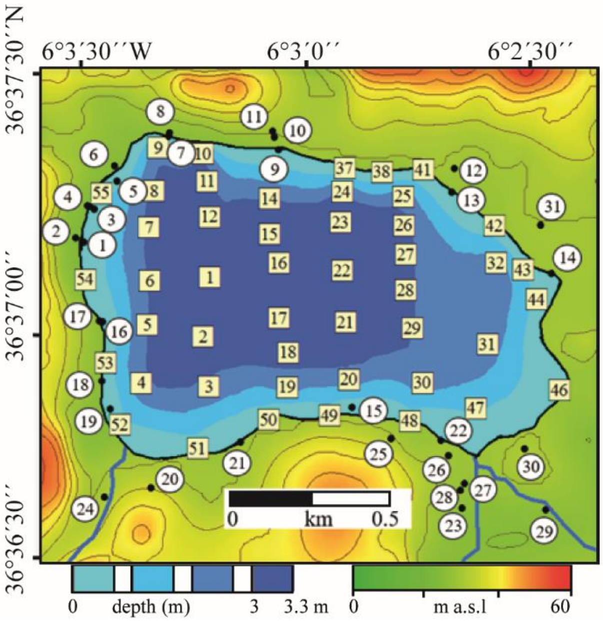

Figure 2.3: Topographic map (green to red m a.s.l.) of the direct surroundings of Laguna de Medina, with the bathymetry (blue in m), and locations of lake surface (centre of squares) and catchment soil (black dots) samples.

The analytical work on the samples was conducted in the laboratories of the University of Cologne. In a first step, the total of 78 samples were freeze-dried, in order to exclude transformation of gypsum ($CaSO_4 \cdot 2H_2O$) to bassanite ($CaSO_4 \cdot ½H_2O$) or anhydrite ($CaSO_4$), which would cause a weight loss of 20.91 % (Stern et al., 1989; Eswaran and Zi-Tong, 1991; Porta, 1998). Subsequently, the bulk sediment samples were split into aliquots for different measurements.

For the grain-size analyses, aliquots of the freeze-dried samples were pretreated with 10 ml $NaCO_3$ at 60°C for 18 hours in order to remove gypsum (Stern et al., 1989). Subsequently, carbonate (10 ml 10 % HCl, 50°C, 3 h), organic matter (5 ml 30 % H_2O_2, 50°C, 18 h), and biogenic silica (5 ml 1 M NaOH, 90°C, 2 x 30 min) were removed. Between these steps, the samples were centrifuged and neutralized with deionized water. Before measurements, the samples were mixed with Na_4P2O_7 (0.05 %) and shaken for at least 12 hours to avoid flocculation of clay minerals. Each sample was measured three times in 116 classes in a range between 0.04 and 2000 µm using the Laser Particle Size Analyser LS 13320 (Beckman Coulter Corp.) and the Frauenhofer optical model. The grain-size distributions were calculated using the program GRADISTAT (Blott and Pye, 2001).

The aliquots for mineralogical and geochemical analyses were ground to <63 µm by hand in agate beakers. Bulk mineralogical contents were determined by X-ray diffraction (XRD) on powder pellets using a diffractometer Bruker D8 Discover with Cu tube (λ = 1.5418 A, 40 kV, 30 mA) and the detector LYNXE_XE (opening angle = 2.9464°). The spectrum from 5° to 90° was measured in 4155 steps of 1 sec. exposure time. The evaluation of the spectra to minerals was computed using Match! (Crystal Impact (2014), Bonn, Germany and SEARCH (Stoe and Cie (2003), Darmstadt, Germany) based on pdf2 (ICDD (2003), Philadelphia, USA). The evaluation of the concentration of the minerals was evaluated using TOPAS Rietveld (Coelho, 2003).

Relative element intensities were determined on pressed powder samples using an X-ray fluorescence (XRF) scanner (ITRAX; Cox Analytical Systems; Davies et al., 2015). Measurements were performed with 1 mm resolution and an exposure time of 60 s using a Cr-tube (settings: 50 kV, 38 mA), which provides a general overview of the elements lighter than Cr (Löwemark et al., 2011).

For the analyses of total inorganic carbon (TIC) and total organic carbon (TOC), ca. 35 mg samples were mixed with 10 g of distilled water and measured via the thermal catalytic oxidation principle in the Dimatoc 2000 (Dimatec Corp.). The contents of total nitrogen (TN) and total sulphur (TS) were measured with a vario Micro cube (Elementar Corp.), in which 5 mg samples were combusted at 1200 °C in a He and O_2 flow and the element concentrations determined on the N_2 and SO_2 released by the thermal conductivity detector.

Interpolation and mapping of the data derived from the lake surface sediment and catchment soil samples were carried out by the ArcGIS software by ESRI using the Kriging method (Oliver and Webster, 1990; Cressie, 1991). The principal component analysis (PCA) was conducted with PAST (Hammer et al., 2001).

The grain-size distributions of the lake surface sediments and the soils in the catchment of Laguna de Medina show a high spatial variability. The lake surface sediments range in mean grain sizes between 4.0 and 362.1 µm (Fig. 2.4a). Coarsest grain sizes, with sand (>63 µm) contents of more than 40 %, occur along the northern and western lake shores (Fig. 2.4b). However, sand is absent at distances >200 m from the shore. Here, silt (2–63 µm) and clay (<2 µm) dominate the sediment composition (Figs. 2.4c and 2.d). Highest silt contents (>60 %) are measured in front of the Arroyo de Fuente Bermeja inlet (Fig. 2.4b). The clay content is highest in the central part of the lake (Fig. 2.4d), but with up to 40 % below the silt fraction. The soil samples show coarsest grain sizes, with more than 50 % sand, in the northern catchment, and are much more fine grained than in the other lake areas (Fig. 2.4).

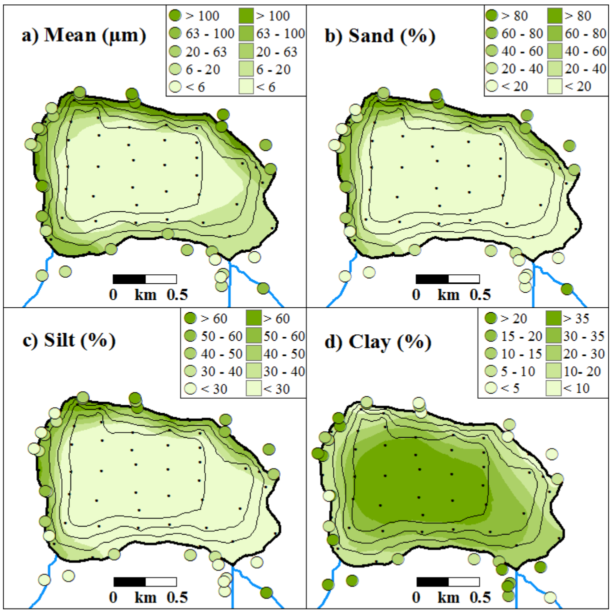

Figure 2.4: Spatial distribution of (a) mean grain size and the volume percentages of (b) sand, (c) silt, and (d) clay in the lake surface sediments (black dots) and catchment soil samples (coloured circles). The major inlet streams are indicated by blue lines, contour lines show 1 m isobaths.

The mineralogical composition of the lake surface sediment and catchment soil samples is dominated by calcite, quartz, dolomite, and gypsum (Fig. 2.5). Furthermore, pyrite, muscovite and some clay minerals occur as minor components. Calcite contents are elevated (>75 %) in soils at the southern shore and in the lake centre (Fig. 2.5a). The soil samples show highest values in the southern and parts of the western catchments. The quartz contents with >60 % are highest in the lake sediments close to the northern shore, and reach intermediate values (30-60 %) close to the western and eastern shores (Fig. 2.5b). This pattern only partly corresponds to the adjacent soil samples, which show similarly high values also in the southeastern catchment. Dolomite exhibits highest concentrations of >20 % in the soil samples close to the Arroyo Fuente Bermeja inlet (Fig. 2.5c). In the lake surface sediments, highest dolomite values of >4 % occur in front of this inlet, but also close to the northwestern lake shore. Gypsum amounts to <5 % in the lake surface sediments, reaching >3 % in the western, central, and eastern part of the lake (Fig. 2.5d). In the catchment soils, the gypsum contents reach values of >5 % but are more patchy and, with the exception of lowest values along the northern shore, do not provide a clear regional pattern.

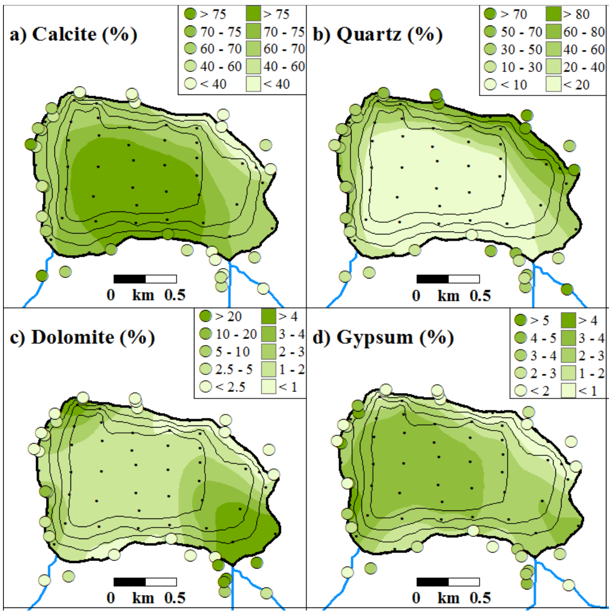

Figure 2.5: Spatial distribution of the volume percentages of (a) calcite, (b) quartz, (c) dolomite, and (d) gypsum in the lake surface sediments (black dots) and catchment soil samples (coloured circles). The major inlet streams are indicated by blue lines, contour lines show 1 m isobaths.

The bulk elemental composition of the lake surface sediments is dominated by calcium (Ca), which shows at least a factor 10^3 higher counts than all other elements. Highest Ca intensities occur in the southern and southwestern lake areas and in many soil samples from the adjacent catchments (Fig. 2.6a). Silicon (Si), in contrast, shows highest intensities in the northern lake and catchment (Fig. 2.6b). Relatively high intensities also occur in front of the inlets reaching the lake in its southwestern and southeastern parts. The distribution of zirconium (Zr) is similar to that of Si, except of a more pronounced minimum at the western shore and more variability of the soil samples in the catchment (Fig. 2.6c). The strontium (Sr) distribution is rather inversely correlated with Si and Zr, showing lowest intensities in the northeastern lake and catchment, and intermediate intensities in the southwestern and southeastern parts at the inlets (Fig. 2.6d). Potassium (K) has a distinct maximum in the southeastern part of the lake, in the vicinity of the Arroyo Fuente Bermeja inlet (Fig. 2.6e). A very similar pattern is shown by the elements aluminium (Al), iron (Fe), titanium (Ti), magnesium (Mg), and rubidium (Rb). The iron/manganese (Fe/Mn) ratio is higher in the eastern than in the western lake and catchment (Fig. 2.6f).

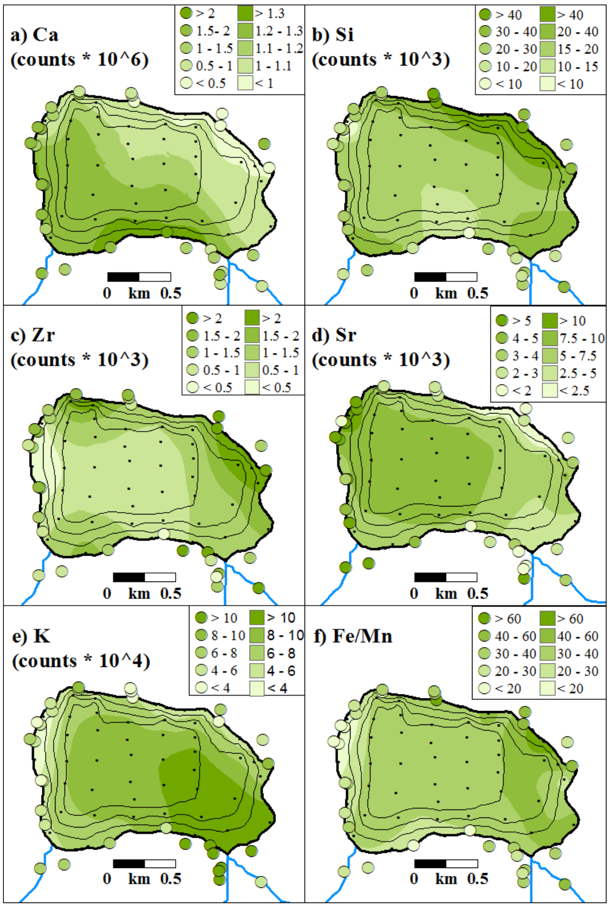

Figure 2.6: Spatial distribution of counts of (a) Ca, (b) Si, (c) Zr, (d) Sr, (e) K, and (f) the ratio of Fe/Mn in the lake surface sediments (black dots) and catchment soil samples (coloured circles). The major inlet streams are indicated by blue lines, contour lines show 1 m isobaths.

TIC is highest (>5 %) in the southern part of the lake (Fig. 2.7a). The soil samples show similar values in the adjacent catchment, but also in most parts of the western and eastern catchments. TOC and TN exhibit very similar patterns (Figs. 2.7b and 2.7c). Distinct maxima occur in the northwestern and eastern lake, with TOC contents of up to 34 % and 23 %, respectively, and TN contents of ca. 1.5 %. Relatively high values of 2-6 % TOC and 0.3-0.5 % TN also occur in the southern and central lake. In the catchment soils, TOC and TN concentrations are much lower and show rather irregular patterns with little similarities in adjacent lake and soil samples. The distribution of TS in the lake sediments shows distinct similarities to those of TOC and TN, with the exceptions that extreme values are missing and that the maximum in the western lake sediments is accompanied by relatively high values in the adjacent catchment soils (Fig. 2.7d). The C/N ratio (TOC/TN) shows a rather simple pattern in the lake sediments, with high values of >10 along all shores and low values of < 10 in the lake centre, but more diverse values in the catchment soils (Fig. 2.7e). The C/S (TOC/TS) ratio (2.7-25.7) has some similarities in the lake sediments with the C/N ratio, however, the maxima are restricted to small areas at the northwestern, southwestern, and eastern shores, and they correspond with maxima in several soil samples from their adjacent catchments (Fig. 2.7f).

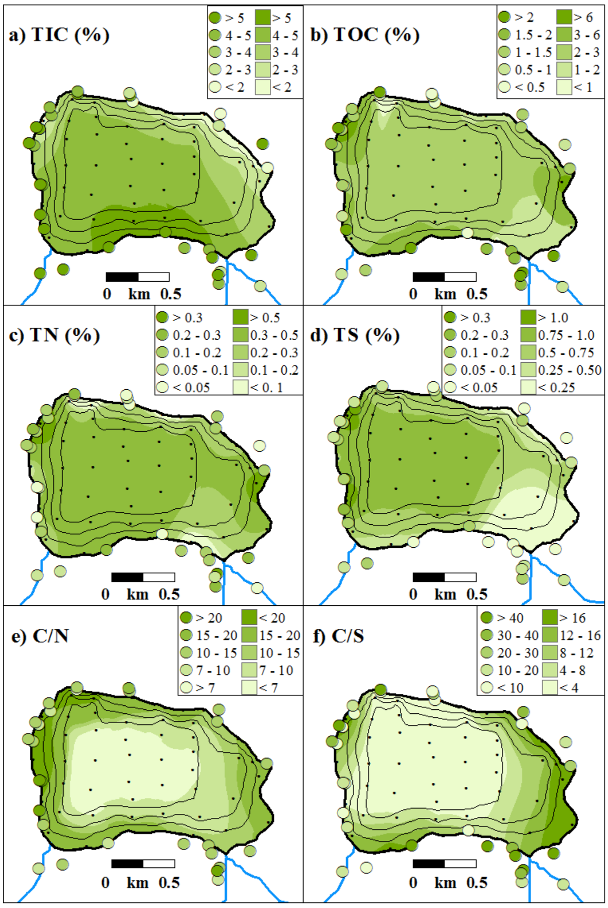

Figure 2.7: Spatial distribution of the volume percentages of (a) TIC, (b) TOC, (c) TN, (d) TS and the ratios of (e) C/N and (f) C/S in the lake surface sediments (black dots) and catchment soil samples (coloured circles). The major inlet streams are indicated by blue lines, contour lines show 1 m isobaths.

The first and second principal components (PC) of the principal component analysis (PCA) of the lake surface sediments of Laguna de Medina explain 55.44 % and 16.79 % of the data, respectively (Fig. 2.8). The outcome plots within the 95% confidence ellipse. Negative loadings of PC1 are found by sand, the mean grain size, Si, Zr, quartz and C/N and C/S ratios. Positive loadings are reflected by the water depth, the fine-grained fractions (clay and silt), gypsum, calcite and TIC and Mn. Positive loadings of PC2 are reflected by TOC, TN and TS. Negative loadings include the elements Ti, K, Al, Rb, Fe and Mg and dolomite.

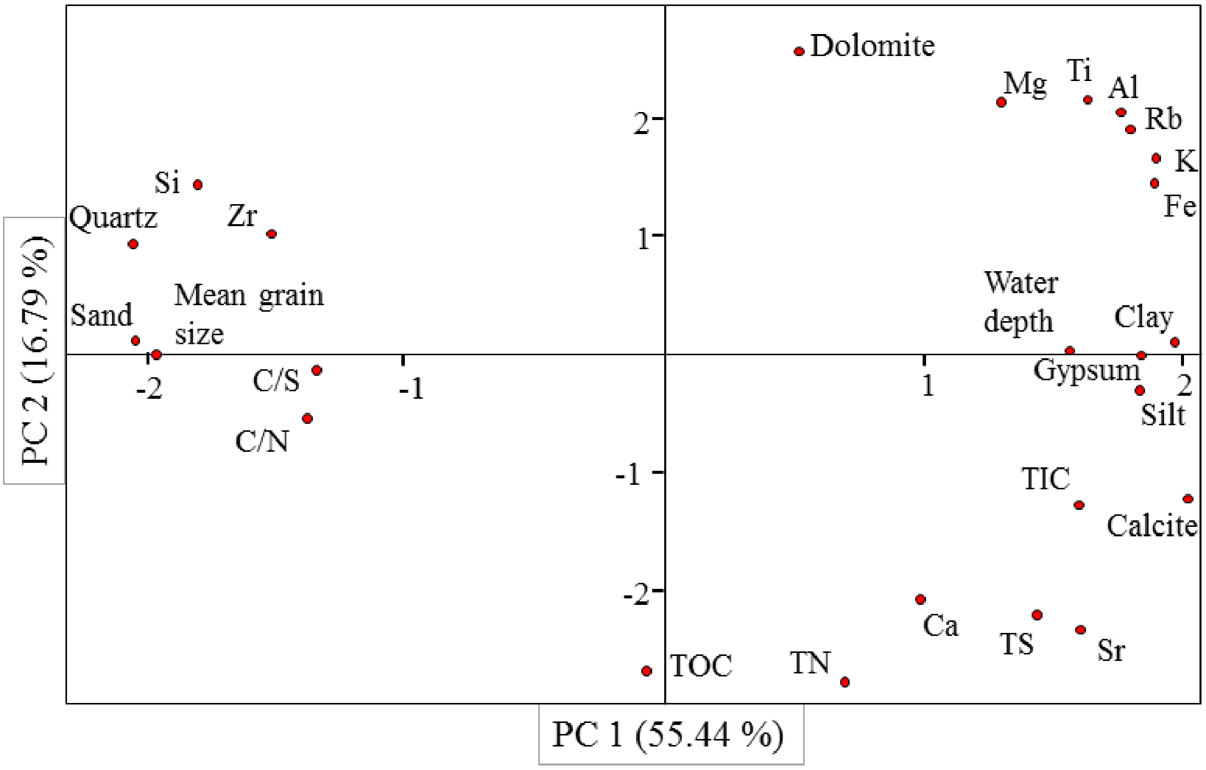

Figure 2.8: Results of the principal component analysis (PCA) of the granulometric, mineralogical, elemental, and geochemical parameters.

2.6 Discussion

Based on the granulometric, mineralogical, and geochemical parameters (Figs. 2.4-2.7), supported by the PCA (Fig. 2.8), the lake surface sediment samples of Laguna de Medina can be divided into six provinces of individual compositions and depositional processes (Fig. 2.9).

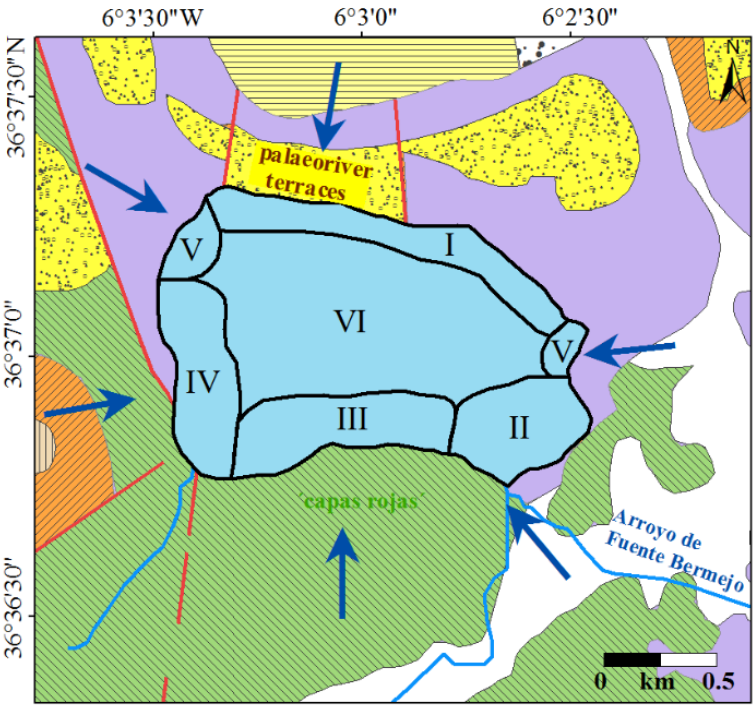

Figure 2.9: Geology in the near surroundings of the Laguna de Medina (cf. Fig. 2.2) and spatial distribution of the six provinces of lake surface sediments with individual compositions and driving forces:

I - input from palaeo river terraces;
II - fluvial sediment supply;
III - ´capas rojas´ influence;
IV - gypsum precipitation;
V - anthropogenic terrestrial organic matter supply;
VI - distal background sedimentation

At the northern shore (Province I), the lake surface sediments differ from those in all other parts of the lake by particularly coarse grain sizes, with high sand contents and a mean grain size of 100 – 362 µm (Figs. 2.4a and 2.4b). Furthermore, quartz, Si, and Zr are clearly enriched (Figs. 2.5b, 2.6b, 2.6c). All these proxies have high negative loadings on the PC1 in common (Fig. 2.8) and a very similar composition is found in the soil samples to the north of the lake. This suggests that sediment supply into the lake from the palaeoriver terraces of the Guadalete to the north, which consist of conglomerates, sands and gravels (IGME, 1984), dominates the sedimentation close to the northern lake shore.

Province II occurs in the southeastern part of the lake, in front of the Fuente Bermeja inlet. The sediments are characterized by high contents of silt (Fig. 2.6b), as well as high intensities of lithogenic elements such as K (Fig. 2.6e), Al, Fe, Ti, Mg and Rb (not shown; Boës et al., 2011), as well as dolomite (Fig. 2.5c). A similar composition is found in the fluvial sediments of the Fuente Bermeja and most of the adjacent soil samples, thus indicating that lake sediment composition is strongly influenced of riverine input by this major inlet.
The chemical and mineralogical composition of the lake sediments suggests that the Fuente Bermeja mainly supplies weathering products of the Triassic Keuper facies, which is widely exposed in the catchment and consists of claystones, sandstones, and partly dolomites (IGME, 1984; Fig. 2.2). The dominance of this sediment source is also reflected by a distinct clustering of dolomite and the lithogenic elements in the PCA, showing positive loadings of PC1 and high negative loadings of PC2. Interestingly, dolomite clusters closer to the lithogenic elements than to the Ca. Ca is dominating in the entire lake, so an extra Ca input from dolomite is not significant. The effect of the Mg, on the other hand, is much more pronounced. That is the reason the dolomites cluster close to the lithogenic elements. The high silt contents of the surface sediments, and its wide distribution throughout the lake (Fig. 2.6b), reflect the main grain size provided by the inlet, but also that this fluvial input constitutes a significant contribution to sedimentation also in other lake parts.

The lake sediments close to the southern shore (Province III) are characterized by high calcite and TIC concentrations, and high Ca intensities (Figs. 2.5a, 2.6a, 2.7b). In the PCA, these proxies show positive loadings in PC1 but negative loadings in PC2. The latter suggests a significantly different sediment source to that of the northern shore (Province I), which is characterized by high concentrations of sediment proxies with positive PC2 loadings that reflect clastic sediment supply. The carbonate-related proxies enriched in Province III, in contrast, rather suggest supply of weathering products from the adjacent Cretaceous ´capas rojas´, a series of Subbetic deep-water marlstones and limestones occurring to the south (IGME, 1984; Vera and Molina, 1999). This sediment source is also reflected in the composition of the soil surface samples to the south of the lake.

Province IV is located in the western part of the lake (Fig. 2.6). It is characterized by high gypsum and TS concentrations, high Sr intensities, and C/N ratios >12 (Figs. 2.5d, 2.6d, 2.7d, 2.7e). The high C/N ratios indicate a high terrestrial influence on organic matter deposition (Meyers and Ishiwatari, 1993). The relatively high Sr concentration could partly be traced back to the Cretaceous carbonates, such as those in the ´capas rojas´ to the south, but also supports direct gypsum supply, which is suggested by elevated gypsum contents. In both cases, Sr is partly related to Ca (Kulp et al., 1952). A Ca, TS, and Sr supply in parts independent on the gypsum supply is also indicated in the PCA, where gypsum loadings around zero on PC2 differ from distinctly negative loadings of Ca, TS, and Sr (Fig. 2.6). The most likely source for terrestrial gypsum supply in Province IV is the western lake catchment. There, however, a patchy pattern in the respective soil samples (Fig. 2.7d) suggests that gypsum is exposed to the surface only locally. Therefore, the high gypsum, Sr, and TS concentrations in Province IV, partly extending further towards the lake centre (Province VI), most likely originate not only from surficial gypsum and carbonate supply but also from infiltrating groundwater, which is enriched with dissolved Ca and SO_4 ions (Burn and Palmer, 2014). This suggestion is supported by low C/S values in the centre of the lake (Fig. 2.7f), which suggest an enrichment of TS by gypsum accumulation.

Province V is divided into two areas in the northwestern and central eastern parts of the lake. These areas are highly enriched in TOC and TN concentrations (Figs. 2.7a and 2.7c), indicating an increased amount of organic matter. TS is moderately enriched in these areas (Fig. 2.7d), suggesting that the sulphur is also partly adsorbed onto organic matter, and not only on the gypsum. This is also visible in the PCA, where TS plots between the organic compounds TOC and TN and the gypsum (Fig. 2.8). Adjacent to the areas in the north western and central eastern parts of the lake, much land is dedicated to agricultural use, like dry cultivation of cereals and sunflower (Reed et al., 2001), using the lake water for irrigation (Fernández-Palacios, 1990). Small gullies, which drain these agricultural areas enter the lake in both of the Provinces V. Hence, the higher TOC and TN concentrations in this province are probably an anthropogenic effect, with more terrestrial organic matter being mobilized and transported into the lake.

Province VI is situated in the ´deep´ centre of the lake, where the influences of wave action and punctuated catchment supply are smallest. Here, low energy favours fine particles as clay and silt to settle (Figs. 2.4b and 2.4c). Sedimentation of gypsum and calcite is significant (Figs. 2.5a and 2.5c), with the former also being reflected by low C/S ratios (Fig. 2.7f). C/N ratios of <10 (Fig. 2.7e) suggest that the organic matter in the surface sediments originates mainly from autochthonous in-lake productivity (algae), with only restricted contribution from terrestrial sources (Meyers and Ishiwatari, 1993). These interpretations are supported by PC1 of the PCA analysis, showing high positive loadings of clay, silt, gypsum, and calcite, and high negative loadings of C/S and C/N (Fig. 2.8).

2.7 Conclusions

Based on the granulometric, mineralogical, elemental, and geochemical composition of the surface sediments in the Laguna de Medina, and the comparison with the composition of catchment soil samples, the following conclusions can be drawn concerning the modern sedimentation in this lake.

Today, regional differences in the sedimentation in the Laguna de Medina, as documented in the sedimentary provinces I to VI (Fig. 2.9), are predominantly controlled by the surrounding geology. This is mainly reflected in the mineralogical and elemental composition of the surface sediments, showing enrichments of quartz, dolomite, calcite, and gypsum, along with the associated elements, close to the northern, southeastern, southern, and western shores, respectively. In addition, enhanced organic matter deposition due to anthropogenic activity in the catchment is indicated close to the eastern and northwestern shores. In the central part of the lake, with a distance greater than 200 m from the shores, sediments are significantly more mixed, even if the sediment supply from the major inlet Arroyo de Fuente Bermejo could be still detected.

No indication was found that lake currents have a strong impact on the modern sediment distribution in the Laguna de Medina. This differentiates this small endorheic lake from larger throughflow lakes, such as Lake Ohrid in the eastern Mediterranean area (Vogel et al., 2010) and Lake El´gygytgyn in the northeastern Russian Arctic (Wennrich et al., 2013). Furthermore, the Laguna de Medina today obviously is too shallow to have significant areal differences in bottom water redox conditions. This is for instance reflected in a Fe/Mn ratio independent on water depth (Fig. 2.4f), a proxy, which in deeper lakes, such as Lake El´gygytgyn, can be used to reconstruct times of anoxic bottom water conditions (Melles et al., 2012). Another difficulty is the double toll of Calcium, because it is partly bound on the calcite and also on the gypsum, so the Ca intensities cannot be used as a proxy for calcite in this lake.

Taking these findings concerning the modern sedimentation in the Laguna de Medina, sediment cores from the central part of the lake should reflect quite well how the identified driving forces have changed in their relative importance throughout the last millennials. Hence, the 25.65 m long core Co1313 recovered from the central part of the Laguna de Medina from its location and length has a high potential to provide new important insights into the regional climatic and environmental conditions in southern Spain during the Holocene.

Laguna de Medina in the morning fog
Picture by Florian Steiniger

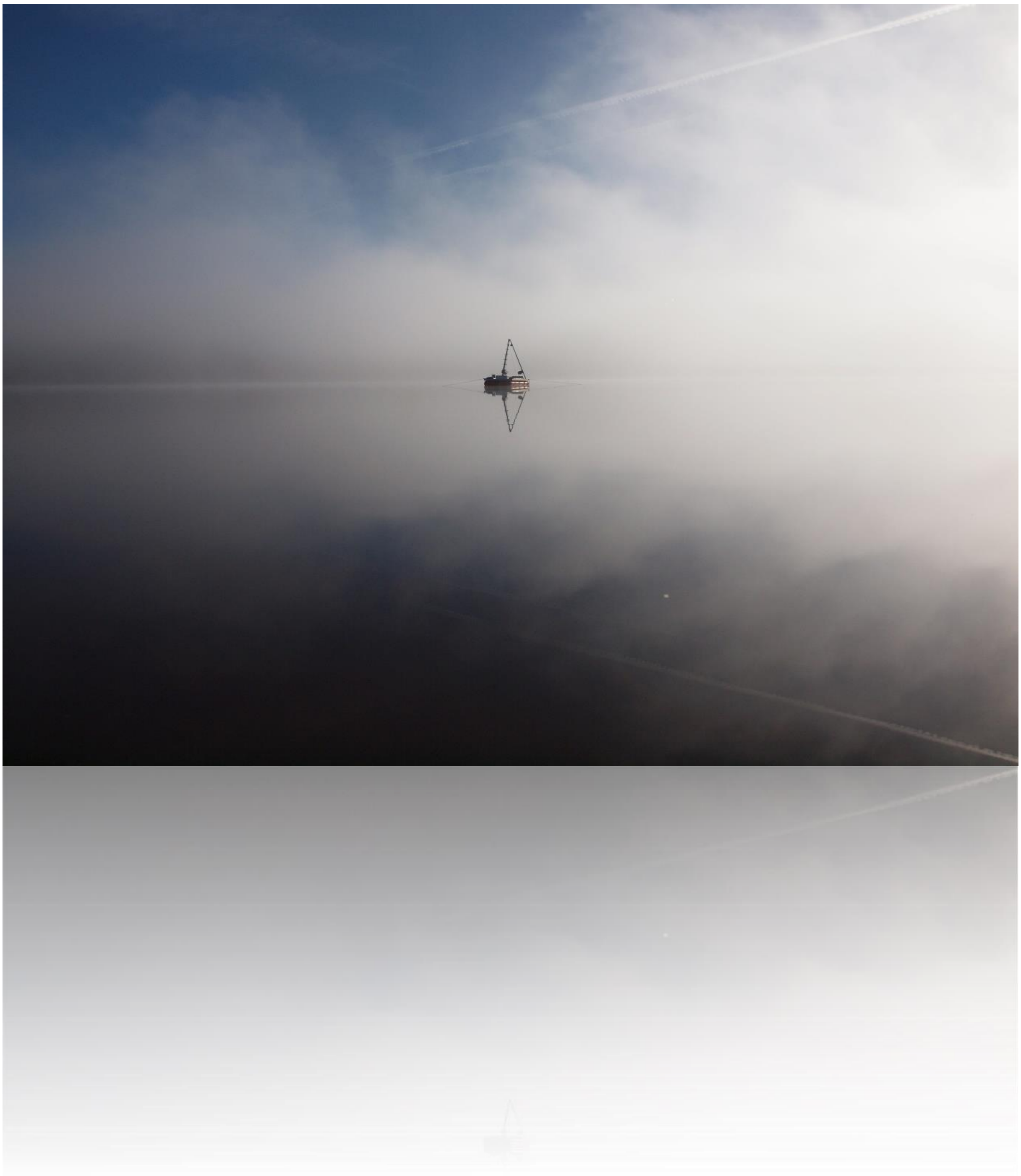

Chapter 3

A high-resolution Holocene palaeoclimate record from the Laguna de Medina, Cádiz, southern Spain

3 A high-resolution Holocene palaeoclimate record from Laguna de Medina, Cádiz, southern Spain

Jasmijn van ´t Hoff[a], Tabea Schröder[b], Finn Viehberg[a], Peter Held[a], Klaus Reicherter[b], Martin Melles[a]

[a] Institute of Geology and Mineralogy, University of Cologne, Zülpicher Str. 49a, 506745 Cologne, Germany
[b] Institute of Neotectonics and Natural Hazards, RWTH Aachen University, Lochnerstr. 4-20, 52056 Aachen, Germany

Corresponding author: Jasmijn van ´t Hoff: jvanthof@uni-koeln.de
Institute of Geology and Mineralogy
University of Cologne
Zülpicher Straße 49a
50674 Cologne, Germany

Key words: Holocene, palaeolimnology, palaeoclimate, Laguna de Medina, southern Spain,

Journal article in preparation

3.1 Abstract

The high-resolution lacustrine sequence from the centre of Laguna de Medina (Cádiz, southern Spain) covers the last 9,600 years, evidenced by 20 calibrated ^{14}C dates. This semi-permanent saline lake gives insight in the palaeoclimatic and -hydrological conditions since the Early Holocene. Due to its basin morphology, the lake is very vulnerable for hydrological changes.

The record provides a detailed history of the depositional regime, the infilling of the sinkhole after its formation, the transition from deep lake with steep sides, to a shallow elongated lake, the chemical evolution of the lake, the influence of the climate, and rapid climate changes during the Holocene.

Based on the sedimentological, geochemical, mineralogical, and ecological (ostracods) data, supported with the statistical analyses of the principal component analysis, the record can be divided into four different periods. The Early Holocene, the period prior to 7,870 cal yr BP, is a warm and wet period with low lake levels. This period is followed by a phase of maximum lake level between 7,870-5,780 cal yr BP, reflected by the laminated facies, and a change in the ostracod assemblage towards more saline species. Interestingly, this humid period has the highest salinity, which is probably the result of enhanced catchment dissolution of the gypsum-rich Triassic geology due to the increased humidity. From 5,780-3,750 cal yr BP, the lake level dropped significantly, mainly reflected by the facies, the reduction of the laminations, and the occurrence of aragonite. However, the lake remains relatively deep, mainly due to its shape, with anoxic bottom water conditions. The last period from 3,750 cal yr BP on is characterized by a progressive aridification with several desiccation phases, enhanced gypsum precipitation, and a dominance of mesohaline ostracods.

Over this long-term trend, several periods of short-term climate change, coinciding with the rapid climate change of the Iberian Peninsula, resulted in periods of aridification. Short arid periods interrupting the long-term trend occurred between 9,160-7,870, 5,780-4,800, 3,150-2,420, 1,950-1,450 (corresponding to the Roman Warm Period), and 1,264-550 (corresponding to the Medieval Climate Anomaly) cal yr BP. One humid period (550-170 cal yr BP) coincides with the last known Rapid Climate Change, reflecting the Little Ice Age.

The sequence of Laguna de Medina reinforces the connection between global changes in the hydrological regime, rapid climate change and North Atlantic Oscillation dynamics.

3.2 Introduction

The Western Mediterranean, and in particular its arid regions, is very vulnerable to even small climatic and hydrological changes (Giorgi and Lionello, 2008). For irrigation of the land, aquifers are exploited. However, the total consumption of ground water in Spain exceeds the yearly input by 163 %, indicating the aquifers are overused (Puigdefábregas and Mendizabal, 1998). As a result, 25 % of the irrigated land already faces problems with soil salinization (Szabolcs, 1990). Due to the onging climate change, droughts are increasing since 1960 (Met Office, 2011), and climate simulations predict a decrease in summer precipitation (Giorgi and Lionello, 2008), and a northward extension of arid lands for the next decades (Gao and Giorgi, 2008). Consequently, soil salinization is expected to increase further, causing huge problems with land irrigation (Puigdefábregas and Mendizabal, 1998).

In order to enhance the quality of the climate prediction for the next decades, it is important to know how climatic settings behave under different boundary conditions. Relatively little is known about these settings since the last glacial on the southern IP, due to the scarcely of long and continuous terrestrial climate archives (Roberts et al., 2008). Since only a few archives cover the entire Holocene (e.g. Carrión et al., 2001a, b; Reed et al., 2001; Fletcher et al., 2007; Martin-Puertas et al., 2008), our knowledge of the Holocene climate history on land is mainly based on information from distal marine sediment cores (e.g. Combourieu-Nebout et al., 1998, 2002, 2009; Sánchez-Goñi et al., 1999; Martrat et al., 2004;Voelker et al., 2006, 2009; Voelker and de Abreu, 2011). Additional terrestrial archives are needed to complement this information by more data reflecting the conditions on land directly. This especially holds true for the precipitation, which cannot be reconstructed properly from marine records.

Amongst the promising archives of the climatic and environmental history of the IP are the sediment records in small endorheic lakes (Spanish: *Salinas*), which are frequent in southern Spain. These lakes may be influenced by temporary desiccation, causing hiatuses in very arid years (Höbig et al., 2016). However, some of the lakes are permanent and thus provide continuous high-resolution records (Moreno et al., 2012). Furthermore, the sediments in these lakes can be highly sensitive to even small climatic changes, in particular of precipitation, because these changes may lead to strong changes in lake level and brine concentration (Fritz, 1996).

Laguna de Medina is such a small and shallow saline lake in southern Spain (Fig. 3.1). The 25.65 m long sediment core Co1313, recovered from the centre of the lake, provides the first continuous and high-resolution terrestrial record for the last 9,600 years from the southern tip of the IP. This study presents a multi-proxy approach of the record, involving sedimentological, mineralogical, geochemical, and paleoecological methods. Due to its exceptionally high temporal resolution, the record reflects not only long-term, millennial-scale climatic and environmental changes, but also short-term, decadal to centennial-scale events (rapid climate changes), and can be linked to oscillations of the NAO.

3.3 Study site

Laguna de Medina (36°37´04”N, 06°03´13”W) is the second largest inland playa lake in Andalucía, southern Spain (de Vicente et al., 2012). Due to its importance for water birds (Amat, 1984), it became a protected Nature Reserve and a Wetland of International Importance included in the Ramsar Convention in 1989 (de Vicente et al., 2012). The lake today is surrounded by agricultural land, dominated by orchards of olive trees, and is used as source for irrigation (Rodríguez-Rodríguez et al., 2012).

Laguna de Medina is a semi-permanent, warm polymictic, and saline lake (Lewis, 1983), with a surface area of 1.2 km^2, and a catchment area of 16 km^2, located 30 m above sea level (Fig. 3.1). The largest inlet, the Arroyo de Fuente Bermeja, enters the lake at its southeastern shore. This temporary inflow, being dry during summer months (Reed et al., 2001), is the most important source of clastic sediment supply (van ’t Hoff et al., 2017). The maximum lake water depth today is 3.5 m, limited by the height of a ditch that overflows when the lake surface exceeds its level (Rodríguez-Rodríguez et al., 2012). During field campaigns in September 2014 and March 2015, the water depths were up to 1.7 m and 3.2 m, respectively. Permanent lakes in the arid Spain require a water depth of >2 m in normal years (Alonso, 1998), indicating Laguna de Medina is a semi-permanent water body that only dries out during very arid years.

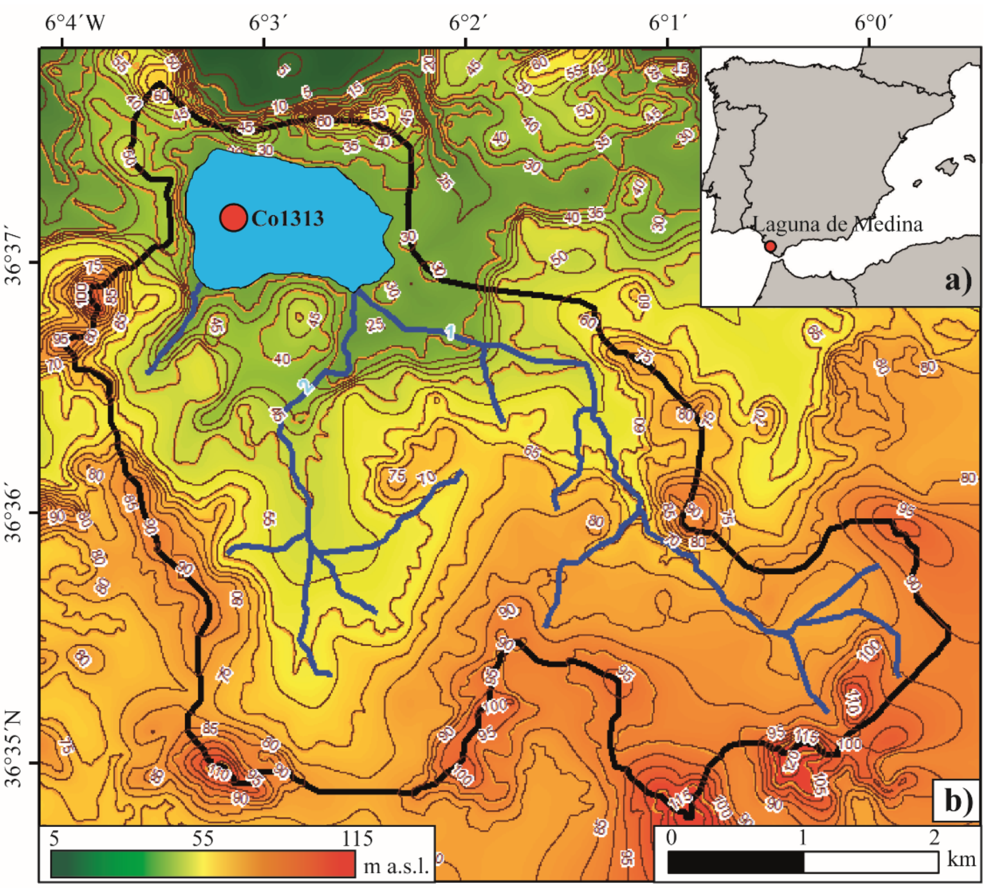

Figure 3.1. Overview of the setting of Laguna de Medina. a) Location of Laguna de Medina on the Iberian Peninsula. b) Digital Elevation Model (in m a.s.l.) of the catchment area (encircled in black) of the Laguna de Medina, and the coring position of Co1313 (red dot). Blue lines indicate the most important inlets.

The lake basin was probably established during the Late Pleistocene, due to diapiric uplift in combination with karstic processes such as dissolution and collapse, resulting in sinkhole (Rodriguez Vidal et al., 1993; Valero-Garcés et al., 2014; Wolf et al. 2014). The southern catchment is dominated by the Cretaceous ´capas rojas´, a series of Subbetic deep-water marlstones and limestones (Vera and Molina, 1999) (Figs. 2.1 and 2.9). In the eastern and western catchment, terrestrial Triassic Keuper facies (claystones, sandstones, dolomites and gypsum) are dominant, and the northern catchment is characterized by coarse sand and gravel from the palaeoriver terraces of the Guadalete (IGME, 1984).

Laguna de Medina today experiences a Mediterranean climate (Peel et al., 2007). The summers are hot and dry, driven by the Azores high pressure system (Sumner et al., 2001). This results in a period of five months with water deficit (Paez, 1991). During the moderate winter, the Azores High shifts southward. This enables mid-latitude storms to reach the region, making the winters relatively wet, with precipitation up to 90 mm per month (Sumner et al., 2001). The average annual precipitation is 525 ± 275 mm/year and the average effective rainfall is 171 mm/year (Rodríguez-Rodríguez et al., 2012). On a decadal scale, the climate variability in southern Spain is mainly influenced by the North Atlantic Oscillation (NAO), with a positive (negative) NAO resulting in more arid (more humid) winters (Wanner et al., 2001; Trigo et al., 2004).

The Laguna de Medina functions as a hydrologically closed system (Fernández-Palacios, 1990). A significant influence of highly saline ground-water inflow results in gypsum precipitation, mainly in the western part of the lake (Eugster and Hardie, 1978; van´t Hoff et al. 2017), and leads to the retention of water during summer times (Reed et al., 2001). However, due to little permeable underground, the influence of ground water is small (Fernández-Palacios, 1990), which makes the lake very vulnerable to variations in precipitation. Today, the lake level is highly affected by seasonal precipitation changes, resulting in summer desiccation in very arid years. The average conductivity is 6.11 mS/cm, but fluctuated heavily (4.65-12.88 mS/cm) during a monitoring study of 84 months by de Vicente et al. (2012). The average total alkalinity is 2.13 meq/l and the pH is 7.98 (de Vicente et al., 2012).

The sediment record at the bottom of Laguna de Medina was first investigated by Reed et al. (2001). Based on paleolimnological proxies (diatoms, ostracods, foraminifera, molluscs, aquatic pollen, and lithology), fluctuations in water level and salinity were reconstructed, which were traced back to significant precipitation changes during the last 9,000 years. These findings significantly complemented marine geological research in the adjacent oceans (Fig. 1.1), which, although they suggest rapid climate change throughout the Holocene, are relatively stable due to the low temporal resolution (Martrat et al., 2007; Fletcher et al., 2009).
The study presented here builds on a new, much longer sediment record from the Laguna de Medina (Co1313), which provides a much better time resolution and is investigated by additional geochemical and mineralogical proxies.

3.4 Material and methods

Field work
The core Co1313 originates from 3 m long core sections, which were retrieved from two parallel sediment cores in the centre of the Laguna de Medina in September 2014 and March 2015 (Fig. 3.1). Coring was conducted from a floating platform with a percussion piston corer (UWITEC Corp., Austria). On site, the cores were cut into up to 1 m long sections, which were stored dark and dry until further processed in the laboratory.

Analytical work
All the analytical work was conducted at the laboratories of the University of Cologne. First, the cores were cut lengthwise into two core halves, which were used for core description and photographical documentation. One core halve was logged with 1 cm resolution for magnetic susceptibility at an MSCL (Multi-Sensor Core Logger, GeoTek; Weber, 1997). The core sections from the parallel holes were correlated to a core composite of 25.65 m length, based on matching of both cores using the sedimentary structures and fluctuations of the magnetic susceptibility in overlapping core parts.
Subsequently, the core composite was scanned for chemical composition with 2 mm resolution at an XRF scanner (ITRAX X-Ray Fluorescence scanner, COX Analytical Systems; Davies et al., 2015). The XRF scans were run with an exposure time of 10 s and Cr-tubes set to 50 kV and 38 mA, thus providing a good overview of the elements lighter than Cr (Löwemark et al., 2011). The XRF data were smoothed using a 19-pt running mean to reduce the noise.

The composite core was subsampled at intervals of 6 cm, leading to 427 discrete samples for geochemical analysis. For the granulometric analysis, every 4th sample was used, resulting in 107 samples. In a first step, the samples were freeze-dried in order to exclude transformation of gypsum ($CaSO_4 \cdot 2H_2O$) to bassanite ($CaSO_4 \cdot ½H_2O$) or anhydrite ($CaSO_4$). Subsequently, the bulk sediment samples were split into aliquots for different measurements.

For the geochemical analysis, one aliquot of the samples was ground to <63 µm to enlarge the surface area. For the analyses of total inorganic carbon (TIC) and total organic carbon (TOC), ca. 35 mg of the ground samples was mixed with 10 g distilled water and measured with a Dimatoc 2000 (Dimatec Corp.). The contents of total nitrogen (TN) and total sulphur (TS) were measured on parallel sample aliquots of 5 mg with a vario Micro cube (Elementar Corp.).

For grain-size analyses, another aliquot was pretreated with 10 ml $NaCO_3$ at 60°C for 18 hours, 10 ml 10 % HCl at 50°C for 3 hours, 5 ml 30 % H_2O_2 at 50°C for 18 hours, and 5 ml 1 M NaOH at 90°C for two times 30 min, in order to remove the gypsum, carbonate, organic matter, and biogenic silica, respectively. Between the different steps, the samples were centrifuged and neutralized with deionized water. Prior to the measurements, the samples were mixed with $Na_4P_2O_7$ (0.05 %) and shaken for at least 12 hours to avoid flocculation of clay minerals. Each sample was measured three times in 116 classes in a range between 0.04 and 2000 µm using a Laser Particle Size Analyser LS 13320 (Beckman Coulter Corp.) and the Frauenhofer optical model. The grain-size distributions were calculated using the program GRADISTAT (Blott and Pye, 2001).

For the mineralogical and elemental powder analyses, 111 aliquots of the ground samples were chosen from interesting parts of the record. Bulk mineralogical contents were determined by X-ray diffraction (XRD) on powder pellets using a diffractometer Bruker D8 Discover with Cu tube (λ = 1.5418 A, 40 kV, 30 mA) and the detector LYNXE_XE (opening angle = 2.9464°). The spectrum from 5° to 90° was measured in 4155 steps of 1 sec. exposure time. The evaluation of the spectra to minerals was computed using Match! (Crystal Impact (2014), Bonn, Germany and SEARCH (Stoe and Cie (2003), Darmstadt, Germany) based on pdf2 (ICDD (2003), Philadelphia, USA). The evaluation of the concentration of the minerals was evaluated using TOPAS Rietveld (Coelho, 2003).

Afterwards, this aliquot was scanned on the XRF scanner with a 1 mm resolution and an exposure time of 60 s using a Cr-tube (settings: 50 kV, 38 mA) for relative element intensities to statistically evaluate the elemental and mineralogical data using a principal component analysis (PCA) conducted with PAST (Hammer et al., 2001). The outcome of the PCA plots within the 95% confidence interval.

The samples for the ostracod and foraminifera analyses were freeze-dried and an aliquot of 5.0 to 12.4 g was submerged in tap water and solidly frozen (-20°C), and later wet-sieved on a 63 µm mesh. The residue was freeze-dried and scanned under a stereomicroscope (magnification 64-fold) for ostracod remains. Carapaxes were counted as two valves, broken valves with more than 50% preserved were counted as a single valve. The taxonomy and ecological interpretation followed the studies by Meisch (2000), Mezquita et al. (2005), and Rasouli et al. (2016). The ostracod species were classified by their salinity preferences (< 0.5 ‰ – freshwater species; 0.5 – 5.0 ‰ mesohaline species; > 5.0 ‰ polyhaline species). Further, the ostracod record was assessed to identify objective intervals by a constrained hierarchical cluster analysis, and used to reconstruct past host water conductivity based on the weighted average ecological preferences of Iberian ostracod species (Mezquita et al. 2005). The ostracod record investigated by Reed et al. (2001) was numerically treated similarly to compare both sedimentary records. A Gaussian LOESS filter was applied to the inferred conductivity data to smooth the results within a 95% confidence interval. All numerical calculations, and analyses were completed with the software package R version 3.2.5 including the libraries: rioja and vegan (R Core Team, 2016).

Radiocarbon dating

Chronostratigraphic information was obtained by radiocarbon measurements of 20 samples. ^{14}C dating was performed on plant material and root fragments of presumably terrestrial origin, in order to avoid falsification by reservoir or hardwater effects from aquatic carbon. All samples were treated using a modified protocol according to Rethemeyer et al. (2013). ^{14}C contents were measured on a 6 MV Tandetron AMS (HVE, The Netherlands) at the University of Cologne (COL, Dewald et al., 2013) and on a NEC compact model 0.5 MV AMS at the ^{14}CHRONO Centre at Queen´s University Belfast (UBA). The ^{14}C dates were calibrated by OxCal v. 4.2 (Ramsey, 2009) using the INT-Cal13 curve (Reimer et al., 2013). The software package Bacon 2.2 (Blaauw and Christen, 2011) using R (R Development Core Team, 2013) was used to construct the age model. Overall stable sedimentation rates (mem.strength = 6, mem.mean = 0.7, thick = 10 cm) and expected sedimentation rates (acc.shape = 1.5, acc.mean = 4) were considered.

3.5 Results

3.5.1 Sedimentology and geochemistry

The sediment record Co1313 is composed of five main lithofacies, based on the sedimentary structures, colours and lithologies (Fig. 3.2). In the first five meters (25.50-20.45 m), the sediments mainly are built up of lithofacies A (Fig. 3.2a). This facies consists of massive carbonate-rich clayey silty sediment without traces of bioturbation and a few poor indications of some laminations (Fig. 3.3). The colour varies between lightbrown and dark brown. It is interrupted twice by lithofacies B (Fig. 3.2b), consisting of massive clayey carbonate-rich silts alternating with weakly laminated sediments with mm thick gypsum and carbonate laminae (Fig. 3.3). The massive sediments are mostly grey. Laminations are mm to cm-fine (0.5-2 cm). For lamination description see Facies C. Facies B becomes more common further up, building up most of the sediment between 19.90-6.51 m, but occurs only once in the uppermost core part, in a depth of 4.30-4.15 m. The first occurrence of lithofacies C (Fig. 3.2c) at 20.45 m depth marks a significant transition in the sediments record, initiated by the onset of the laminated sediments. Facies C consists of highly laminated sediments with mm think gypsum and carbonate layers (Fig. 3.3). Mm-fine laminations are varying in colour between green, white, yellow and brown and in grain-sizes between clay-size up to 3 mm. Coarse grained laminae consist of gypsum. It repeatedly occurs between up to 8.30 m depth, most frequently between 20.45-13.23 m, alternating with facies B.

In facies B and C, white mottles occur between 20.45-6.51 m (indicated by the red stars in Fig. 3.3), which consist of 80-90% elemental sulphur (Fig. 3.2f).

The uppermost 6.51 m of the record consists of an alternation of lithofacies D and E (Fig. 3.3). Facies D (Fig. 3.2d) is built up of massive carbonate-rich clayey silts with traces of bioturbation, mainly of roots. The colour varies between dark brown and brown-greyish. Lithofacies E (Fig. 3.2e), consists of massive carbonate-rich clayey silts with white and/or green mottling of carbonates and gypsum evaporates and traces of bioturbation. The colour varies between light-brownish and brown-greyish. White mottling consisting of 1-3 mm and green mottling consisting of 1-5 mm large spots.

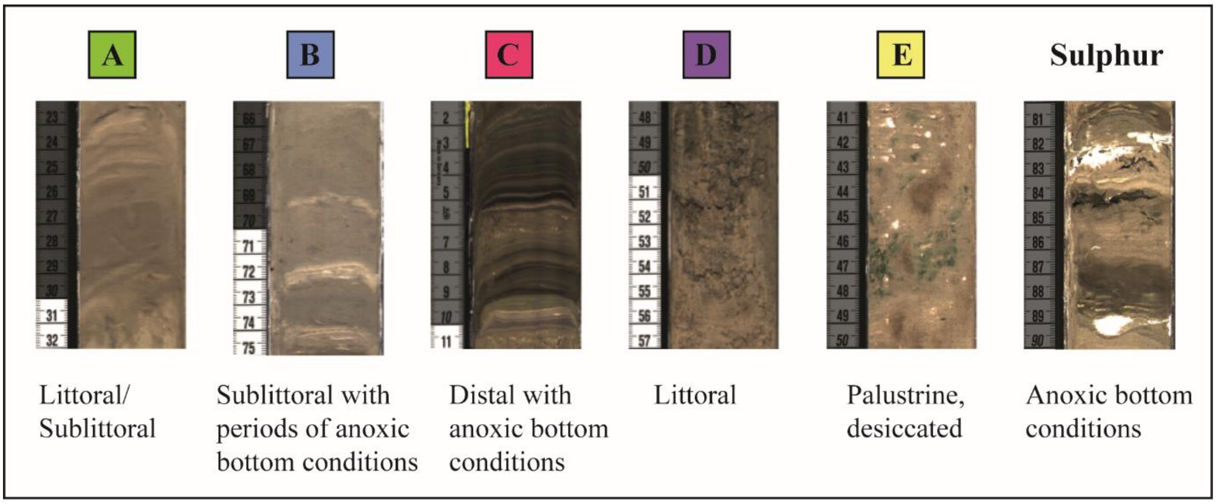

A representative picture of the five different facies (A-E) and the sulphur mottles, including the sedimentological characteristics and the interpretation.

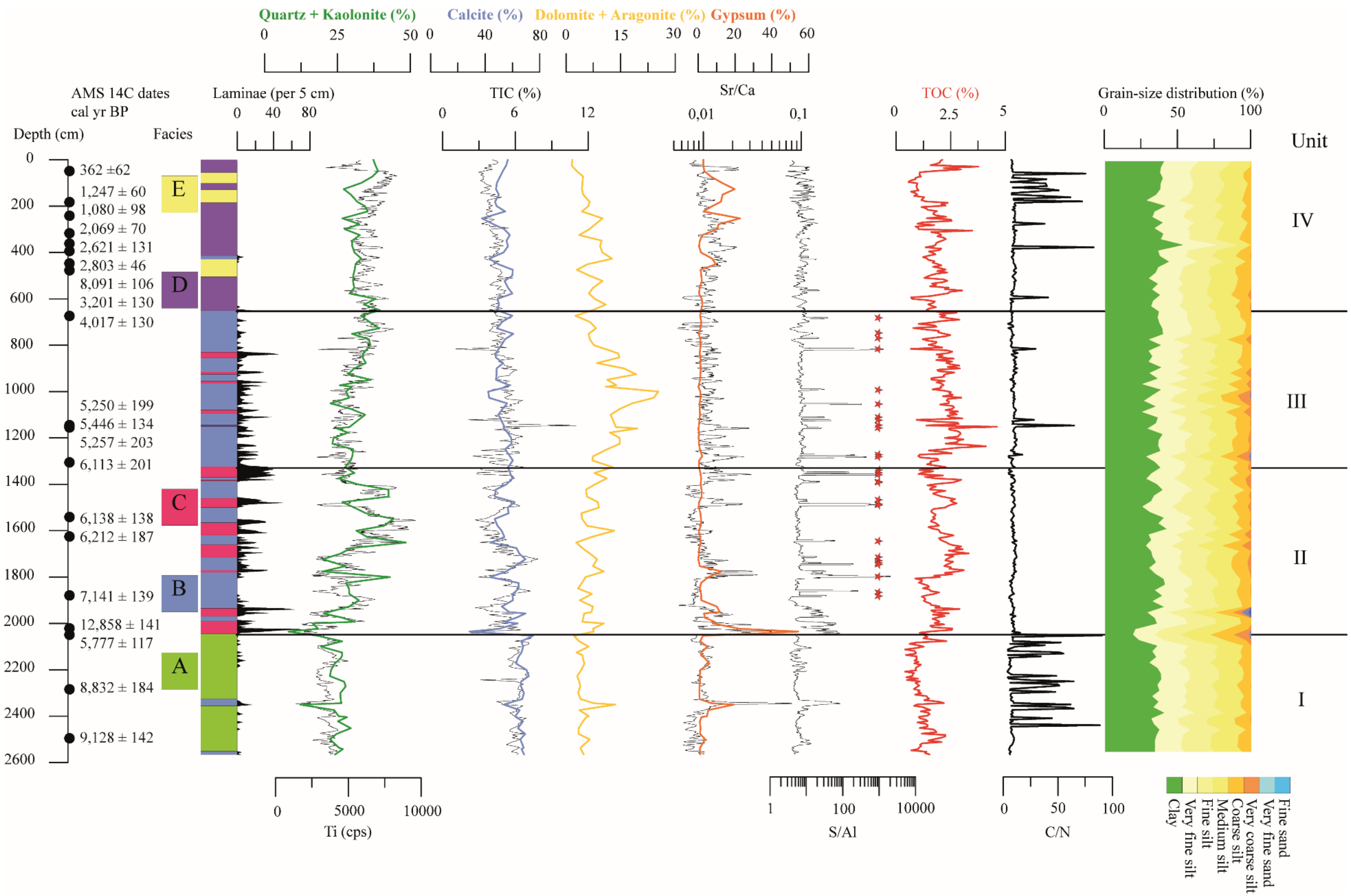

Figure 3.3. AMS data, sedimentary facies, laminae, units, geochemical, mineralogical, and granulometric proxies for core Co1313.

The mineralogical composition is dominated by calcite (50-70%), kaolinite (10-20%), and quartz (10-20%), and single layers with gypsum enrichments of up to 50 % (Fig. 3.3) which are also visible as light, coarse-grained bands by naked eye. Besides, dolomite, aragonite, pyrite, halite, muscovite, and some clay minerals occur in minor amounts.

The grain-size distribution of the clastic sediment components is dominated by silt (60-70 %) and clay (30-40 %). About 90 % of the grains fall within the fractions clay to medium silt (<16 µm). The grain-size distribution shows little fluctuations downcore (Fig. 3.3). The mean grain-size ranges between 3.0 and 11.4 µm, with only 2 outliers up to 13.1 and 15.8 µm, induced by the input of (fine) sand, only occurring in 20.50-19.50 m sediment depth (Fig. 3.3).

Variations in the magnetic susceptibility coincide with concentration changes of quartz, kaolinite, and the elements Titanium (Ti) Rubidium (Rb), Iron (Fe), Potassium (K), Aluminium (Al), and Silicon (Si), which all show an increased variability between 20.50-14.00 m (Figs. 3.3 and 3.5). The Sr/Ca ratio matches variations of gypsum in the lower core part very well, with highest variations in the laminated parts. Highest intensities are found in the laminated parts, as well as in the upper part of the record. S/Al has its own character, with maxima in the sulphur mottles (Fig. 3.2e), which only occur in lithofacies C and D (Fig. 3.3).

The total inorganic carbon (TIC) follows the same trend as calcite, decreasing towards the top of the record (Fig. 3.3). The total organic carbon (TOC) shows an increasing trend towards the top of the record (Fig. 3.3). The C/N ratio is high (>17) in several intervals until 20.50 m, stable and low (<7) until 6.00 m and again high (>15) and unstable towards the top of the record (Fig. 3.3).

The sediment record alternates between homogeneous and laminated sediments. The most remarkable shift occurs at 20.45 m, with the transition from massive homogeneous to laminated lithofacies, inducing an increase in complexity and variability of the sediment proxies (Fig. 3.3). Above 14.00 m, most of the proxies lose their variability and remain relatively stable towards the top, except for the minerals dolomite, aragonite and gypsum, as well as the C/N ratio. These proxies remain instable and vary towards the top of the record. The laminations disappear around 6.40 m, the sediments are now homogeneous and bioturbated.

Clustering of the geochemical and mineralogical proxies is strengthened by the outcome of the principal component analysis (PCA, Fig. 3.5). The first three components of the PCA of 111 samples explain 83.1 % of the total variance of the record. Negative loadings of PC1 are reflected by the minerals calcite, dolomite, aragonite and gypsum, the elements Ca, Sr and S, and the TIC. Positive loadings include the magnetic susceptibility (MS), the minerals quartz and kaolinite, and the elements Rb, Fe, Ti, K, Al and Si. Positive loadings of PC2 are reflected by the minerals gypsum, dolomite and aragonite and the elements S and Sr. Loadings clustered around zero contain the MS, the minerals quartz and kaolinite, and the elements Rb, Fe, Ti, K, Al and Si. Negative loadings are reflected by calcite, TIC, and Ca. Positive loadings of PC3 (not shown) are reflected by the contents of TOC and N.

3.5.2 Ecological proxies: Ostracods and Foraminifera

The ostracod record is continuous throughout the analysed samples (Fig. 3.4). In total, the fossil fauna holds 16 taxa (Tab. 3.1) that are known to be halotolerant species (Athersuch et al., 1989; Meisch, 2000; Mezquita et al., 2005; Rasouli et al., 2016).
Seven ostracod zones were identified by a constrained hierarchical cluster analysis of the relative abundance record.

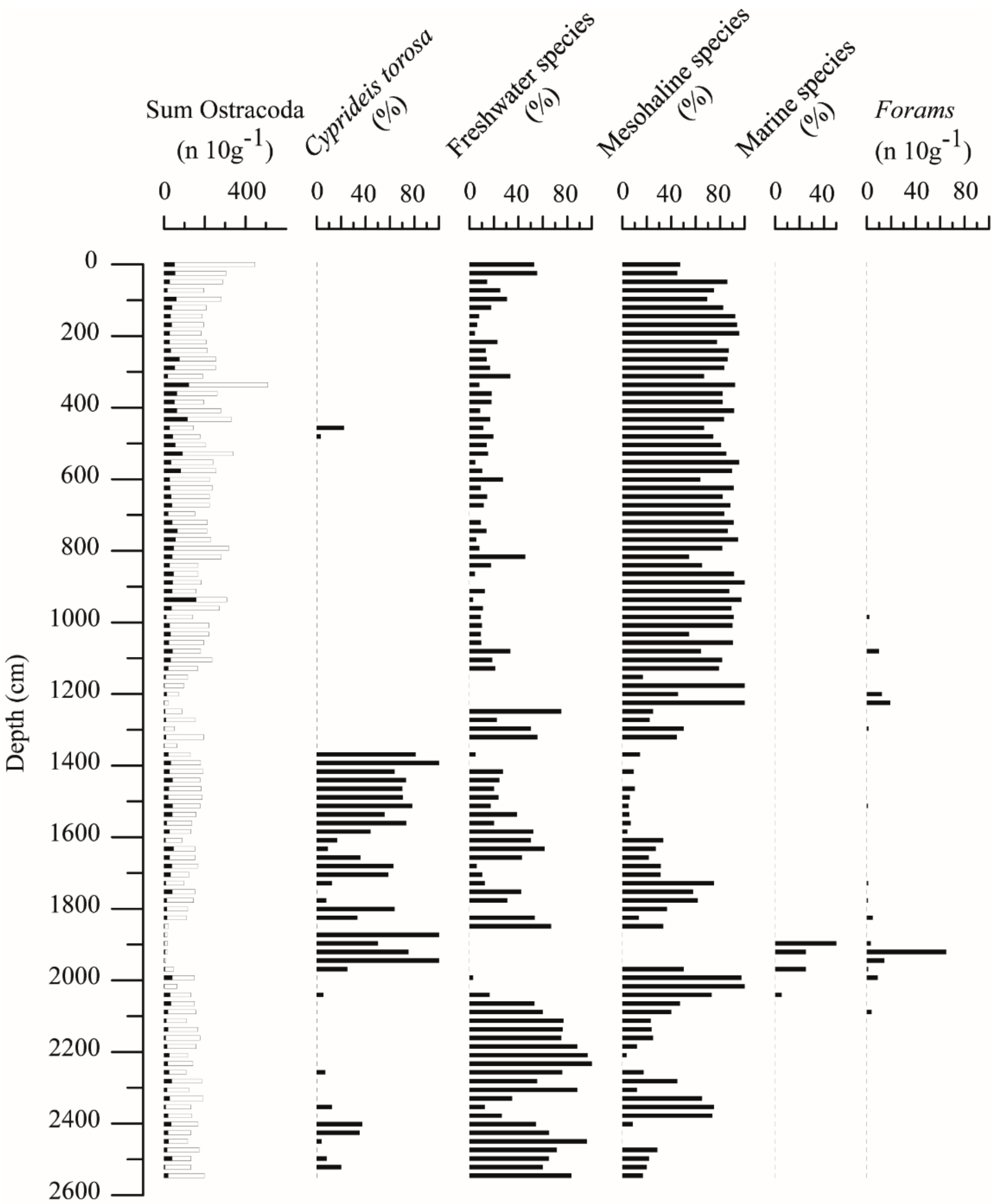

*Figure 3.4. Sum of total abundance of adult (filled bars) and juvenile (open bars) ostracods, and relative abundance of ostracod assemblages (*Cyprideis torosa*, freshwater species, mesohaline species, polyhaline species, and absolute abundance of Foraminifera [Forams]) for Laguna de Medina.*

The first ostracod zone (O1; bottom to 20.40 m) is characterised by a well-established freshwater fauna with some influence of mesohaline species. The following ostracod zone (O2; 20.40-19.44 m) is dominated by mesohaline species, especially *P. newtoni*. The third ostracod zone (O3; 19.44-18.48 m) holds polyhaline species incl. *C. torosa* and foraminifera species, i.e. *Ammonia beccarii.* The next zone (O4; 1848-1560 m) is a mix of freshwater species, here especially *Ilyocypris* sp., mesohaline species and the occurrence of polyhaline *C. torosa*. The succeeding species assemble of the adjacent zone (O5; 15.60-13.44 m) is dominated by *C. torosa*, which is accompanied by mainly freshwater species and minor abundance of mesohaline species. Then a sharp transition occurs in the following ostracod zone (O6; 13.44-12.24 m), as valves of *C. torosa* disappear and the species assemblage splits in freshwater, mesohaline waters and only few peaks of polyhaline species (i.e. *E. mareotica*). The top most zone (O7; 12.24 m to top) comprises a stable domination of valves of mesohaline species and successively fading of singular occurrence of polyhaline species (i.e. *E. mareotica*). *C. torosa* has a last occurrence between 4.80 and 4.56 m.

The occurrence of foraminifera tests is sporadic and restricted to samples of the lower part of the core. *Ammonia beccarii* (Linnaeus, 1758) was the only species found in our core samples.

Table 3.1. List of ostracod taxa in core Co1313 and previous study from Reed et al. (2001). The calculated optimum conductivity (optiCOND) as given in Mezquita et al. (2005) is used to classify species in freshwater (0-1.5 mS cm^{-1}), mesohaline (1.5-8.0 mS cm^{-1}) and polyhaline (>8.0 mS cm^{-1}) groups.

Taxa name	**Co1313**	**Reed et al. (2001)**	**optiCOND (mS cm^{-1})**	**Group**
Ostracods:				
Candona neglecta (Sars, 1887)	X	X	0.457	Freshwater
Cyprideis torosa (Jones, 1850)	X	X	31.623	Polyhaline
Cypris bispinosa (Lucas, 1849)	X		1.479	Freshwater
Darwinula stevensoni (Brady and Robertson, 1870)	X	X	1.230	Freshwater
Eucypris mareotica (Fischer, 1855)	X	X	48.978	Polyhaline
Eucypris pigra (Fischer, 1851)	X		0.676	Freshwater
Herpetocypris intermedia Kaufmann, 1900	X		0.891	Freshwater
Heterocypris incongruens (Ramdohr, 1808)	X		1.148	Freshwater
Heterocypris salina (Brady, 1868)	X	X	2.089	Mesohaline
Ilyocypris sp.1	X	X	1.023	Freshwater
Leptocythere sp.1	X		NA	Polyhaline
Limnocythere inopinata (Baird, 1843)	X		2.455	Mesohaline
Loxoconcha elliptica (Brady, 1868)	X		19.953	Polyhaline
Plesiocypridopsis newtoni (Brady and Robertson, 1870)	X	X	5.128	Mesohaline
Sarscypridopsis aculeata (Costa, 1847)	X		7.943	Mesohaline
Trajancypris clavata (Baird, 1838)	X		1.660	Mesohaline
Foraminifera: *Ammonia beccarii* (Linnaeus, 1758)	X	X	NA	

3.5.3 Chronology

The age-depth model for the Laguna de Medina is based on 20 ^{14}C dates, and provides a chronology for the last 9,600 years (Tab. 3.2). Except for three dates (UBA-32743, COL3423, and COL3291), the calibrated dates provide a systematic sequence of increasing age with increasing depth. The $\delta^{13}C$ values of the measured samples are in the range of -48.3 to -12.9 ‰, although most of the samples are within the range of -25 to -20 ‰, suggesting the organic material is from terrestrial origin (Meyers and Ishiwatari, 1993).

Table. 3.2. Results of AMS radiocarbon measurements conducted on the sediment record Co1313 from the Laguna de Medina

Lab sample no.	Depth (cm)	Age (yr) uncalibrated	± (yr)	Age (yr) calibrated	± (yr)	$\delta^{13}C$ (‰)
COL3288	48 – 50	287	44	362	62	-36.8
UBA-32745	183 – 185	1345	24	1247	60	-15.7
UBA-32746	242 – 244	1160	29	1080	98	-20.9
UBA-32747	317 – 319	2098	26	2069	70	-16.0
COL3412	360 – 364	2537	43	2621	131	-21.2
UBA-32748	394 – 396	2694	25	2803	46	-18.4
UBA-32743	447 – 449	7291	52	8091	106	-23.0
UBA-32744	477 – 479	2998	33	3201	130	-20.7
COL3413	672 – 676	3669	42	4017	130	-20.5
COL3414	1144 – 1146	4573	46	5250	199	-22.8
COL3415	1146 – 1151	4675	46	5446	134	-15.9
COL3416	1154 – 1156	4586	45	5257	203	-16.8
COL3417	1303 – 1307	5341	104	6113	201	-48.3
COL3419	1540 – 1542	5351	45	6138	138	-24.6
COL3420	1624 – 1626	5450	59	6212	187	-24.8
COL3421	1878 – 1880	6253	55	7141	139	-21.4
COL3423	2020 – 2022	10967	63	12858	141	-23.9
COL3291	2048 – 2050	5023	40	5777	117	-28.2
COL3425	2283 – 2285	8001	61	8832	184	-21.1
COL3427	2493 – 2497	8128	53	9128	142	-12.9

3.6 Discussion

3.6.1 Origin of allochthonous and autochthonous sediment components

The principal component analysis (PCA) shows clustering of elements, minerals, the magnetic susceptibility (MS), and geochemical data. The PCA can be defined into five sediment components, reflecting the sedimentation and the conditions of the lake from a desiccated or shallow lake towards a deep lake (Fig. 3.5). This typical sequence is found in many saline lakes on the Iberian Peninsula (e.g. Martín-Puertas et al., 2011).

The PC1 reflects the difference between in-lake sedimentation (endogenic components), as the gypsum, evaporite and carbonate component on the negative end, and allochthonous sedimentation, reflected by the terrestrial component on the positive end (Fig. 3.5). PC1 can be used as an indicator for changes in sediment supply. The endogenic components (gypsum, evaporite and carbonate) are indicative for (highly) concentrated shallow (or desiccated) environments, whereas high lake levels coincide with a terrestrial origin (Martín-Puertas et al., 2011). The terrestrial input is indicative for the presence of an active inlet (Renaut and Gierlowski-Kordesch, 2010). The Arroyo de Fuente Bermejo in the southeastern part of the lake is the main carrier of the terrestrial components (van ’t Hoff et al., 2017). However, a significant change in grain-size distribution is not noted during phases of increased terrestrial input, so the influence of wind can be neglected. The modern sedimentation patterns indicate the influence of coarse-grained sediments is limited to the first 200 m from the shore lines (van ’t Hoff et al., 2017).

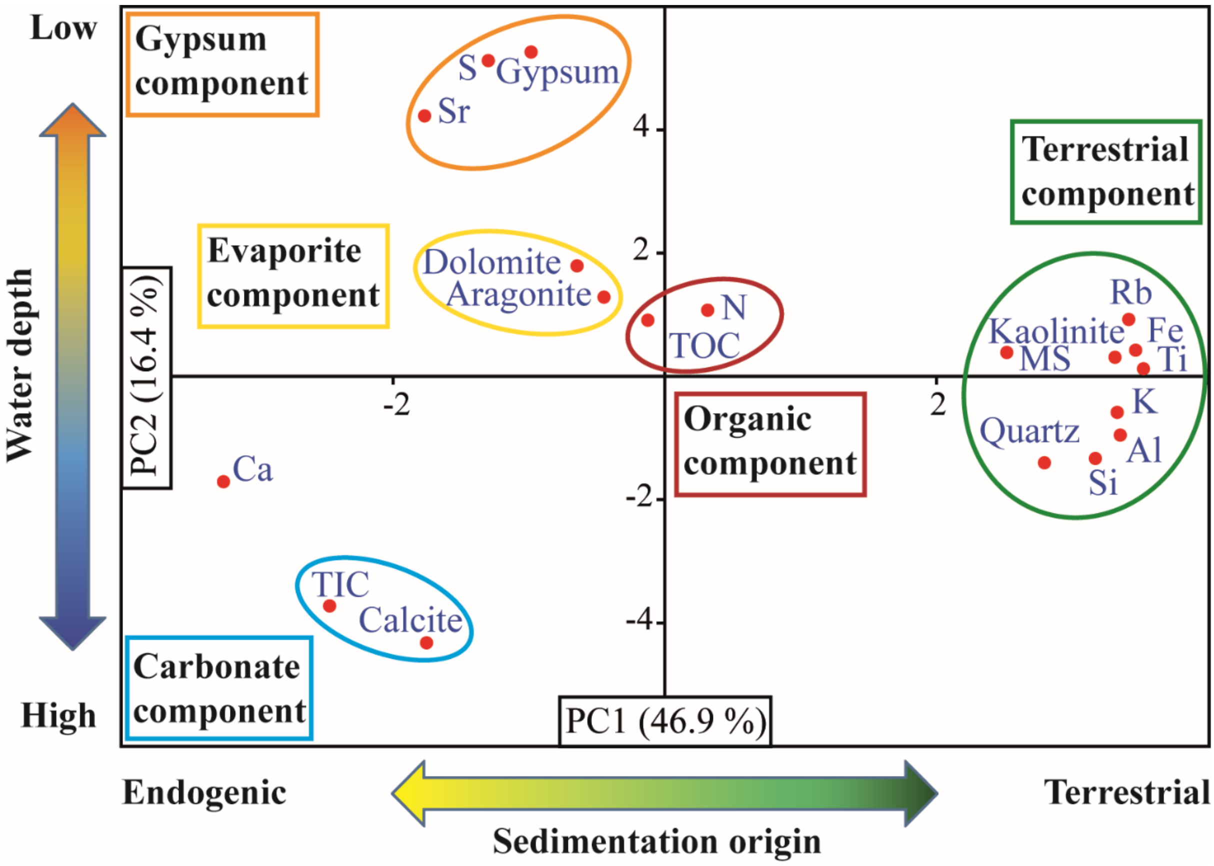

Figure 3.5. Outcome and interpretation of the PCA of the results of the geochemical, mineralogical data, and the magnetic susceptibility. The arrows indicate interpretation of the axes.

Shallow lakes have been featured by excessive natural fluctuations in water levels, driven by irregular precipitation patterns (Alvarez-Cobelas et al., 2005). This results in desiccation in arid years. The PC2 reflects these natural fluctuations from desiccation to the deep lake very well. This typical evaporitic sequence (Giralt and Juliá, 2003), due to evaporation and concentration processes, is clearly reflected in the Laguna de Medina. When the lake level decreases, carbonates, sulphates and chlorites are the main endogenic salts that precipitate (Eugster and Hardie, 1978). During a lake refilling phase, siliciclastic input and carbonate precipitation form the major mineral composition (Giralt et al., 1999).

1. The gypsum component reflects gypsum precipitation, which is enriched due to dissolution of the Triassic underground (IGME, 1984), and coincides with a shallow lake with highly saline conditions, or a desiccated lake with a gypsum crust (Stein et al., 1997). The high Sr intensities reinforces this assumption, since Sr exchanges with Ca in gypsum as salinity or evaporation increases (Santisteban et al., 2016).
2. During the first infilling phase, dissolution of the gypsum crust takes place, increasing the salinity. This favours precipitation of dolomite and aragonite (Vegas et al., 2010).
3. When the gypsum crust is entirely dissolved, and the input of fresh water continues, the lake is developing toward more fresh conditions, favouring precipitation of calcite as found in the carbonate component (Martín-Puertas et al., 2011).
4. During the lake level high-stand, the terrestrial component is sedimented, indicating an increase in lake surface, weathering of the Keuper facies in the catchment and higher alluvial input via the Arroyo de Fuente Bermejo (van 't Hoff et al., 2017).

PC3 reflects the organic component, and is identified by high values of N and TOC. The TOC concentration is highest during anoxic periods of lake level high stands, because of the good preservation of organic matter (Meyers and Lallier-Vergès, 1999).

The element Calcium (Ca) normally is a good indicator for the presence of carbonate, but Ca correlates very badly with both TIC and calcite (r^2 is 0.58 and 0.41 resp.), and plots in the PCA between the evaporite and endogenic carbonate component. This bad correlation indicates a more complex pattern with two different origins, namely gypsum ($CaSO_4 \cdot 2H_2O$) and carbonates (aragonite, calcite ($CaCO_3$), and dolomite ($CaMgCO_3$)).

Anoxic bottom conditions evidenced by native sulphur mottles

The S in the record are not only traced back to gypsum, but also partly of sulphur mottling. The sulphur mottling occurs in the laminated parts of the sediment record. The white spots pushes the laminated sediments away, and consists of diagenetic elemental sulphur (red stars in Fig. 3.3). Offsetting of the existing sediments by native sulphur is also found in Lake Lisan in Israel (Torfstein et al., 2008). Native sulphur is formed during anoxic periods due to bacterial sulphate reduction (BSR), in lakes with SO_4^{2-} concentrations >100 µM (Rudd et al., 1986; Ziegenbalg et al., 2010). Dissolution of gypsum by precipitation and the supply of dissolved gypsum via the ground water delivered SO_4^{2-} for microbial sulphate reduction. Organic matter is oxidized by sulphate-reducing bacteria, which leads to production of reduced sulphur species (Feely and Kulp, 1957). This happens in the lower water body of the stratified lake, or within the bottom sediments (Ziegenbalg et al., 2010). Highest concentrations of elemental sulphur were recovered in near-surface sediments (Urban et al., 1999). Therefore, it is likely the diagenetic sulphur spots in this core are formed close at the water-sediment surface, indicating anoxic bottom conditions during the deposition of facies B and C (Fig. 3.6).

Hydrogen sulphide is either abiologically or biologically oxidized to native sulphur, but the exact mechanisms are still unknown (Machel, 1992). In fact, in hypersaline lakes, accumulation of native sulphur was not detected yet in Holocene sequences (Ziegenbalg et al., 2010; Lindtke et al., 2011).

3.6.2 Genesis of the facies

The record of Laguna de Medina can be divided into four units (Fig. 3.3), mainly based on the alternation of the different lithofacies (Fig 3.6). Unit 1 is dominated by facies A, with some interruption of facies B. Unit 2 consists of an alternation of facies B and C, with a dominance of facies C. Unit 3 consists also of an alternation of facies B and C, here with a dominance of facies C. Unit 4 is characterized by an alternation of facies D and E.

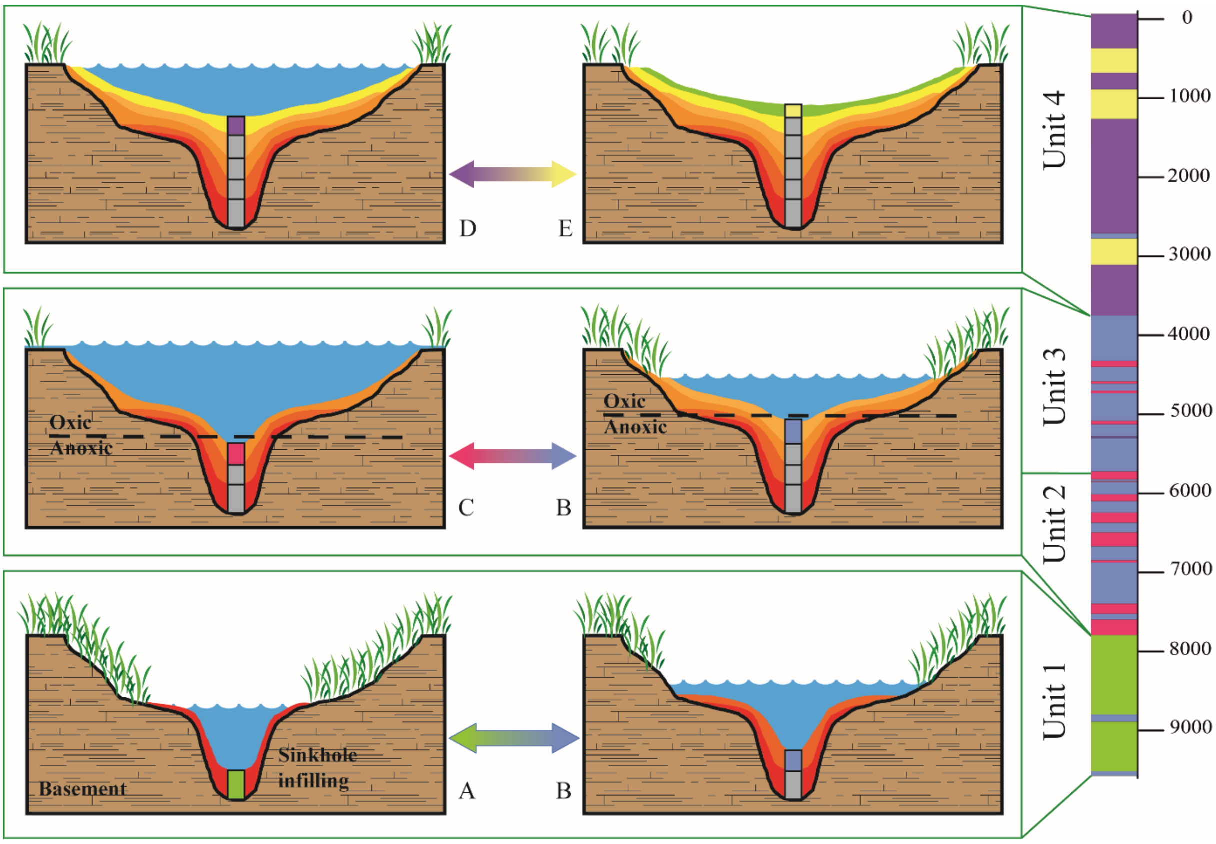

Figure 3.6. Basin Fill; Model of different stages of the Laguna de Medina during the deposition of the facies in the former sinkhole

Lithofacies A (Characterizing for Unit 1, Fig. 3.6) reflects a period of moderate heavily fluctuating water levels and salinity, indicated by the conductivity and the C/N ratio (Figs. 3.3 and 3. 8). Several peaks of high C/N ratios indicate pulses of terrestrial organic matter in a lacustrine environment (Meyers and Ishiwatari, 1993). The terrestrial component is high during phases of traces of small laminations, indicating enhanced fluvial supply from the Arroyo de Fuente Bermejo (van 't Hoff et al., 2017). However, generally, the terrestrial component is low, reflecting a low energy regime, little alluvial influence, and a relatively arid period (Valero-Garcés et al., 2014). The carbonate component is high in facies A, suggesting a relatively high water table with enhanced weathering of the adjacent marl- and limestones. However, the lack of lack of laminae suggest a moderate water table. The high carbonate content can also be the result of the instable period after the collapse of the sinkhole, and reflecting a change in ground water regime and enhanced erosion due to a change in the hydrological setting. However, it is not exactly known when the sinkhole collapsed, so this hypothesis cannot be tested.
Facies B (dominant in Unit 3, Fig. 3.6) reflects a relatively humid period with a fluctuating, and relatively high salinity (Fig. 3.8). The fluctuating behaviour of the lake level is reflected by the alternation of deposition of massive clayey silts during shallower phases and laminations during deeper phases (Valero-Garcés et al., 2014). The terrestrial component is moderate, reflecting moderate fluvial input during a period with relatively low precipitation. The evaporite component is highest in this facies,

representing a period of moderate lake levels and relatively high salinity. The diagenic sulphur mottles indicate anoxic bottom conditions (Ziegenbalg et al., 2010).

Facies C (mainly present in Unit 2, Fig. 3.6) represents a humid period with the maximum lake level, high salinity with anoxic bottom conditions (Ziegenbalg et al., 2010), characterized by the occurrence of finely laminated sediments (Valero-Garcés et al., 2014) (Fig. 3.8). The occurrence of *Loxoconcha elliptica*, *Leptocythere sp*. and even foraminifera confirm a high salinity. TOC is highest during this period, probably due to the high water level, and the anoxic bottom water conditions, preserving the organic matter (Meyers and Lallier-Vergès, 1999; Ziegenbalg et al., 2010). Here, the terrestrial component is highest, indicating enhanced fluvial supply from the Arroyo de Fuente Bermejo due to enhanced precipitation, and a high lake level (Valero-Garcés et al., 2014; van ’t Hoff et al., 2017). The carbonate component is relatively high, although lower than in facies A, probably due to the predominant influence of the terrestrial components. In general, the gypsum component is low, with the exception of some peaks, which indicate desiccation events, or highly concentrated waters (Martín-Puertas et al., 2011). The high lake level disables the precipitation of gypsum, despite the high salinity (Torfstein et al., 2008).

In other Spanish lakes, like Lake Arreo (Corella et al., 2013) and Lake Zoñar (Martin-Puertas et al., 2008; 2011), changes between stratified and mixed waters are reflected by the alternation of massive and laminated facies. This fluctuating water level is clearly show in the alternation of facies B and C in Unit 2 and 3. Stratification and the occurrence of anoxic conditions is mainly controlled by the water depth (Wetzel, 2001). Stratification is limited by a minimum water depth of 6 m (Shaw et al., 2002). Both facies B and C are characteristic for a deep-water phase, although fluctuating (Fig. 3.6 Unit 2 and 3).

Facies D, reflects an arid period with shallow lake levels, indicated by traces of bioturbation, especially of roots (Valero-Garcés et al., 2014). The gypsum component is relatively low, probably because of dissolution of the gypsum crust during infilling of the lake after desiccation. This also explains the relatively high evaporite component in comparison with the gypsum component. Carbonate and terrestrial component increase, indicating periods of filling after desiccation. The C/N ratio is low, indicating a lacustrine origin of the organic matter (Meyers and Ishiwatari, 1993).

Facies E reflects an arid period with very shallow waters, and periods of desiccation. The carbonate and evaporite mottling, and bioturbation are indicators for desiccation (Valero-Garcés et al., 2014). The gypsum component is relatively high, suggesting periods of aerial exposure and gypsum precipitation. The evaporite component is low during these phases, indicating no phases of infilling. The calcite content is decreasing towards the top, reflecting a decreasing water level. The high C/N peaks reinforces this statement, indicating enhanced terrestrial organic influence (Meyers and Ishiwatari, 1993). The terrestrial component is low, indicating a low energy regime and little alluvial input (Valero-Garcés et al., 2014). The Arroyo de Fuente Bermejo is presumably dry during these arid periods.

3.6.3 Age model

In southern Spain, most of the lakes are shallow saline water bodies (<0.50 m), which are characterized by excessive natural fluctuations in water levels, driven by the five months summer water deficit and the irregular precipitation patterns of the Mediterranean climate (Alvarez-Cobelas et al., 2005; Peel et al., 2007). This results in desiccation in arid years, leading to hiatuses and preservation problems for organic matter. Organic material may even be absent in shallow lakes with annual desiccation events, such as the Laguna de Salada (Cádiz; Chapter 4) and Laguna Salada (Campillos; Schröder et al., 2017). Laguna de Medina only dries out in exceptionally arid years, leading to relatively good preservation of organic matter. This allowed to radiocarbon date the material of terrestrial origin, thereby bypassing the hard water effect. Furthermore, previous studies faced difficulties with radiocarbon dating of bulk organic material in carbonate-rich areas, because of the hard water effect (e.g. Höbig et al., 2016).

The results of the age model suggest that most of the ^{14}C ages are reliable (Fig. 3.7). However, the resulting age/depth succession is bracketed by a few ^{14}C ages, which obviously are erroneous. This includes the ^{14}C dates of samples UBA-32746 (242-244 cm depth), and COL3291 (2048-2050 cm), which obviously are too young, in the order of 100 and 2000 years, respectively. The small errors of UBA-32746 may for instance be due to bioturbation or penetration of younger roots into older sediments (Kaland et al., 1984). The larger error of COL3291 might be due to contamination of younger bacteria or humic acids, because the piece of wood was not bleached properly during the preparation (Kaland et al., 1984). Too old ages are found in the samples UBA-32743 (447-449 cm), COL3417 (1303-1307 cm), and COL3423 (2020-2022 cm), in the order of 5000, 100 and 5000 years, respectively. A too low carbon content (280 µm) in sample COL3417 could explain the small error. The larger errors might represent the input of reworked organic material from older sediments outside the lake during periods of increased catchment erosion (Nambudiri et al., 1980; MacDonald et al., 1991).

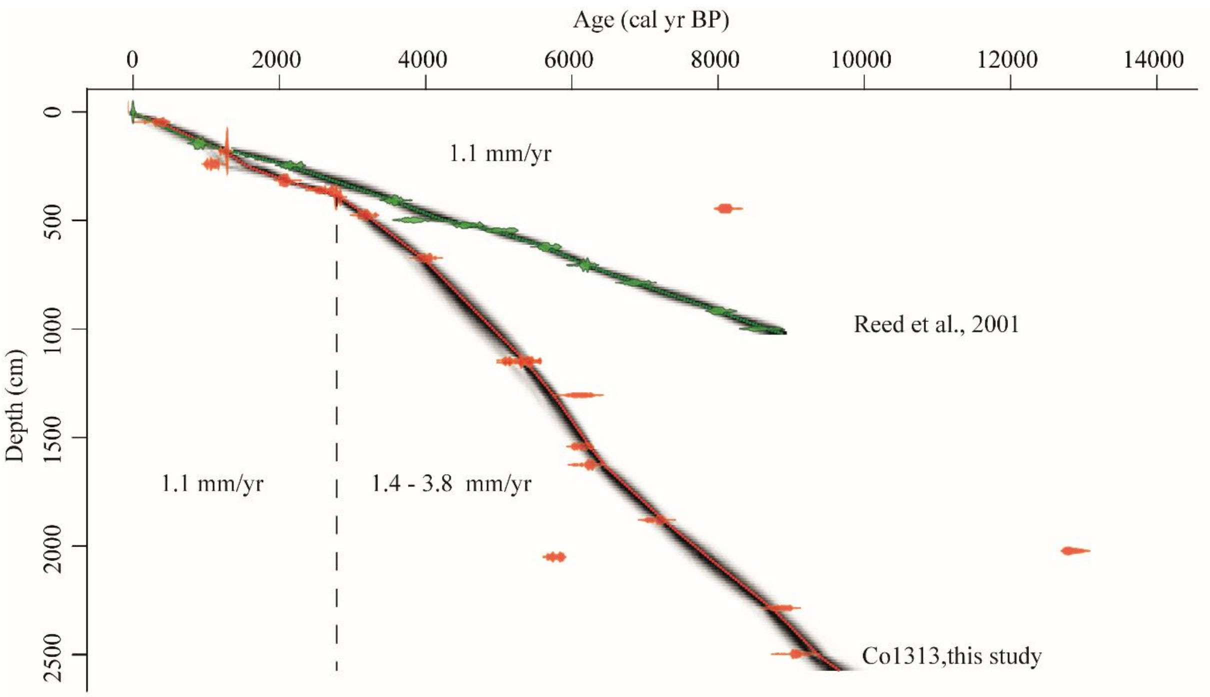

Figure 3.7. Age-depth model for Laguna de Medina. The orange ages represent this study, the green ages reflect the ages by Reed et al., 2001.

3.7 Interpretation

3.7.1 Comparison with the Reed et al. (2001) record from Laguna de Medina

This high-resolution record from the Laguna de Medina is not the first sediment core retrieved from this lake. Former studies (Reed et al., 2001; Roberts et al., 2008) were focused on the palaeoecological changes based on diatoms, pollen and ostracods, and $\delta^{18}O$ of ostracods, and covers the last 9,000 years. Although retrieved from the same lake, the core Co1313 and the core of Reed et al. (2001) show some remarkable differences. Most striking feature between the two sediment records is the difference in sedimentation rate. The Reed record is 10 m long, covers the last 9,000 year, and has a constant sedimentation rate of 1.1 mm/yr. This in contrast to our core, which is 25.65 m long, and includes the last 9,600 years with sedimentation rates varying between 1.1-3.8 mm/yr. The sequence until 2,820 cal yr BP has the highest sedimentation rate (3.8 mm/yr). The modern sedimentation rate is around 1.1 mm/yr (Fig. 3.7).
According to Reed et al. (2001), the lake has always been relatively shallow. However, sedimentological features in our record, as the facies, the laminations, and the sulphur mottles suggest periods of a deep lake with anoxic bottom water conditions (Shaw et al., 2002; Ziegenbalg et al., 2010). A possible solution for this discrepancy can be found in the genesis of the lake (Fig. 3.6), whose origin was controlled by karstic processes (Durán Valsero et al., 2009), leading to a funnel-shaped sinkhole with steep margins (Palmquist, 1979). Steep-sided lakes are beneficial to stratification, contributing to a dynamic depositional environment with abrupt changes in geochemical and limnological factors, e.g. oxic/anoxic conditions at the lake bottom (Renaut and Gierlowski-Kordesch, 2010).
In lakes with such a hyperboloid morphology (Lehman, 1975), sediment from the littoral zone is redeposited in the deeper basin of the lake (Davis, 1968; 1973). Probably, the Reed core was retrieved from the margin of the lake, and our core was taken inside of the steep walls of the sinkhole, explaining the high sedimentation rate in Co1313 in contrast to the low sedimentation rate of the Reed core.
In the margins, the sediments are more often exposed to the air, which could cause hiatuses, enhanced gypsum precipitation, and bad preservation of organic matter (Meyers and Lallier-Vergès, 1999; Martin-Puertas et a., 2008; Valero-Garcés et al., 2014). In the Reed core, the gypsum content fluctuated between 40-90 %, this in contrast to our record, where the gypsum varies between 0-20 %, with only one exception to 50 % (Fig. 3.8). The aerial exposure during lower lake levels in the margins, also explains the variances in preservation and quality of the pollen and diatoms. In the Reed core, the upper 5 m do not contain any diatoms and in the lower 5 m, the diatoms are poorly preserved. The pollen are badly preserved in the entire record. This in contrast to the excellent preservation of the diatoms (H. Vossel, pers. comm. 2016) and pollen (T. Schröder, pers. comm. 2017) in Co1313.
Although retrieved from different sites in the lake, the two cores show some striking similarities. The salinity, based on the ostracod assemblages (Mezquita et al., 2005), follows the same trend, showing two peaks around 7,400 and 6,000 cal yr BP (Fig. 3.8). The highest salinity coincides with the maximum lake level. This paradox is found in the Reed core as well, which might be explained by a change in ground water regime or due to redissolution of gypsum in the catchment. The coherence between the salinity and Ti between 7,870-5,780 cal yr BP suggests enhanced catchment erosion, which increases the input of dissolved salts, and gypsum into the lake. The high water table avoids gypsum precipitation, which only takes place during desiccation events. In the Reed core, highest gypsum concentrations are found during this period, reinforcing the hypothesis this core was retrieved from the margins, which are much more sensitive to small lake level fluctuations.
The sedimentation rates of the two cores vary widely between 9,600-2,820 cal yr BP. Co1313 has a fluctuating sedimentation rate between 2.9-3.5 mm/yr. The Reed core has a stable sedimentation rate of 1.1 mm/yr. From about 2,820 cal yr BP, both of the age models merge and have a relative stable sedimentation rate of 1.1 mm/yr towards the top (Fig. 3.7). This suggest, from 2,820 cal yr BP on, the sinkhole is completely filled up and the morphology of the lake is more or less equal in both coring sites (Lehman, 1975).

3.7.2 Long-term palaeoclimate reconstruction / Long-term depositional history

The differences in ages between the two records from Laguna de Medina indicate the lake was not always as shallow as it is nowadays (Figs. 3.7). The geochemical proxies and the lithofacies confirm this hypothesis (Figs. 3.6 and 3.8). Four main limnological units are identified based on shifts in the lithofacies, and the mineralogical, elemental, and ecological (ostracods) proxies (Fig. 3.8).

Unit 1: Dry and warm Early Holocene (9,590 – 7,870 cal yr BP)
Unit 1 reflects the period just after the sinkhole formation, the lake was a deep hole with steep margins, and functioned as a new water basin for the precipitation in the catchment. Unit 1 represents a phase of moderate waters with rapid fluctuations in salinity, as indicated by the freshwater and mesohaline ostracod assemblages- The lake level is relatively low, as indicated by the peaks in C/N ratio, which suggest an alternation between lacustrine and terrestrial origin of the organic matter (Meyers, 1997). The period is interrupted by one desiccation event around 8,870 cal yr BP, as evidenced by gypsum precipitation. The rapid changes in salinity are indicated by the alternation of the ostracod species *Plesiocypridopsis newtoni*, *Cyprideis torosa*, *Darwinula stevensoni* and *Ilyocypris sp*.
On the southern IP, the Early Holocene (prior to 8,000 cal yr BP) is a warm period with arid conditions, associated with an increase in xerophytic, and steppe vegetation (Pantaléon-Cano et al., 2003: Fletcher et al., 2007; Schneider et al., 2016), and a drop in lake level (Carrión, 2002; Morellón et al., 2008) (Fig. 3.8). The Alboran Sea has a relatively low SST, causing arid conditions on land because of the low evaporation quotient (Cacho et al., 2002). Several desiccation events are recognized during this period in the Mediterranean region, although the timing is not synchronous, for example in Lake Siles two desiccation events at 9,300 and 8,400 cal years BP occurred.

Unit 2: Maximum lake level during the Holocene Climate Optimum (7,870 – 5,780 cal yr BP)
The start of unit 2 is marked by a strong desiccation event around 7,970 cal yr BP, denoted by gypsum precipitation, as well as the onset the laminated sediments. Unit 2 reflects a humid period, with increased precipitation, as reflected by the increased terrestrial components (Fig. 3.8). The dominance of facies B and C indicate the maximum water level >6 m (Shaw et al., 2002). Diagenetic sulphur spots reinforce this argument, indicating anoxic bottom water conditions (Ziegenbalg et al., 2010). Unit 2 is characterized by a remarkable shift in ostracod assemblages towards more saline conditions, indicated by an increase in *Cyprideis torosa*, and the occurrence of *Loxoconcha elliptica*, *Leptocythere sp*. and even foraminifera. Paradoxically, this period represents the maximum lake level and the highest salinity. Reed et al. (2001) found this paradox as well, which can either be explained by a change in ground water influx, or by redissolution of gypsum and salts in the catchment (see Chapter 3.7.1).
During this period, the sinkhole is rapidly filled up with sediments, with a sedimentation rate of 3.5 mm/yr. In comparison with other lakes, e.g. Lake Zonar (1.50 mm/yr), Lake Siles (0.08 mm/yr), Laguna de Fuente de Piedra (0.50 mm/yr), and Sierra de Gádor (0.37 mm/yr), the sedimentation rate is extremely high in this unit (Carrion, 2002; Carrión et al., 2003; Martín-Puertas et al., 2008; Corella et al., 2011; Höbig et al., 2016). Such high sedimentation rates are normally found in estuarine environments after the rapid sea level rise, e.g. in the Guadiana estuary in Portugal (Fletcher et al., 2007). The high sedimentation rate is caused by the hyperboloid form of the lake, removing sediment from the littoral zone to the deepest part of the lake (Davis, 1968; 1973; Lehman, 1975).
In the Spain, roughly the period between 8,000-5,500 is a humid period, reflecting the Holocene Climate Optimum (Fletcher and Zielhofer, 2013). For the core in the margin of Laguna de Medina, Reed et al. (2001) found the highest lake levels between 6,320-4,800 cal yr BP based on diatoms, Roberts et al. (2008) found a maximum lake level 8,000-6,700 cal yr BP based on stable isotopes. In the Segura Mountains in southern Spain, between 7,420-5,300 cal yr BP, a period with increased summer droughts and a warm and wet climate is found (Carrión et al., 2010). In the pollen sequences, an increase in mesophytic species (Fig. 3.8) is found in Lake Siles (S Spain) and Cañada de la Santa Cruz (S Spain) (Carrión et al., 2001b; Carrión, 2002). Interestingly, the new sediment record from Lake Sidi Ali (Morocco) is characterized by a long-term lake level low stand from 6,600-5,400 cal yr BP, probably induced by a decrease in winter rain (Zielhofer et al., 2016).

Unit 3: Lake level shallowing, transition towards more arid conditions (5,780 – 3,750 cal yr BP)
Unit 3 reflects a period of relatively high lake level >6 m (Shaw et al., 2002), although lower than Unit 2, indicated by the dominant occurrence of facies B. The salinity dropped and fluctuates, *Cyprideis torosa* disappears. The aragonite, and dolomite concentrations are high, indicating shallower, and brackish water. However, the bottom water conditions are still temporarily anoxic, as approved by the occurrence of diagenetic sulphur spots (Ziegenbalg et al., 2010).
During this period, the sinkhole is continuously filled up with a sedimentation rate of 3.2 mm/yr, changing the bathymetry of the lake from a lake with steep sides towards a shallow lake.
In Spain, many lakes show a drop in lake level from about 5,500 cal yr BP. In de Sierra de Gádor (SE Spain), maximum lake levels are found (based on pollen) until 5,500 or (based on lacustrine evidences) until 5,900 cal yr BP (Carrión et al., 2003). In Lake Siles (S Spain), the maximum lake level is found until 5,400 cal yr BP (Carrión, 2002), and in San Rafael (SE Spain) until 5,500 cal yr BP (Yll et al., 1994). Palynological records from the Algarve coast (S Portugal) show an aridification and a trend towards more xerophytic species from 5,000 cal yr BP on (Schneider et al., 2016). The drop in lake level is initiated by an aridification trend due to a change towards more positive NAO values (Olsen et al. 2012). In the Sahara, the African Humid Period ended around 5,500-5,000, resulting in increasing aeolian sediment transport, suggesting an aridification (Swezey, 2001; deMenocal et al., 2000; Bard, 2013).

Unit 4: Dry and warm Late Holocene with increased aridification and desiccation (3,750 cal yr BP – today)
Unit 4 reflects a shallow lake, with periods of desiccation, as indicated by the evaporite mottles in facies E (Valero-Garcés et al., 2014). This Unit starts with the disappearance of the laminations and the diagenetic sulphur spots. The ostracods suggest a mesohaline lake (Fig. 3.8).
Many lakes in Spain have indications for several periods of desiccation, although not synchronous, e.g. Lake Siles (S Spain) and Lake Zoñar (S Spain) (Carrion, 2002; Martín-Puertas et al., 2008). Lake Estanya (N Spain) has an almost continuous low lake level (Morellón et al., 2008, 2011), and pollen from Lake Siles, the Sierra Gádor, Villaverde and San Rafeal (all S Spain) indicate xerophytic species (Yll et al., 1994; Carrión, 2002; Carrión et al., 2001a; 2003; Pantaléon-Cano et al., 2003). Microcharcoal, related to an enhanced fire regime due to droughts, is increased in Lake Siles and Cañada de la Cruz (both S Spain) (Carrión et al., 2001; Carrión, 2002).

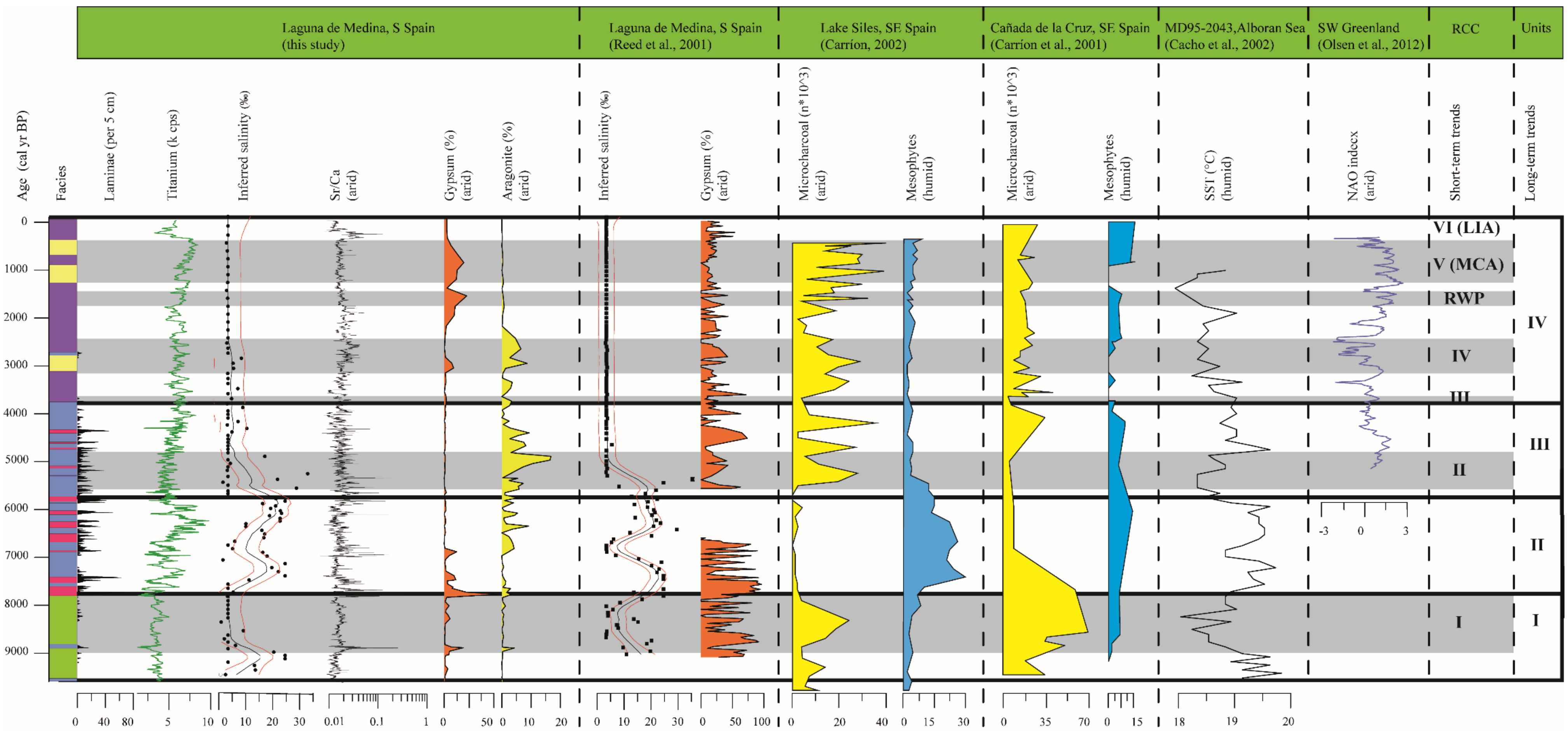

Figure 3.8. Overview of the arid and humid phases in Laguna de Medina, compared with the former record of Laguna de Medina (Reed et al., 2001), Lake Siles (Carrión, 2002), Cañada de la Santa Cruz (Carrión et al., 2001b), marine core MD95-2043 (Cacho et al., 2002, and the NAO index (Olsen et al., 2012). Grey bars indicate arid periods.

3.7.3 Short-term climate events: Rapid Climate Change

Research of the Holocene palaeoclimate based on glacier investigations by Denton and Karlén (1973) indicated six periods of rapid climate change (RCC): 9,000–8,000, 6,000–5,000, 4,200–3,800, 3,500–2,500, 1,200–1,000, and 600–150 cal years BP (Mayewski et al., 2004). In the Western Mediterranean region, three RCC´s are predominantly recognized, 6,000-5,000, 3,500–2,500, and 600–150 (Fletcher and Zielhofer, 2013). Generally, the RCC´s resulted in an aridification, characterized by a lake level drop, a change to more arid-tolerant vegetation, and an enhanced fire regime (Carrion, 2002; Fletcher et al., 2007; Morales-Molino et al., 2013), at the timing of a SST cooling in the Western Mediterranean Sea (e.g. MD95-2043; Cacho et al., 2002). Only the last RCC, at the timing of the LIA, is reflected by an increase in humidity. In Laguna de Medina, most of the known Holocene RCC´s are found in the record (Fig. 3.8, grey bars).

Interestingly, well-known climate events as the 8.2, 6.4, and 4.2 ka events are not recognizable in the sediment record. These events, coinciding with the Bond events, are best recognizable in the North Atlantic region (Bond et al., 1997), although also recognized in Spain. Reed et al. (2001) did found a trend towards more desiccation around 7,985 cal yr BP, and linked this to the 8.2 event. However, in our record, this period is characterized by a change towards more humid conditions. The reason these events were not found in our record is still unclear. Presumably, the lake was too deep and stable during these periods, or the deep channel was not sensible enough for these changes.

Other small events were found in the Medina record. There are desiccation events of gypsum precipitation and high salinity at 7,770, 7,660, 7,500, 6,920, 6,870, 6,070, 5,820, and 5,800 cal yr BP, as indicated by the Sr/Ca peaks (Martín-Puertas et al., 2010).

RCC I (9,160-7,870 cal yr BP)

From 9,160-7,870 cal yr BP, repeated pulses of terrestrial organic matter reach the lake, characterizing a low lake level due to an arid period (Meyers and Ishiwatari, 1993). One desiccation event occurred 8,890-8,830 cal yr BP. Arid period I coincides with the RCC 9,000-8,000 cal yr BP. Although not jet convincingly found in the Western Mediterranean, in other regions this is a severe event. In the high latitudes, this cooling event led to an increase in glaciers, enhanced ice-rafting and strengthened atmospheric circulation (Mayewski et al., 2004). Whereas in the low latitudes, this event resulted in a period of aridification, e.g. in Africa, where this event resulted low lake levels or desiccation (deMenocal et al., 2000; Gasse, 2000). This RCC coincides with an increase in microcharcoal in Lake Siles and Cañada de la Cruz (Fig. 3.8) on the IP (Carrión et al., 2001b; Carrión, 2002). A drop in the sea surface temperature (SST) is found in the Alboran Sea, resulting in less evapotranspiration leading to arid condition on the IP (Cacho et al., 2002).

RCC II (5,780-4,800 cal yr BP)

This RCC is one of the abrupt climate changes, which is best recognized in the Western Mediterranean region (Fletcher and Zielhofer, 2013). It is indicated by the ´cool poles, dry tropics´ pattern, and features ice-rafting in the North Atlantic Ocean (Bond et al., 1997; Mayewski et al., 2004).

In Laguna de Medina, RCC II (5,780-4,800 cal yr BP) initiates the end of the maximum lake level, although the lake level was still relatively high after 5,780 cal yr BP. RCC II resulted in the short-term disappearance of fresh water ostracods. Four desiccation events are recognizable based on the Sr/Ca ratio at 5,800 5,630, 5,520, and 5,320 cal yr BP (Fig. 3.8).

During this RCC, foraminifera are found between 6,130-4,800 cal yr BP, indicating a highly saline lake. The aragonite concentration is highest during this period, reflecting a concentrated brine due to enhanced evaporation (Pérez et al., 2002).

In the Alboran Sea, a drop in SST resulted in a reduction of evaporation, which initiated an aridification on land (Cacho et al., 2002). In other regions in the Western Mediterranean, the aridification resulted in a drop of lake level, e.g. desiccation of Lake Siles (Carrión, 2002). In Lake Estanya, this resulted in the onset towards a long-term drier hydrological regime (Morellón et al., 2011). This RCC event initiated the end of the African Humid Period, changing the Saharan desert from a greenly vegetated environment to a hyperarid desert (Fontes et al., 1985; deMenocal et al., 2000; Gasse, 2000), and initiates the onset to long-term aridification signals over the southern IP (Carrión et al., 2010).

RCC III (around 3,750 cal yr BP)
Evidence for the RCC event between 4,200-3,800 cal yr BP is scarce, especially on the IP (Mayewski et al., 2004). Also in Laguna de Medina, this event is not convincing. It is although very likely, RCC III initiated the transition from the deep water facies B and C towards more drier conditions with the occurrence of the low water facies D and E around 3,750 cal yr BP. The onset in Laguna de Medina coincides with a high NAO phase, resulting in more aridity (Olsen et al., 2012).
In Europe, the effects on glaciers are weak, in comparison with North America (Mayewski et al., 2004), but in Africa, enhanced drier conditions are found (Gasse, 2000).

RCC IV (3,150-2,420 cal yr BP)
The aridification effects of RCC IV (3,150-2,420 cal yr BP) are good recognizable on the IP. Pollen records show a decline in forests, indicating a phase of drier, and cooler conditions (Combourieu Nebout et al., 2009; Fletcher and Sánchez Goñi, 2008), or even a trend towards more xerophytic species (Fletcher et al., 2007). In Laguna de Medina, this event is clearly recognizable in the facies, with the transition towards facies E, indicating desiccation, and the increase in gypsum and aragonite between 3,150-2,420 cal yr BP, reflecting aridification. In Lake Siles, an increase in microcharcoal and a desiccation phase was found between 3,500-2,700 cal yr BP (Carrion, 2002). Lake desiccation or a significant drop in lake level is also found in other lakes on the IP, e.g. in Lake Zoñar, Laguna de Gallocanta, and in the Sierra de Gador (Pérez et al., 2002; Martín-Puertas et al., 2008; Jiménez-Moreno and Anderson, 2012).

Roman Warm Period (1,950-1,450 cal yr BP).
The short arid period occurring 1,950-1,470 cal yr BP coincides with the Roman Warm Period (RWP). This arid period is the warmest period in the last 2,000 years. It is characterized by an increase in xerophytic vegetation and a drop in lake level (Corella et al., 2011; Moreno, et al., 2012). In Laguna de Medina, this period is reflected by the gypsum peak, coinciding with a positive NAO phase (Olsen et al., 2012).
This period is characterized by a high input of Saharan dust, and minor fluvial input in the Algerian-Balearic basin (Nieto-Moreno et al., 2011). In la Basa de la Mora, an increase in *poaceae* is indicative for the aridification during the RWP (Moreno et al., 2012).

RCC V + Medieval Climate Anomaly (1,264-550 cal yr BP)
This northern European humid RCC coincides with a predominantly positive NOA phase (Olsen et al., 2012), which results in aridification on the IP (Wanner et al., 2001; Trigo et al., 2004). This period is directly followed by a large hydrological change representing the Medieval Climate Anomaly (MCA) from 1,050-650 cal yr BP (Moreno, et al., 2012).
In Laguna de Medina, it is hard to distinguish the transition between these two arid periods, therefore they are described as one period. This arid period is reflected by the occurrence of facies E, an increase in gypsum and aragonite, and the peaks in C/N ratio between 1,264-550 cal yr BP. The timing of this event is almost synchronous with aridification features in Lake Zoñar, where aridity was found from 1,350–730 cal yr BP (Martín-Puertas et al., 2008).
Lower lake levels are also found in northern Spain, in Lake Arreo from 1,060-650 cal yr BP (Corella et al., 2013), Estanya Lake from 800-650 cal yr BP (Morellón et al., 2011), Lake Montcortés from 1,260-490 cal yr BP (Corella et al., 2011), and in Central Spain in Laguna de Taravilla, where the lack of a good age model difficult the timing (Valero Garcés et al., 2008). An increase in microcharcoal is found in Lake Siles, reflecting arid periods with an enhanced fire regime (Carrión, 2002).

RCC VI (600-150 cal yr BP Little Ice Age)

Subsequently to the MCA, the Little Ice Age (LIA) started. This RCC is the only one that deviates from the ´cool poles, dry tropics´ RCC´s. This one is indicated by ´cool poles, wet tropics´ (Mayewski et al., 2004). The northern regions suffer a temperature drop of 1-3° C (Sousa et al., 2006). Generally, the LIA, which induces increased precipitation on the IP, occurred between 650-100 cal yr BP (Moreno et al., 2012). However, the in the Mediterranean region, the LIA is divided in three main humid periods: 380-320, 170-150, and 120-80 cal yr BP (Sousa and García-Murillo, 2003).

In the record of Laguna de Medina, the period after the MCA stays arid with some interruptions of more humid phases. Generally, the period between 600-150 cal yr BP coincides with a humid period. The LIA starts at 550 cal yr BP. Three humid periods occur around 542-457, 362-324, and after 170 cal yr BP. After 170 cal yr BP, it is hard to interpret the proxy data, because the core is extremely water saturated, and the XRF data are influenced by the water content, and therefore not reliable. The second humid phase in Laguna de Medina coincides perfectly with the first humid phases noticed in southern Spanish archives. Both of them occur during negative NAO phases, which resulted in increased precipitation (Trigo et al., 2004; Olsen et al., 2012).

3.8 Conclusions

The sediment core Co1313 was retrieved from the deepest part of the Laguna de Medina, in the former sinkhole. This gave the opportunity to analyse a high-resolution sediment record, which covers the last 9,600 years. Supported by the PCA, which shows the differences in origin of the sediments, and the lake level fluctuations, a palaeoclimalitogical and –hydrological reconstruction was made. The palaeoclimate reconstruction for Laguna de Medina shows the long-term climate evolution of the lake, which can be divided into four units. The period prior to 7,870 cal yr BP reflects the warm and dry Early Holocene. From 7,870-5,780 cal yr BP, the lake experiences its maximum lake level, with anoxic bottom water conditions. In the period until 3,750 cal yr BP, the lake has still a high lake level with anoxic bottom water conditions, but an aridification trend, and a transition towards a shallower lake level is already recognizable. The period from 3,750 cal yr BP on reflects the arid Late Holocene. The lake is shallow, and endured several periods of desiccation.
Over this long-term trend, several short-term climate changes are recognizable, coinciding the RRC of the Mediterranean region. Severe arid RCC are found 9,160-7,870, 5,780-4,800, 3,150-2,420, 1,950-1,450 (corresponding to the RWP), and 1,264-550 (corresponding to the MCA) cal yr BP. The last RCC is the humid period coinciding with the LIA 550-170 cal yr BP.
The sequence of Laguna de Medina reinforces the connection between global changes in the hydrological regime, rapid climate change and NAO dynamics.

Laguna Salada during a desiccation event
Picture by Jasmijn van ´t Hoff

Chapter 4

A Holocene palaeoclimate record from the Laguna Salada, Cádiz, southern Spain

4 A Holocene palaeoclimate record from Laguna Salada, Cádiz, southern Spain

Jasmijn van ´t Hoff[a], Tabea Schröder[b], Klaus Reicherter[b], Martin Melles[a]

[a] Institute of Geology and Mineralogy, University of Cologne, Züpicher Str. 49a, 506745 Cologne, Germany
[b] Institute of Neotectonics and Natural Hazards, RWTH Aachen University, Lochnerstr. 4-20, 52056 Aachen, Germany

Corresponding author: Jasmijn van ´t Hoff: jvanthof@uni-koeln.de
Institute of Geology and Mineralogy
University of Cologne
Zülpicher Straße 49a
50674 Cologne, Germany

Key words: limnology, palaeoclimate, Holocene, Laguna Salada, southern Spain,

Journal article in preparation

4.1 Abstract

The multi-proxy study of a sediment core from Laguna Salada, Cádiz, provides a record of changes in climate and humidity of the last 8,500 years in southern Spain, evidenced by three ^{14}C AMS dates.
The lake originated 8,500 cal yr BP due to collapse of the karstic environment, resulting in a sinkhole. This is clearly visible by an increase of coarse grain-sizes between 8,500-8,100 cal yr BP. Maximum lake level occurred from 8,500-5,900 cal yr BP, coinciding with the Mid-Holocene climatic optimum. This phase ended with an arid phase 5,900-2,500 cal yr BP, reflecting the Late Holocene aridification. In the last 2,500 years, the sedimentation rate increased, representing enhanced erosion due to human influence. Two humid periods, coinciding with the Iberian Roman Humid Period (2,500-1,100 cal yr BP) and the Little Ice Age (750-250 cal yr BP), and an arid period, reflecting the Medieval Climate Anomaly (1,100-750 cal yr BP) were found in the sediment sequence.
The humid, and arid periods are synchronous with the general climate patterns on the Iberian Peninsula (IP), triggered by the North Atlantic Oscillation (NAO).

4.2 Introduction

The arid southern Spain is very vulnerable, even for small climatic changes (Giorgi and Lionello, 2008). Especially with the focus on the ongoing climate change, climate models predict an aridification of arid areas (IPCC, AR5). This will lead to an increase in droughts, a continuing overexploitation of aquifers and an increase in water stress. The groundwater discharge already decreased strongly during the last century, because of a decrease in precipitation, and an increase in evapotranspiration (Aguilera and Murillo, 2009). Overexploiting of these aquifers will lead to more water stress and a higher risk of salinization (Puigdefábregas and Mendizabal, 1998).
Precipitation is decreasing, but on the other hand, heavy rainfalls are likely to become more frequent, causing more erosion (Jiménez Cisneros et al., 2014). This will affect semiarid areas, as southern Spain, the most. Especially highly cultivated areas are very vulnerable for soil erosion (García-Ruiz, 2010). Bussi et al. (2013) show, a single erosion event produced up to 43 % of the total sediments over almost 20 years.

In southern Spain, small endorheic depressions established during the Late Pleistocene and Early Holocene in the karstic and evaporative areas (Valero-Garcés et al., 2014). Many of them are called *´Salada´*, after the high salinity of the lakes (Pardo, 1948). The lakes are shallow, with a brine mainly consisting of Cl-SO_4-Na-Ca-Mg. During the arid summer months, this results in precipitation of gypsum, halite, dolomite and calcite (Dantín, 1942; Schütt, 1998; Martín-Puertas et al., 2011). With the focus of the ongoing climate change, the decrease in precipitation, and the increase in evapotranspiration will have enormous effects on the small shallow lakes. The period of summer desiccation will increase, and possibly, the lakes will eventually desiccate permanently.

One of these small endorheic depressions is Laguna Salada, a shallow lake with a water depth of 0.5 m, and annual summer desiccation (Alonso, 1998). This lake is very suitable for palaeoclimate studies, since it reacts strongly on aridification trends during the Holocene.
This study focusses on the effects of climatological changes during the Holocene on a small Spanish limnological system. Other papers focus mainly on relatively deep lakes (Pérez-Obiol and Julià, 1994; Martín-Puertas et al., 2008), but also the shallow lakes do have a huge potential for palaeoclimate reconstruction (Höbig et al., 2016). One of the advantages is, these lakes react on even small climatic and hydrological changes. On the other side, this can also be a problem, causing hiatuses. In general, these *´Saladas´* make it possible to establish a more detailed overview of the desiccation events of the area during the different climatic phases in the Holocene (Pérez et al., 2002).

The palaeoclimatological and -hydrological evolution of Laguna Salada, Cádiz, has been researched by studying a 12 m sediment sequence drilled in the centre of the lake. This record, which covers the entire limnological history of the lake since its establishment, shows the different arid and humid phases during the last 8,500 years.

4.3 Study site

Laguna Salada (36°37´04"N, 06°03´13"W) is a small endorheic lake situated roughly 13 km north from Cádiz, southern Spain (Fig. 4.1). The entire complex is a nature reserve since 1989, and Laguna Salada is also protected by the Ramsar Convention on Wetland of International Importance (Ramsar, Iran, 1971). The area is an important area for wintering and nesting water birds, including the endangered species *Oxyura leucocephala*, *Fulica cristata* and *Porphyrio porphyrio* (Fernández-Palacios, 1990).

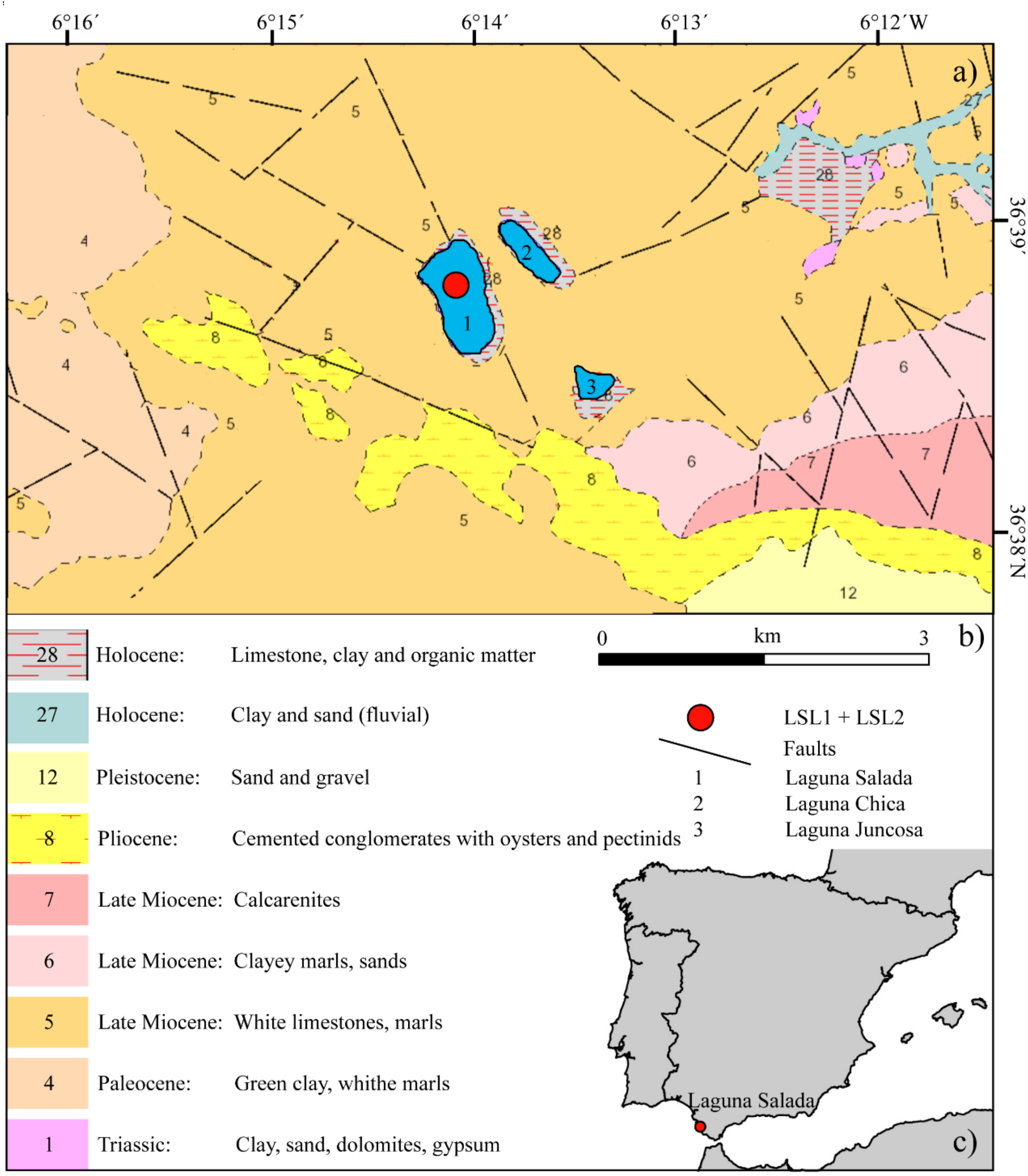

Figure 4.1: Maps of the study area. a) Geological map of the surroundings of Laguna Salada, including the major stratigraphic units and fault systems (modified after IGME, 1984). The coring location is indicated with a red dot and the three lakes are identified with the numbers 1-3. b) Legend for a). c) Location of Laguna Salada on the Iberian Peninsula

Laguna Salada is the biggest of the three lakes of the natural reserve ´Complejo Endorreico del Puerto de Santa María´, which consists furthermore of Laguna Chica and Laguna Juncosa. It is located 28 m above sea level (a.s.l.) and has a surface area of 27 ha and a catchment area of 157 ha. Laguna Chica and Laguna Juncosa have a surface area of 8 and 4 ha, and a catchment area of 118 and 77 ha, respectively. The lakes are mainly fed by rainfall. Lagunas Salada and Chica have a maximum water depth of about 0.5 m, and desiccate annually during the arid summer. Laguna Juncosa, mainly due to its small size, is temporal, and is only present during periods of heavy rain. The area is surrounded by salt cedar (*Tamarix spp*.), reed (*Typha dominguensis*), rushes (*Juncus acutus*), and other xerophytic species (Junta de Andalucía, 2003).

Like many other small endorheic basins in southern Spain, Laguna Salada was formed during the Late Pleistocene-Early Holocene, due to karstic processes (Valero-Garcés et al., 2014). The catchment consists mainly of ´*Albarizas*´, white marls with diatoms and foraminifera (Calderón and Arana, 1896). Patches of conglomerates with oyster and pectinides occur in the southern and eastern catchment (IGME, 1984) (Fig. 4.1).
The climate is a Mediterranean marine climate, with hot and dry summers, and moderate and relatively wet winters (Peel et al., 2007). The summer results in a five month water deficit, resulting in annual lake desiccation. The average annual precipitation is 613 mm/yr (Rodríguez-Rodríguez et al., 2012).

Laguna Salada is highly saline, with precipitation of clay-gypsum in the arid seasons. The salinity depends on the water depth, with high salinities during periods of a low water table. The brine consist of Cl-SO_4-Na-Ca-Mg ions, the pH fluctuates between 7.4 and 9.3 (Junta de Andalucía, 2003).
The surrounding areas are heavily used for agriculture, mainly vineyards. This leads to an increase in erosion and the enhanced silting up of the lakes. Laguna Salada is also used as supply sources for irrigation water.

4.4 Material and methods

Field work
The cores were retrieved in 1 m long sections from two parallel sediment cores (LS1 and LS2) from the centre of the desiccated lake in September 2014 with a cobra drill hammer. Post-recovery, the cores were stored dark and dry.

Analytical work
In the laboratories of the University of Cologne, the cores were halved lengthwise and described. Subsequently, the cores were photographed and scanned with a 2 mm resolution (settings: 50 kV, 38 Ma, 10 s) at a XRF scanner (ITRAX X-Ray Fluorescence from COX Analytical Systems), using Cr-tubes (Davies et al., 2015).
To reduce noise, XRF data were smoothed using a 5-pt running mean. Correlation of the sections was done optically, and based on the Ca and S results from the XRF scanning, leading to a composite core of 12 m length.

For the analytical work, the composite core was firstly sampled at intervals of 6 cm. Secondly, the samples were freeze-dried, and subsequently, the bulk sediment samples were split into three aliquots for different measurements.
For the grain-size analyses, the pretreatment of the 55 samples was done following van ’t Hoff et al. (2017). Each sample was measured three times in 116 classes in a range between 0.04 and 2000 µm using the Laser Particle Size Analyser LS 13320 (Beckman Coulter Corp.), and the Frauenhofer optical model. The grain-size distributions were calculated using GRADISTAT (Blott and Pye, 2001).
To analyse the geochemical composition, 176 samples were ground to <63 µm. The analyses of total inorganic carbon (TIC), and total organic carbon (TOC) were conducted on 35 mg of sediment mixed with 10 g distilled water on a Dimatoc 2000 (Dimatec Corp.).
The contents of total nitrogen (TN) and total sulphur (TS) were measured on 5 mg sample with a vario Micro cube (Elementar Corp.)

The principal component analysis (PCA) was conducted with PAST (Hammer et al., 2001), based on the XRF, TOC, TIC, TS, and TN data of 53 samples.

Radiocarbon dating
Radiocarbon analysis of three samples was performed on terrestrial plant material to exclude the hard water effect. The datings were conducted by Beta Analytic (Miami, USA), using Accelerator Mass Spectrometry (AMS). The ^{14}C dates were calibrated using the INT-Cal04 curve (Reimer et al., 2013). The age model was conducted by linear interpolation between the age points, assuming a constant sedimentation rate between the age points.

4.5 Results and Discussion

4.5.1 Chronology

The age model for Laguna Salada is a chronology for the last 8,500 years (Fig. 4.2), based on three AMS ^{14}C ages (Tab. 4.1), which were obtained on terrestrial organic matter. The year of the coring campaign (2014) was taken as the date of the sediment–water interface. The $\delta^{13}C$ values of the three samples vary between -24 to -20 ‰, indicating a terrestrial origin of the organic material (Meyers and Ishiwatari, 1993).

Table 4.1: Radiocarbon ages of terrestrial plant material samples from Laguna Salada (ages calibrated using INT-Cal04 (Reimer et al., 2013)).

Lab sample Label	Depth (cm)	age (y) uncalibrated	+-(y)	age (y) calibrated	δ13C	Sample mat.
Surface	0	Sept. 2014	1	-64.7	-	reference
Beta – 445440	6.02-6.04	2,420	30	2,498	-23.1	Plant material
Beta – 429887	9.72-9.74	6,750	30	7,678	-23.4	Plant material
Beta – 429888	10.92-10.93	7,390	40	8,280	-20.6	Plant material

Small lakes often cause problems concerning the creation of the age model (Höbig et al., 2016). Preservation of the organic matter is depending on presence of a permanent water body (Meyers and Lallier-Vergès, 1999). In small lakes with annual desiccation, like the *´Lagunas´* in southern Spain, the TOC content is often very low, making it difficult to pick a reliable amount of terrestrial organic matter. Arid periods with prolonged permanent desiccation cause problems concerning the chronological interpolation (Rodó et al., 2002). In Laguna Salada (Cádiz), with the exception of the section 12.00-8.50 m, the TOC is <1 %. The lack of organic matter causes the low-resolution age model.
Laguna Salada (Campillos), a small saline lake in SE Spain, is one of the examples for a *´Laguna´* dealing with difficulties to obtain a reliable chronology (Schröder et al., in review). In this lake, the partial lack of organic matter, and the occurrence of several hiatuses difficult the interpretation of the sediments based on an age model.
Several processes in the lake influence the ages of the obtained organic matter. Bioturbation and root penetration may make dates younger, while catchment erosion may increase the ages (Kaland et al., 1984). Although it is hard to test the reliability of the age model on only three dates, the age model seems reliable, with increasing ages with increasing depths. However, the ages should be used with caution.

4.5.2 Sedimentation rate

The sedimentation rate varies throughout the core (Fig. 4.2). The section 12.00-11.40 m is not included in the sedimentation rates, because these sediments reflect the weathered bedrock.
The lower part (11.40-9.72 m), which coincides with the origin of the lake, has a sedimentation rate of 1.8 mm/yr. The relatively high sedimentation rate might be a consequence of the instability just after the collapse of the karstic environment, resulting in a sinkhole.
The middle part (9.72-6.02 m) has a low sedimentation rate of 0.7 mm/yr. Low sedimentation rates during arid periods is linked to aridity in Lake Salines, where Burjachs et al. (2016) presume erosion or deflation as the cause for the low sedimentation rates. Sedimentation rates are often low during lake level low stand or desiccation, because of erosion (deflation due to wind action), and the lesser amounts of accumulated sediments (Rodó et al., 2002; Cohen, 2003; Hupy, 2004; Magny et al., 2007). Long periods of desiccation increases the problems of chronological interpolation, causing hiatuses (Rodó et al., 2002).
In the upper six meters (upper 2,500 cal yr BP), the sedimentation rate increases to 2.3 mm/yr. Since the Roman Period (~2,000 cal yr BP), increased human activity is found on the IP, often associated with deforestation, enhanced erosion, silting up of lakes, and farming expansion (García-Ruiz, 2010; Moreno et al., 2011). This high sedimentation rate is probably the result of the intensification of the agricultural areas in the surrounding of the lake (Carrión, et al., 2003). Modern studies showed the lake is silting because of heavy agricultural use (Junta de Andalucía, 2003).

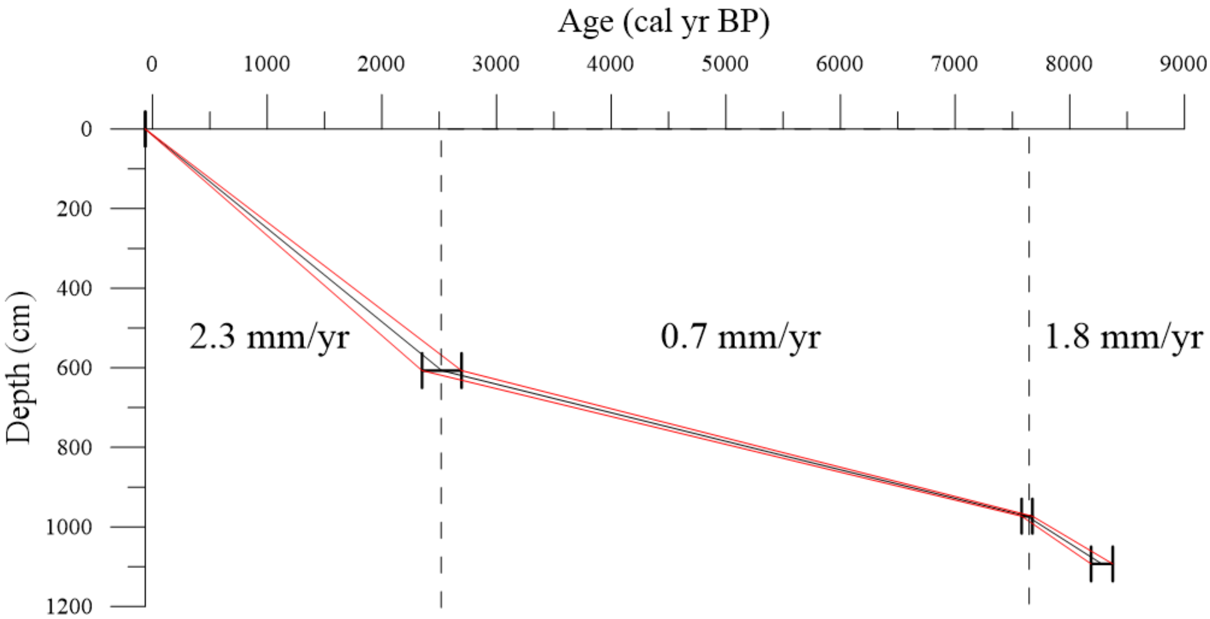

Figure 4.2: Age-depth model of calibrated radiocarbon ages (Reimer et al., 2013) for Laguna Salada based on linear interpolation.

4.5.3 PCA: Origin of allochthonous and autochthonous sediment components

To explain the dependency relationship of the different proxies, a PCA was conducted (Hammer et al., 2001). The first three principal components (PC) of the PCA explain 57.3, 15.2, and 9.8 % of the data, respectively (Fig. 4.3). The outcome of the data points plots within the 95% confidence ellipse.
The PCA plot shows elemental and geochemical data, and can be divided into four different components. The organic component consists of TOC and TN, and is mainly explained by positive loading of PC3 (not shown). The carbonate component is characterized by the elements Sr, Ca, and the TIC, and has positive loadings of both PC1 and PC2. The evaporite component only consists of TS and has negative loadings of both PC1 and PC2. The terrestrial component includes the elements Si, Al, K, Ti, Fe, and Rb. This component has positive loadings for PC1 and negative to slightly positive loadings for PC2.

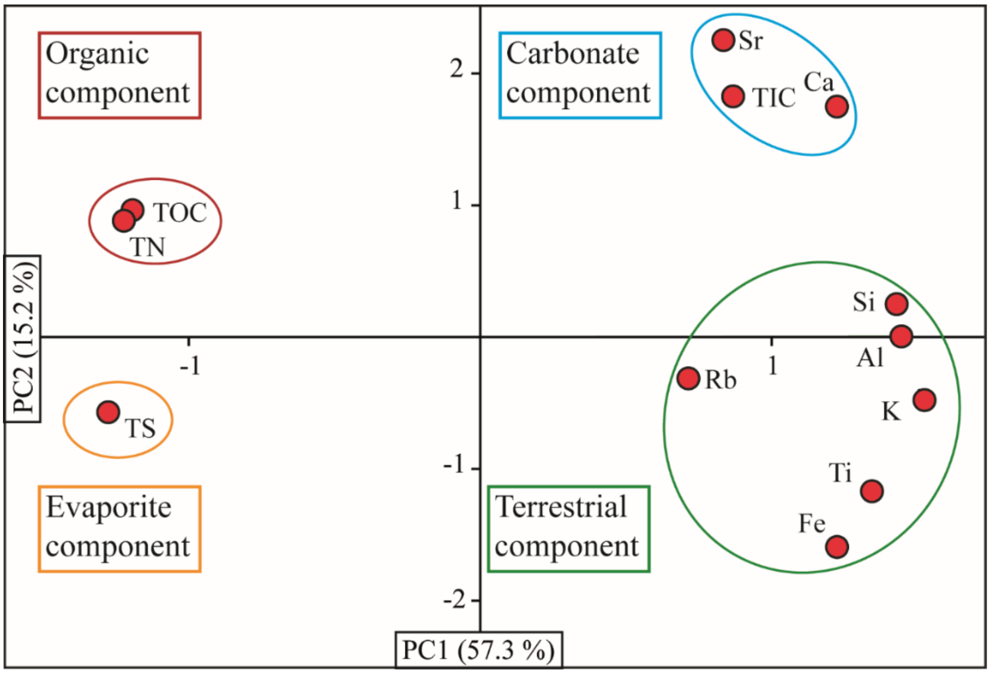

Figure 4.3: Outcome and interpretation of the Principal Component Analysis.

The terrestrial component reflects the input of sediment from outside of the lake, and is often used as an indicator for high lake level (Giralt and Juliá, 2003; Martín-Puertas et al., 2011). However, the surrounding geology of this lake is overprinted by carbonates (Fig. 4.2), difficulting the interpretation of the terrestrial component, because it is overprinted by the carbonate component. Maxima of the terrestrial component might be caused by the dilution effect by the carbonate component. During humid periods, erosion leads to an increase of the carbonate component, overprinting input of the terrestrial component. The carbonate component is also partly from terrestrial origin, but a differentiation between authigenous and terrigenous influence cannot be made based on the PCA.

The evaporite component reflects gypsum precipitation, and is relatively low throughout the core. Gypsum is not abundant in the catchment, only in the east some patches of gypsum occur (Fig. 4.2). The influence of gypsum via groundwater is low, the lake is mainly fed by rainwater (Junta de Andalucía, 2003). However, the influence of groundwater cannot be neglected during the initial phase of the lake. The collapse of the sinkhole probably caused a shift in the hydrological settings in the surroundings of the lake, resulting in a slightly increased evaporite component.

Interestingly, Sr plots closely to TIC, and Ca. In saline lakes, Sr is often a good indicator for palaeosalinity, due to the exchange of Sr for Ca under saline conditions (Dodd and Crisp, 1982; Santisteban et al., 2016), and plots closely to TS. In this case, the high amount of carbonates in comparison to gypsum overprinted the signal of Sr in the gypsum. The S/Al ratio in this lake is much lower as in other saline lakes, like e.g. Laguna de Medina (Chapter 3).

Based on the PCA, following proxies were selected to reflect the geochemical variability in the Salada record (Fig. 4.4). For the organic component, both TOC and TN contents are shown, extended with the C/N ratio, which allows to divide the organic matter from a terrestrial, and a limnological origin (Meyers and Ishiwatari, 1993). The Ca/Ti ratio, and the TIC concentration reflect the periods of high carbonate precipitation, and low terrestrial input (Corella et al., 2013). Ti indicates periods with enhanced terrestrial input (Boës et al., 2011). The S/Al ratio represents the evaporite component, reflecting periods of gypsum precipitation due to a low lake level of entire desiccation (Roca and Julià, 1997).

5.5.4 Palaeoclimatological / Palaeohydrological reconstruction

The sediment record of Laguna Salada covers the entire lacustrine history of the lake, starting in the weathered bedrock. Based on the lithology (Tab. 4.2), sedimentology, geochemical and granulometric results, the sequence can be divided into six phases of different palaeoclimatological and –hydrological periods (Fig. 4.4), and is compared with archives form the IP (Fig. 4.5).

Table 4.2: Lithostratigraphic description and interpretation for Laguna Salada

Depth (cm)	**Lithology**	**Interpretation** Based in the facies classification of Valero-Garcés et al., 2014
0-36	Dark grey organic-rich clayey silts with evaporative mottles (green, yellow, white), and gypsum nodules	**Palustrine-Littoral:** Deposited in shallow or desiccated environment. Periods of subaerial exposure and evaporite formation.
36-270	Light to dark brown clayey silts with traces of bioturbation, evaporite mottling and gypsum nodules. The mottles are green, yellow and white, with gypsum grains. 180-200 cm: Dark grey clayey silts with fragments of shells.	**Littoral:** Deposited in shallow or desiccated environment. Periods of subaerial exposure and evaporite formation.
270-633	Light brown clayey silts with less green mottles and some dark brown bands and shells fragments (bivalves).	**Sub-Littoral:** Deposited in a moderate deep environment (dark bands and shells), with a few periods of shallowing (mottles).
633-971	Massive dark grey clayey silts with traces of bioturbation and evaporite mottles	**Littoral:** Deposited in a shallow environment with periods of desiccation.
971-1134	Dark grey sandy silts with many shell fragments (bivalves) and a high component of organic matter	**Distal:** Deposited in a deep environment, with a permanent water body.
1134-1200	Yellow-beige carbonate-rich silt. No lacustrine sediments anymore	**Substratum:** No lacustrine deposits, this is weathered bedrock.

I: Stable landscape prior to 8,500 cal yr BP (12.00-11.40 m)

The landscape was presumably stable prior to 8,500 cal yr BP. The sequence starts in the weathered bedrock, consisting of yellow-beige sediments, which are silt dominated (80 %), with a small sand content (9 %). The weathered bedrock is completely different in colour, and composition from the rest of the core (Tab. 4.2). The mean grain-size is 21 µm. The terrestrial component is relatively high, reflecting the influence of weathering on the original bedrock. The carbonate content is high, with a low gypsum content. TOC (<0.50 %) and TN (0.02 %) are low. The C/N ratio is high, indicating a terrestrial origin of the accumulated organic matter in the weathered bedrock (Meyers and Ishiwatari, 1993).

II: Collapse of the sinkhole 8,500-8,100 cal yr BP (11.40-10.50 m)

The stable phase ends abruptly with the collapse of the karstic environment, resulting in a sinkhole, and the onset of the lacustrine environment. The sediments are sandy silts with a high organic component, and many shell fragments (bivalves), reflecting a period of a relatively deep lake (Moreno et al., 2011; Valero-Garcés et al., 2014). The onset of the collapse of the sinkhole is clearly reflected in the grain-size distribution by the input of sand (up to 82 %). The mean grain-size fluctuates between 21-163 µm. The sedimentation rate is with 1.8 mm/yr relatively high, induced by the coarse grain-size, and the instability of the steep walls. Ti and Ca/Ti show the same strong fluctuations, reflecting the instable character of the sinkhole just after its collapse with some pulses of increased terrestrial material and carbonates (Corella et al., 2013). The C/N ratio, which varies between 7-12, reflects a lacustrine origin of the organic matter (Meyers and Ishiwatari, 1993). The increased TOC and TN are likely a result of better preservation due to the increased water table (Meyers and Lallier-Vergès, 1999).

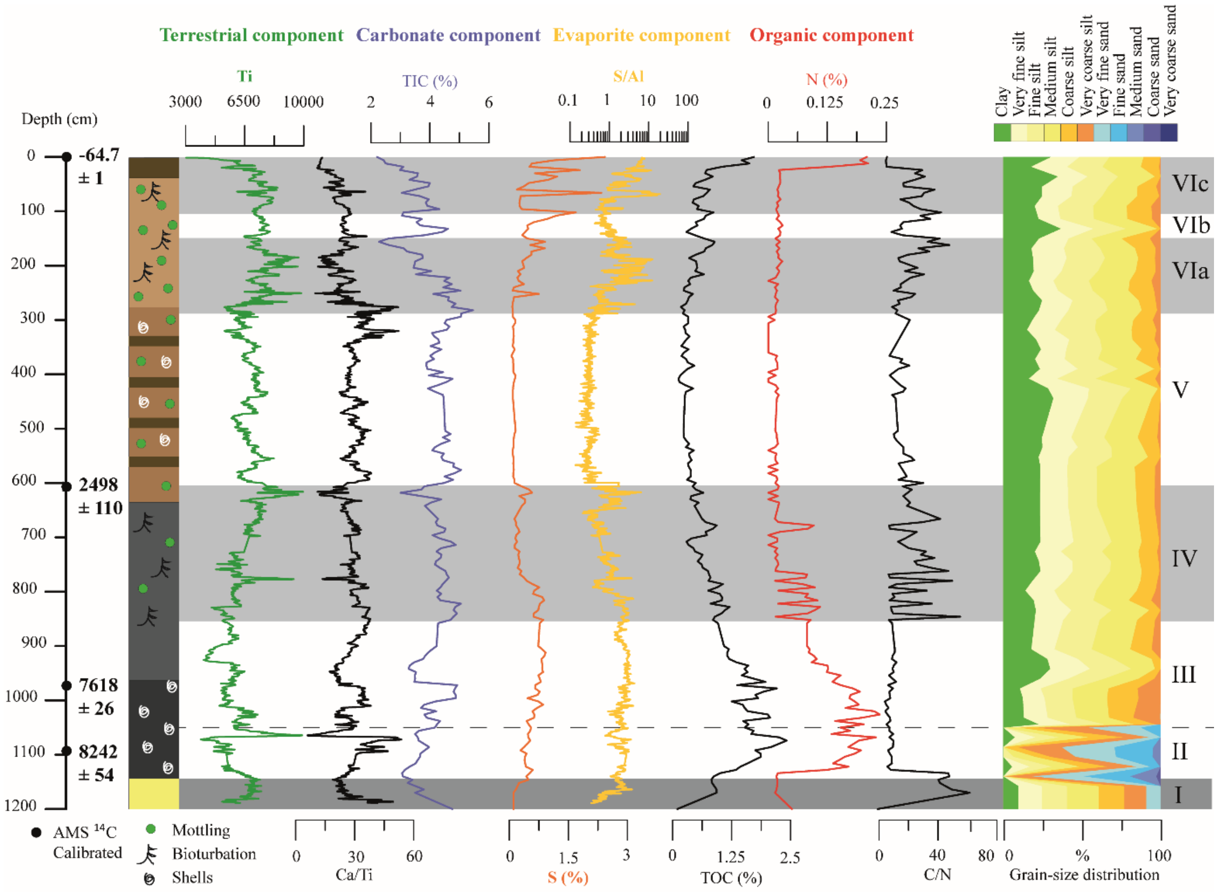

Fig. 4.4: Lithology, geochemical and granulometric data for Laguna Salada, as well as the different phases. Arid phases are indicated by light grey bars. The substratum is indicated by a dark grey bar. Valid calibrated AMS data are also indicated

III: Initial phase of the lake 8,100-5,900 cal yr BP (11.40-8.52 m)

After the stabilization of the walls of the sinkhole, there is no more input of sand, and the grain-size distribution becomes relatively stable. The sediments are now dominated by silt (70-90 %) and clay (10-30 %). The organic component is most dominant during this humid period (Fig. 4.4), reflecting the initial phase of the lake. The high water level induces the good preservation of organic matter (Meyers and Lallier-Vergès, 1999). During this lacustrine period, characterized by the low C/N ratio (Meyers and Ishiwatari, 1993), the TOC (max. 2.40 %) and TN (max. 0.25 %) are high and slowly decreasing. This indicates either a drop in productivity or in preservation of the organic matter (Meyers and Lallier-Vergès, 1999), reflecting a decreasing humidity (Moreno et al., 2011).

This humid phase coincides with the Middle Holocene humidity maximum (roughly between 8,000-5,500 cal yr BP). this humid period was clearly reflected in the Saharan vegetation records, reflecting aperiod in which the Saharan desert turned ´green´ (Gasse et al., 1990). This period with a warm and moist climate is reflected by the maximum lake level in e.g. Lake Siles, Lake Gallocanta, Laguna de Medina, and a lacustrine deposit in the Sierra de Gádor (Reed et al., 2001; Carrion, 2002; Carrión et al., 2003; Luzón et al., 2007; Roberts et al., 2008). In the fluvial system of the Guadalete River, soil development due to preservation by a continuous vegetation cover reflects this humid phase between 8,000 and until 6,000 cal yr BP (Wolf et al., 2014).

IV: Late Holocene aridification 5,900-2,500 cal yr BP (8.52-6.06 m)

Around 5,900 cal yr BP, the permanent lake changes into a semi-permanent lake. This is best reflected in the C/N ratio, which varies between 9-60, representing pulses of lacustrine and terrestrial input of organic matter (Meyers and Ishiwatari, 1993). During this arid period, the lake level is unstable, with several desiccation events. This is an unfavourable environment for the preservation of organic matter, resulting in a low organic component. TOC is further decreasing, whereas TN varies a lot. Peaks in S/Al reflect increased gypsum precipitation during periods of desiccation (Celia Martín-Puertas et al., 2008). Ca/Ti is relatively stable and Ti is slightly increasing, reflecting an increase in terrestrial input.

The Late Holocene is a period of progressive aridification, although the onset is not synchronous on the IP (Fletcher and Zielhofer, 2013). The timing and the intensity are still in debate, since records show a complex system with several arid and humid periods (Morellón et al., 2008). The onset from a humid to an arid phase is around 5,500-5,000 cal yr BP, and coincides with a change towards more positive NAO values (Sánchez Goñi et al., 2002; Moreno et al., 2012; Olsen et al., 2012). Low lake levels and desiccation are found all over the IP, e.g. in Laguna de Medina, Lake Siles, Lake Zoñar, and Lake Gallocanta (Reed et al., 2001; Carrion, 2002; Luzón et al., 2007; Martín-Puertas et al., 2008; Morellón et al., 2008). In the Guadalete fluvial system, the arid period occurred between 4,300-2,400 cal yr BP is indicated by landscape stability due to a low sediment supply (Wolf et al., 2014). In north Africa, lowest lake levels were found from 6,000 cal yr BP on (Lamb et al., 1999).

V: Iberian Roman Humid Period; 2,500-1,100 cal yr BP (6.06-2.88 m)

After the unstable period with desiccation events, the lake stabilizes, and has a constant water table. TOC (<0.50 %) and TN (<0.03 %) are low, and the C/N ratio indicates a lacustrine phase with some small inputs of terrestrial organic material (Meyers and Ishiwatari, 1993). Ti is generally low, but indicates some pulses of enhanced terrestrial input. Also in the Montcortés Lake (N Spain), a low input of terrestrial components characterize this humid period (Corella et al., 2011). The TS (<0.10 %) and S/Al are low and stable, indicating a permanent water table (Martín-Puertas et al., 2008). TIC is relatively high, reflecting enhanced carbonate precipitation due to a higher water table, or enhanced dissolution of the adjacent carbonates in the catchment due to enhanced precipitation (Roca and Julià, 1997).

This humid period 2,500-1,100 cal yr BP coincides with the overall more humid period on the IP, the Iberian Roman Humid Period (Moreno et al., 2012). This humid period was found in Lake Zoñar (S Spain), the Basa de la Mora sequence (SE Spain), in the Somolinos tufa lake record (C Spain), and in Montcórtes Lake (N Spain) (Martín-Puertas et al., 2009; Corella et al., 2011; Currás et al., 2012; Pérez-Sanz et al., 2013). Some lakes in north Africa show a humid period with high lake levels, e.g. Lake Sidi Ali (Morocco) (Lamb et al., 1999).

VI: Aridification /Desiccation 1,100 cal yr BP-now (2.88 m-top)

The second arid period (VIa; 1,100-750 cal yr BP) in the Laguna Salada matches the Medieval Climate Anomaly (1,500-650 cal yr BP; Moreno, et al., 2012). The lake changes from a permanent lake to a temporary lake. The increased gypsum precipitation, which is reflected by the TS content and S/Al ratio, represents a desiccated period. Desiccation is increasing towards the top of the record (VIc). The modern lake is known to desiccate annually. The terrestrial component is high during this phase, presumably an anthropogenic effect of increased erosion of the agricultural areas during the wet winter periods (Boës et al. 2011; Bussi et al., 2013). This is reinforced by the high sedimentation rate of 2.3 mm/yr.

This progressive aridification is interrupted by a short relatively humid phase (VIb: 750-250 cal yr), without gypsum precipitation (low S/Al ratio). The age model of the Salada is not good enough for an evident comparison. However, the timing suggests this humid period could be the LIA, found 650-100 cal yr BP (Sousa and García-Murillo, 2003). The LIA is known as a generally cold and humid period with stronger climatic variability (Valero Garcés et al., 2008; Moreno et al., 2012). A switch towards more negative NAO values resulted in heavy rainfall (Olsen et al., 2012). This is noted by relatively high lake levels, e.g. in Lake Zoñar (Martín-Puertas et al., 2008, 2009), and an intensive period of sedimentation in the Guadalete fluvial system (Wolf et al., 2014).

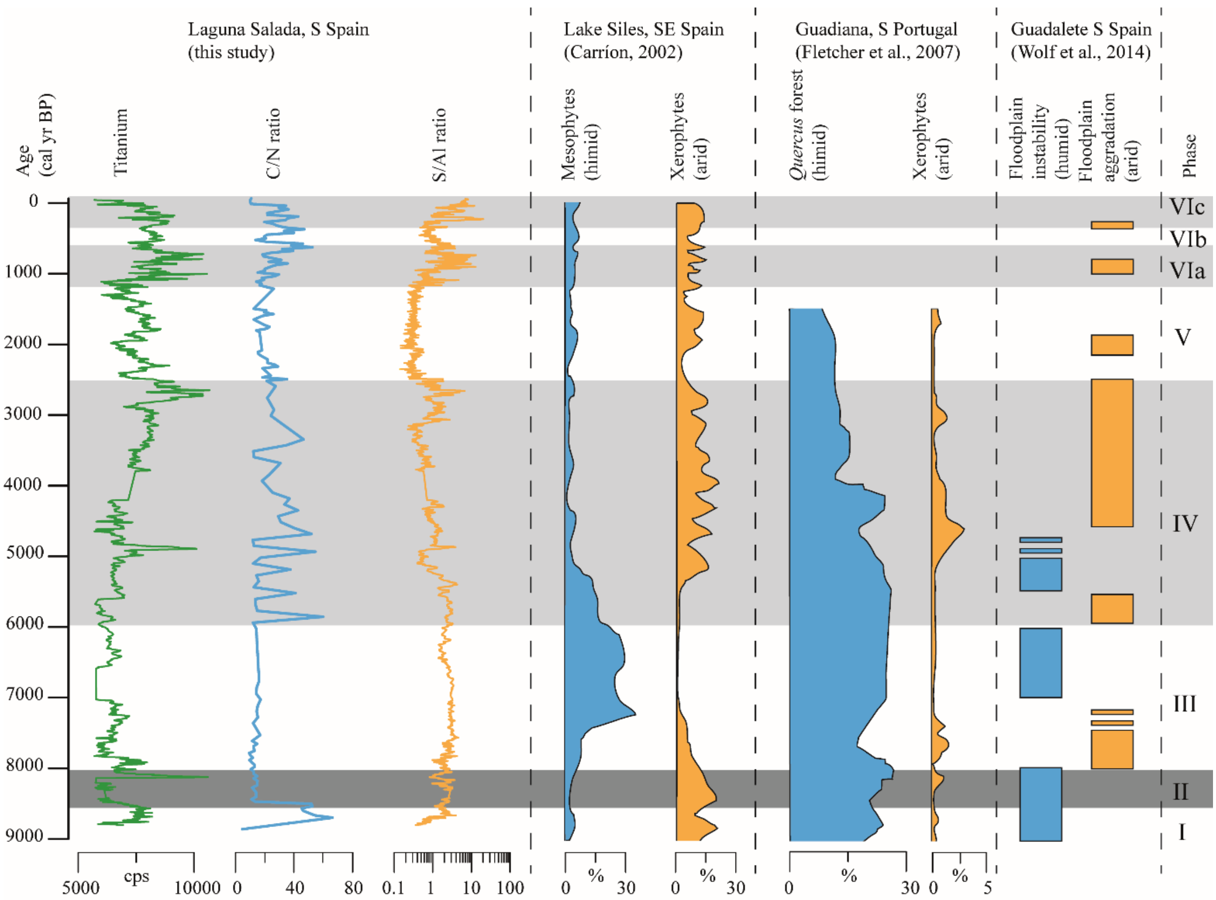

Fig. 4.5: Summary of the Holocene arid (grey bars), and humid periods in Laguna Salada, and a compilation of palaeoclimatological archives from southern Iberia. Titanium, C/N, and S/Al from Laguna Salada compared with the mesophytic and xerophytic pollen percentages from Lake Siles (Carrion, 2002), pollen percentages of Quercus *and xerophytes from the Lower Guadiana Basin (Fletcher et al., 2007), periods of floodplain stability and aggradation of the Guadalete River (Wolf et al., 2014).*

4.6 Conclusions

Palaeoclimate reconstruction for the Laguna Salada represents the entire limnological history of the lake, reflecting humid and arid periods. The lake developed due to collapse of the karstic system, resulting in a sinkhole around 8,500 cal yr BP. The limnological history of the lake can be divided into six palaeohydrological periods. The period prior to 8,500 cal yr BP reflects a stable landscape, before the establishment of the lake. The lake originated 8,500-8,100 cal yr BP, as the result of collapse. The sinkhole was rapidly filled up with water during the humid period 8,100-5,900 cal yr BP. This period is characterized by the maximum lake level, synchronous with the Mid-Holocene Climate Optimum. The arid period from 5,900 cal yr BP - today reflects the onset of the Late Holocene aridification. This progressive aridification is disrupted by two humid periods. The Iberian Roman Humid Period (2,500-1,100 cal yr BP), and the Little Ice Age (750-250 cal yr BP). The arid period (1,100-750 cal yr BP) intermitting these humid periods coincides with the Medieval Climate Anomaly. The last 300 years (from 250 cal yr BP) reflect the modern arid times, with annually desiccation of the lake.
Despite the chronological uncertainties due to the poor amount of fixed age points, the palaeoclimatological trends of the Laguna Salada are in trend with the climatic development across southern Iberia, and contribute to a better understanding of the Holocene climate variability.

Laguna de Medina and the platform
Picture by Florian Steiniger

Chapter 5

Synthesis

5.1 Synthesis

Terrestrial palaeoclimate archives are sparse in southern Spain, and reconstructions are mainly based on distal low-resolution marine records. The principle aim of this thesis was to obtain a reliable reconstruction for the development of Holocene climate in southern Spain based on lacustrine archives. Due to the scarcity of deep natural lakes, two shallow saline lakes (´*Salinas*´) were cored during two coring campaigns: Laguna de Medina and Laguna Salada.
Several questions came up during this thesis, in this chapter, these questions are answered.

5.1.1 How do the modern processes help to unravel the palaeoprocesses?

For a better understanding of the modern processes, a study was performed on lake surface sediment and soil catchment samples of the Laguna de Medina. Based on the geochemical, mineralogical, and granulometric data, the lake was divided into six different provinces with different influences. Some interesting and helpful conclusions for the interpretation of the long sediment record were obtained (van ’t Hoff et al., 2017).

In the modern situation, sand does not reach the coring site, and is only deposited within 200 m from shores. Thus, the absence of sand in the long core implies that the coring position was always distant to the lakeshores, and does not reflect a climatic signal. Moreover, the modern sediments contain terrestrial components (K, Al, Fe, Ti, Mg, and Rb). These sediments are brought into the lake via the most important inlet, the Arroyo de Fuente Bermejo in the southeastern part of the lake. This inlet is dry during summer months, and arid periods. Increased terrestrial input in the long record indicates enhanced catchment erosion, and a more sufficient fluvial supply due to enhanced precipitation.
The modern samples contain a high calcite content, which is delivered to the lake by dissolution of the adjacent ´capas rojas´, a series of marlstones and limestones. This finding from the modern samples is in particular important, since calcite is often interpreted as authigenoc bioproduction. Based on the analogue study, however, it became clear that increased carbonate content in the long core is rather attributed to enhanced erosion due to increased precipitation, than being a signal of increased productivity. The PCA of the long sediment sequence of Laguna de Medina shows an increased carbonate content during periods of relatively high lake levels, reflecting increased erosion and dissolution of the ´capas rojas´ during high lake levels.
Gypsum in the modern samples is restricted to the eastern part of the lake. Probably, the ions from dissolved Triassic gypsum from the catchment are brought into the lake by upwelling groundwater. Another source for gypsum into the lake is the weathering and dissolution of the Keuper facies, which is directly brought into the lake via surface water. Based on this finding, and increase in salinity in the record can be caused by a change in ground water regime, enhanced weathering of the Keuper facies (enhanced precipitation), or result from desiccation of the lake (enhanced evapotranspiration). Increased gypsum precipitation is restricted to the arid period (Stein et al., 1997).
In the centre of the lake, at the location of core Co1313, distal background sedimentation occurs. The sediments consist mainly of silt and clay, and contain a mixture of the other components. Entangling the sediments of the long record will prove when the influence of which modern province was dominating the sediments.

The study focused on the lake surface sediment and soil catchment samples in Laguna de Medina delivered a modern analogue for the interpretation of the long sediment sequence from deepest part of the lake.

5.1.2 How can we obtain a reliable age model?

Laguna de Medina is a semi-permanent lake, which desiccates only during very arid years. Laguna Salada is a temporal lake, and desiccates annually. Due to the shallowness of the lakes, both react very sensitive on even small climate changes (Giorgi and Lionello, 2008). However, such shallow saline basins are insufficient environments for the preservation of organic matter (Meyers and Lallier-Vergès, 1999).

Obtaining reliable chronologies is a challenging task in many saline archives (Santiago Giralt et al., 1999; Höbig et al., 2012, Schröder et al., in review). Desiccation phases may result in the loss of organic matter (Meyers and Lallier-Vergès, 1999). Many processes result in a shift to older ages, as the input of reworked catchment material during erosion phases, or the hard water effect (Eichinger, 1983; Valero-Garcés et al., 2000). Other processes, like root penetration, bioturbation or the influence of younger humic acids (the result of not properly bleaching the samples before the measurements) result in a shift towards younger ages (Kaland et al., 1984).

The TOC content varies around 1.5-2.5 % in Laguna de Medina, which was enough to pick a reliable amount of terrestrial organic matter for radiocarbon dating. Terrestrial organic matter was picked to bypass the hard water effect (Eichinger, 1983). Twenty samples were radiocarbon dated. Most of the dates seemed reliable, providing a consistent age-depth relationship. However, five of the samples seemed erroneously, by producing age reversals. Two of the dates had a significant younger age, which could only be explained by bioturbation or the contamination of humic acids (Kaland et al., 1984). Three dates had a significant older age, this could be explained by the input of reworked material (Kaland et al., 1984). More in Chapter 3.6.3.

For Laguna Salada, sampling of suitable organic material for radiocarbon dating was very hard, and failed in the upper 8 m, where the TOC <1 % already reflected the wide lack of organic matter. Only the part from 11.30-9.00 m contains 1.5-2.5 % organic carbon, allowing to pick a sufficient amount of organic matter. Therefore, the age-depth model for Laguna Salada relies only on three radiocarbon dates. This makes is impossible to control whether these ages are reliable, or contain (small) errors. Likewise, for another Laguna Salada (Campillos), organic remains suitable for radiocarbon dating were sparse. This small saline lake in SW Spain desiccates annually, resulting in a low organic carbon content, and the hiatuses difficult the interpretation of the dates (Schröder, in review).

To obtain a reliable age-model in the future, some proposals to improve the current age-model with different techniques are listed:

An approach to improve this age model with additional dates, is to date shells or snails parallel to the existing ages obtained from organic matter. The parallel dating enables the calculation of the hard water effect on the shells or snails. This was already effectively used by Reed et al. (2001) to bypass the hard water effect. Knowing the calculated hard water effect for this lake gives the opportunity to date more shell fragments or snails from other parts of the record, and subtract the hard water effect on the newly obtained ages to improve the chronology.

Another method to obtain a chronology on only small amounts of organic matter is to date pollen grains. This is a better method than dating bulk sediment, especially in limestone-rich settings due to the hard water effect (Brown et al., 1989). Attempts to date pollen in Laguna Salada (Campillos) failed due to the absence of pollen. Future studies have to demonstrate whether pollen are sufficient present in the record for Laguna Salada (Cádiz).

For new studies in such shallow saline environments, it is recommended to core the sedimentary sequences with black liners to avoid interaction of sun light with the minerals. This allows optically stimulated luminescence (OSL) dating to determine the age of burial (sedimentation) using the quartz or feldspars in the record. This technique is very well suited for Holocene sediments (Aitken, 1998).

Another method that can be very useful in small saline lakes is palaeomagnetic analysis of the sediments. Especially for older (>100ka) records, polarity change gives robust reliable dates. But also for shorter records, proxies for the strength and direction of the Earth's magnetic field can be correlated to reference records, available for the past 700 ka (Constable & Korte, 2015).

5.1.3 What are good proxies to reconstruct the palaeoclimatological conditions in saline environments?

Saline limnological environments like Laguna de Medina and Laguna Salada contain typically a brine of Ca-Na-Mg-Cl-SO_4, resulting in gypsum precipitation (Eugster and Hardie, 1978). Enhanced gypsum precipitation during arid phases and lake desiccation is found in many salt lakes over the world (Pérez et al., 2002; Torfstein et al., 2008; Pérez-Sanz et al., 2013). The typical evaporation cycle in a saline lake starts with gypsum precipitation. An increase in water level results in the redissolution of the gypsum crust, and dolomite and aragonite precipitate. The input of enhanced fresh water will lead to carbonate precipitation, and in the end to the input of terrestrial components (Roca and Julià, 1997; Giralt and Juliá, 2003; Martín-Puertas et al., 2011).

The principal component analysis (PCA) based on the geochemical, mineralogical data, and the magnetic susceptibility of 111 samples from Laguna de Medina reflects these four stages very well. Gypsum (or TS content) is very suitable to reconstruct desiccation events in the Holocene, and functioned in Laguna de Medina and Laguna Salada very well. The gypsum concentration (or TS content) was significantly higher in Laguna de Medina during arid periods. The precipitation of gypsum is a complex system with influences of the climate, geology, ground water, and dissolution processes. However, the precipitation of gypsum is restricted to arid periods, and a good indicator for aridification events in the Holocene (Torfstein et al., 2008; Martín-Puertas et al., 2011).

Periods of a high water level disable the precipitation of gypsum during humid periods (Torfstein et al., 2008). The analysis of the lake surface sediment, and soil catchment samples of Laguna de Medina indicates an area of enhanced gypsum precipitation in the lake, probably due to enhanced upwelling of gypsum-ion-rich ground water.

Laguna Salada, although desiccating every year, does only show a small increase in gypsum during arid events. The main difference between these two lakes is the surrounding geology. Both lakes are situated in a karstic and evaporitic catchment, consisting of carbonates, marls, Keuper facies, and gypsum. The catchment of Laguna Salada consist mainly of carbonates, the 'alborizas'. Keuper facies and gypsum only occur in small patches in the catchment (IGME, 1984).

Aragonite turned out to be a good indicator for the start of aridification of the Late Holocene in Laguna de Medina, and was also used to reflect arid periods of RCC. The carbonate content (characterized by calcite precipitation) was more complex to interpret, because of the carbonate-rich catchments for both of the lakes. However, in general, the higher carbonate content reflects enhanced erosion, and dissolution during a high lake level (Giralt et al., 1999; Martín-Puertas et al., 2011). The terrestrial component (characterized by K, Al, Fe, Ti, Mg, and Rb) reflects the periods of increased fluvial activity due to enhanced precipitation, and coincides with a high lake level. In Laguna de Medina, the increased terrestrial component reflects very well the maximum lake level.

Other proxies that were used in this thesis are the Sr/Ca ratio and the C/N ratio. The Sr/Ca ratio is often used in saline environments to reconstruct the salinity (Dodd and Crisp, 1982), because Sr exchanges for Ca under very arid or saline conditions (Santisteban et al., 2016). For the Laguna de Medina, this proxy clearly reflects the desiccation. In Laguna Salada, this proxy was not applicable. The carbonate content (Ca) dominated the sequence, Sr was only available in very small intensities. The PCA reflected this very well, by a cluster of carbonates and Sr in the one corner, and the TS in the other corner.

The C/N ratio was very useful to interpret the origin of the organic matter in the sediment cores. This ratio clearly differentiated between periods of enhanced organic matter from terrestrial origin, reflecting lake level low stands, and periods with organic matter from lacustrine origin (algae), characterizing for periods with lake level high stands (Meyers and Ishiwatari, 1993).

The salinity, in Laguna de Medina based on the occurrence of ostracod assemblages (Mezquita et al., 2005), gave insight in an interesting paradox. The period with the maximum lake levels correlates with the maximum salinity. With the use of other proxies (e.g. Ti), the hypothesis is that increased salinity is a result of enhanced weathering and dissolution in the catchment (consisting of gypsum-rich Keuper facies), delivering dissolved evaporites into the lake. The highly concentrated brine led to an increase in salinity, but the high lake level disabled the precipitation of gypsum.

5.1.4 Are the Holocene climate events synchronous in the two records, and how about the entire Iberian Peninsula?

Based on the proxies, the two records could be divided into several arid and humid periods. The long-term trend is relatively synchronous in both of the records. The period prior to ~8,000 cal yr BP reflects the warm and arid Early Holocene. The period between 8,000-5,500 represents the humid climatic optimum in the Middle Holocene, characterized by maximum lake levels. The period from 5,500 cal yr BP on reflects the progressive aridification trend in the Late Holocene.
This long-term trend is interrupted by several short-term climate changes, the rapid climate changes (Mayewski et al., 2004; Fletcher and Zielhofer, 2013). In the high-resolution record of Laguna de Medina, this gave the opportunity to investigate the timing, duration, and effects of the Holocene RCC´s on the limnological evolution, and to compare them with rapid climate change in other Iberian archives (Fig. 5.1).

The long-term trend is more of less synchronous in both studied cores, and is similar to the Iberian Holocene climate trend. The Early Holocene (prior to 8,000 cal yr BP) is a warm and arid period with low lake levels and an increase in xerophytic vegetation (Fig. 5.1). The Early Holocene is found in Laguna de Medina prior to 7,870 cal yr BP. Laguna Salada is too young, and its initial phase too instable to recognize the Early Holocene. Iberian archives indicate the Mid Holocene (8,000-5,500 cal yr BP) as a humid phase with increased lake levels and a rise in mesophytic vegetation. In Laguna de Medina and Laguna Salada, maximum lake levels are found 7,870-5,900 cal yr BP and 8,500-5,900 cal yr BP, respectively. These findings are in line with many Iberian archives (Fig. 5.1), like in Lake Siles and Cañada de la Cruz, where an increase in microcharcoal indicate an increase in fire regime, and a low lake level due to aridity (Carrión, 2002).
After 5,500 cal yr BP, most of the Iberian archives reflect a progressive aridification trend, resulting in a drop in lake level, and a transition towards xerophytic vegetation, induced by a general trend towards more positive NAO values (Olsen et al., 2012). In Laguna de Medina, the lake level is still relatively high until 3,750 cal yr BP, but the progressive aridification trend is already visible from 5,900 cal yr BP. In Laguna Salada, this transition is found from 5,900 cal yr BP on. In Lake Siles, the Guadiana Basin, Canadaa de la Cruz, and the four sites from the Segura Mountains (d) reflect this humid period with an increase in mesophytic vegetation (Carrión et al., 2001a; 2001b; Carrión, 2002; Fletcher et al, 2007). High lake levels are found in many Iberian lakes, like Lake Siles, and Lake Estanya (Carrión 2002; Morellón et al., 2009), but also in African lakes as Lake Sidi Ali, Sebkha Melalla, and Hassi el Mejnah (Gasse et al., 1999; Lamb and van der Kaars, 2008).

Short-term trends are mainly visible in the Laguna de Medina record. However, during the last 2,500 years, also Laguna Salada reflects a transition in arid and humid periods.

The Iberian Roman Humid Period or the Roman Warm Period (RWP) is reflected in Iberian archives between 2,600-1,600 cal yr BP (Morellón et al., 2012), and is found in Laguna de Medina between 1,950-1,450 cal yr BP, and in Laguna Salada between 2,500-1,100 cal yr BP. The difference in the onset and the duration of the RWP can be the result of the poor age control for Laguna Salada. A change in solar forcing caused this humid period (van Geel et al., 1996; 1999).
The subsequent arid period of the Medieval Climate Anomaly (MCA; 1,050-1,600 cal yr BP) is detected in several Iberian archives, e.g. in Lake Zoñar, Taravilla, Arreo, and Estanya (Martin-Puertas et al., 2008; Valero-Garcés et a., 2008; Morrellón et al., 2009; Moreno et al., 2012; Corrella et al., 2013). The MCA is reflected by enhanced gypsum precipitation in both Laguna de Medina (1,050-650 cal yr BP), and Laguna Salada (1,100-750 cal yr BP).
The aridity trend in the Late Holocene is interrupted once more by the humid Little Ice Age (LIA; 650-100 cal yr BP). This period, induced by a change towards more negative NAO values (Olsen et al., 2012), is characterized by relatively high lake levels, e.g. in Lake Zoñar and Lake Arreo (Martín-Puertas et al., 2008, 2009; Corella et al., 2013). In Laguna de Medina, the LIA is found between 650-150 cal yr BP, and in Laguna Salada between 750-250 cal yr BP.

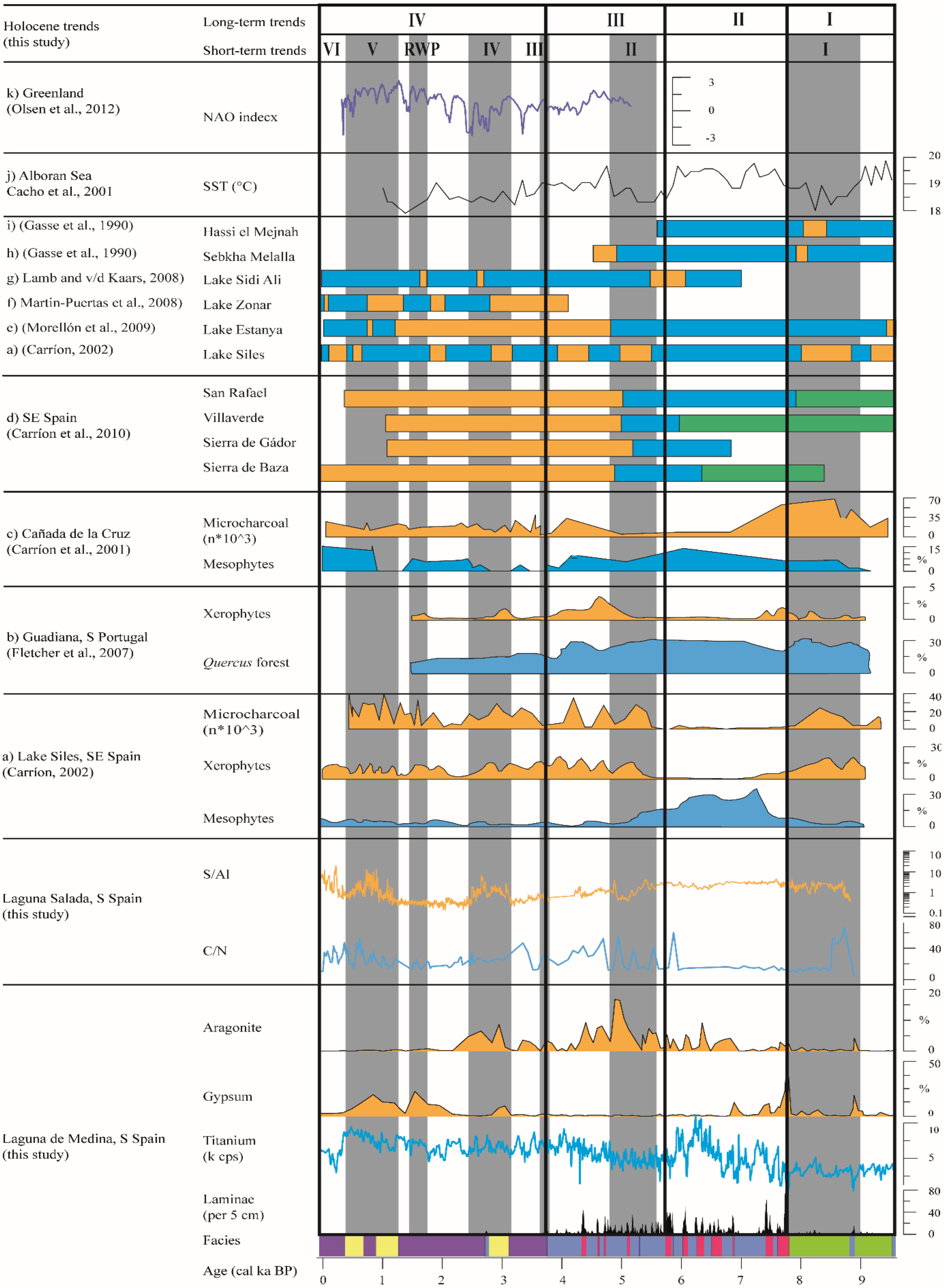

Figure 5.1. Overview of the arid and humid phases in Laguna de Medina and Laguna Salada compared with Lake Siles (Carrión, 2002), the Guadiana Basin (Fletcher et al., 2007), Cañada de la Santa Cruz (Carrión et al., 2001b), palynological data from Sierra de Bara, Sierra de Gádor, Villaverde and San Rafael (Carrión et al., 2010), and from Lake Siles (Carrión, 2002), Lake Estanya (Morellón et al., 2009), Lake Zoñar (Martin-Puertas et al., 2009), Lake Sidi Ali (Lamb and v/d Kaars, 2008), Sebkha Melalla (Gasse et al., 1990) and Hassi el Mejnah (Gasse et al., 1990), and marine core MD95-2043 (Cacho et al., 2002, and the NAO index (Olsen et al., 2012). Grey bars indicate arid periods. Yellow indicates xerophytic pollen, blue indicates mesophytic pollen and green indicates a mixture.

5.2 Importance of Laguna de Medina and Laguna Salada for the CRC 806

This thesis is part of the CRC 806 ´Our Way to Europe´. In the archaeology, the impact of climatic and environmental changes is becoming more important. This resulted in a close collaboration between the geologists and archaeologists of the C cluster. The Spanish archaeological sites of Solutrean and Magdalenian technocomplexes (about 24,000 to 17,0000 cal BP) are clustered close to the shores in the north, east and south of the IP and close to the Tagus River in Portugal. Laguna de Medina and Laguna Salada were selected, because of their close situation to a cluster of Solutrean sites in southern Spain. This would give the opportunity to compare the palaeoclimatological and -environmental data with the cultural changes and the results from the C1 project.

In this regard, core Co1313 from Laguna de Medina looked very promising. A rough interpolation based on the older study from Reed et al. (2001) suspected an age around 23,000 years for the 25.65 m long record. However, with the establishment of the age model, it turned out the record was only 9,600 years. Also Laguna Salada, 8,500 cal yr BP, does not reach the Pleistocene-Holocene boundary.
Laguna de Medina and Laguna Salada are too young for a comparison between climatological and environmental forcing on the cultural processes within the Solutrean technocomplexes.

However, the records proved to be very good palaeoclimate archives for the Holocene. Especially Laguna de Medina turned out to be highest-resolution archive for Holocene climate changes on the Iberian Peninsula. This high-resolution record is therefore very promising for further studies concerning human impact on the environment (currently analysed by T. Schröder in the framework of the CRC 806), and the effect of rapid climate change on the human behaviour and impact.

5.3 The future for Laguna de Medina and Laguna Salada in the light of the ongoing climate change

The records of Laguna de Medina and Laguna Salada showed the impact of the past climatological changes in the ecosystems. With the focus on the ongoing climate change, some question about the Spanish limnological ecosystems came up (Álvarez-Cobelas et al., 2005b):

- Will they still exist at the end of the century?
- Will they still be permanent or will they become temporary?
- Will the biochemistry or biota change?

The ongoing climate change will have devastating effects on small shallow lakes as the two analysed in this thesis. Irrigation plays a very important role in southern Spain. In the last decades, a significant increase in demand for irrigation water is signalised, as the result of an increase in economic productivity. However, since 2005, farmers are forced to modernise the irrigation techniques to save water (Expósito and Berbel, 2017). The water of Laguna de Medina and Laguna Salada are both used for irrigation purposes for the surrounding agricultural areas. This influences the already water level, which is already fluctuating by natural changes, enormously (Rodríguez-Rodríguez et al., 2012).
With the focus on the ongoing climate change, droughts will increase and precipitation will decrease (Bolle, 2003; de Castro et al., 2004; Met Office, 2011), resulting in reduced water availability for surface waters (Álvarez-Cobelas et al., 2005a).

Laguna Salada will suffer first from reduced water availability. The temporary lake with annual desiccation is highly vulnerable for small climate changes (Giorgi and Lionello, 2008). It is very likely, the desiccation period will start earlier in the year and will be extended (Williams, 2002). The surrounding agricultural areas are highly sensible for erosion (García-Ruiz, 2010). Enhanced erosion is already noticeable in the record since the Roman Period. During this period with increased human influence, the sedimentation rate increased to 2.3 mm/yr. Interpolation of this sedimentation rate to the end of the century results in an extra ~20 cm sediment. On a maximum lake level of 50 cm, this is a significant change. Soon, Laguna Salada will be completely silted up, and not be a depression in the landscape anymore.
This has many consequences for the flora and fauna. The lake is protected by the Ramsar Convention on Wetland of International Importance (Ramsar, Iran, 1971), because of its importance for wintering and nesting water birds (Fernández-Palacios, 1990). However, without a water body, water birds will choose another place to nest or overwinter (Davis et al., 2010).

Laguna de Medina has a higher lake level, currently only desiccating in very arid years. A high correlation between the lake level and the salinity of the lake is found, especially after the increased water abstraction for irrigation since 1948 (Tello Ripa and López Bermúdez, 1988). The higher lake level means a longer retention of the water, increasing the salinity, probably also affecting the species living in the lake. Taking the sedimentation rate of 1.8 mm/year in account, this will result in a sedimentation of about 25 cm more until the end of the century. This is a relatively high amount for the lake. However, it will not have devastating effects on the limnological system jet.
The ongoing climate change will likely change the semi-permanent lake into a temporal lake, which becomes similar to the modern configuration of Laguna Salada. However, this will not take place before the end of the century. Nesting and overwintering water birds are very likely to still use the lake at the end of the century.

Most important sentence is for both of the lakes (Álvarez-Cobelas et al., 2005b): *´Many endangered Mediterranean limnosystems will survive if, and only if, Mediterranean societies appreciate them (which is not the case right now)´.*

References

Aguilera, H., & Murillo, J. M. (2009). The effect of possible climate change on natural groundwater recharge based on a simple model: A study of four karstic aquifers in SE Spain. *Environmental Geology*, 57(5), 963–974.

Aitken, M. J. (1998). *An introduction to Optical Dating*. Oxford: Oxford University Press.

Alonso, M. (1998). Las lagunas de la España Peninsular. *Limnetica*, 15, 1–176.

Álvarez-Cobelas, M., Catalán, J., & García de Jalón, D. (2005a). Impacts on inland aquatic ecosystems. In J. M. Moreno (Ed.), *Effects of Climate Change in Spain* (pp. 109–142). Ministerio de Medio Ambiente, Madrid.

Álvarez-Cobelas, M., Rojo, C., & Angeler, D. G. (2005b). Mediterranean limnology: Current status, gaps and the future. *Journal of Limnology*, 64(1), 13–29.

Amat, J. A. (1984). Las poblaciones de aves acuáticas en las lagunas andaluzas: composición y diversidad durante un ciclo anual. Ardeola, 31, 61–79.

Arnell, N., Bates, B., Lang, H., Magnuson, J. J., & Mulholland, P. (1996). Hydrology and freshwater ecology. In J. T. Houghton, L. G. M. Filho, B. A. Callander, N. Harris, A. Kattenberg, & K. Maskell (Eds.), *Climate Change 1995* (pp. 325–363). Cambridge: Cambridge University Press.

Athersuch, J., Horne, D. J., & Whittaker, J. E. (1989). Marine and brackisch water ostracods (superfamilies Cypridacea and Cytheracea). (E.J. Brill, Ed.), Leiden, 359 pp

Bard, E. (2013). Out of the African Humid Period. *Science*, 342(2013), 808–9.

Blaauw, M., & Christen, J. A. (2011). Flexible paleoclimate age-depth models using an autoregressive gamma process. *Bayesian Analysis*, 6(3), 457–474.

Blott, S. J., & Pye, K. (2001). Technical Communication Gradistat: a Grain Size Distribution and Statistics Package for the Analysis of Unconsolidated Sediments, *Earth surface processes and landforms*, 1248, 1237–1248.

Boës, X., Rydberg, J., Martinez-Cortizas, A., Bindler, R., & Renberg, I. (2011). Evaluation of conservative lithogenic elements (Ti, Zr, Al, and Rb) to study anthropogenic element enrichments in lake sediments. *Journal of Paleolimnology*, 46(1), 75–87.

Bolle, H.-J. (2003*). Mediterranean Climate. Variability and Trends*. (H.-J. Bolle, Ed.). Springer Verlag, Berlin.

Bond, G., Showers, W., Cheseby, M., Lotti, R., Almasi, P., DeMenocal, P. Priore, H. Cullen, I. Hajdas, Bonani, G. (1997). A Pervasive Millennial-Scale Cycle in North Atlantic Holocene and Glacial Climates. *Science*, 278(5341), 1257–1266.

Brown, T. A., Nelson, D. E., Mathewes, R. W., Vogel, J. S., & Southon, J. R. (1989). Radiocarbon dating of pollen by accelerator mass spectrometry. *Quaternary Research*, 32(2), 205–212.

Burjachs, F., Jones, S. E., Giralt, S., & Fern, J. (2016). Late Glacial to Early Holocene recursive aridity events in the SE Mediterranean Iberian Peninsula : The Salines playa lake case study. *Quaternary International*, 403, 187–200.

Burn, M. J., & Palmer, S. E. (2014). Solar forcing of Caribbean drought events during the last millennium. *Journal of Quaternary Science*, 29(8), 827–836

Bussi, G., Rodríguez-Lloveras, X., Francés, F., Benito, G., Sánchez-Moya, Y., & Sopeña, A. (2013). Sediment yield model implementation based on check dam infill stratigraphy in a semiarid Mediterranean catchment. *Hydrology and Earth System Scienc*es, 17(8), 3339–3354.

Cacho, I., Grimalt, J. O., Pelejero, C., Canals, M., Sierro, F. J., Flores, J. A., & Shackleton, N. (1999). Dansgaard-Oeschger and Heinrich event imprints in Alboran Sea paleotemperatures. *Paleoceanography*, 14(6), 698–705.

Cacho, I., Grimalt, J. O., & Canals, M. (2002). Response of the Western Mediterranean Sea to rapid climatic variability during the last 50,000 years: a molecular biomarker approach. *Journal of Marine Systems*, 33–34, 253–272.

Calderón, & Arana, S. (1896). La diatomita y los yacimientos diatomáceos de Morón. *An. Soc. Esp. Hist. Nat.*, XV, 477–493.

Carrión, J.S., Andrade, A., Bennett, K. D., Navarro, C., & Munuera, M. (2001a). Crossing forest thresholds: inertia and collapse in a Holocene sequence from south-central Spain. The Holocene, 11(6), 635–653.

Carrión, J.S., Munuera, M., Dupre, M., Andrade, A., 2001b. Abrupt vegetation changes in the Segura Mountains of southern Spain throughout the Holocene. *Journal of Ecology* 89, 783e797.

Carrión, J. S. (2002). Patterns and processes of Late Quaternary environmental change in a montane region of southwestern Europe. Quaternary Science Reviews, 21, 2047–2066.

Carrión, J. S., Sánchez-Gómez, P., Mota, J. F., Yll, R., & Chaín, C. (2003). Holocene vegetation dynamics, fire and grazing in the Sierra de Gádor, southern Spain. *The Holocene*, 13(6), 839–849.

Carríón, J. S., N, F., González-Sampérez, P., Sánchez-Quirante, L., Finlayson, J. C., Fernandez, S., & Andrade, A. (2007). Holocene environmental change in a montane region of southern Europe with a long history of human settlement. *Quaternary Science Reviews*, 11–12, 1455–1475.

Carrión, J. S., Fernández, S., Jiménez-Moreno, G., Fauquette, S., Gil-Romera, G., González-Sampériz, P., & Finlayson, C. (2010). The historical origins of aridity and vegetation degradation in southeastern Spain. Journal of Arid Environments, 74(7), 731–736.

Coelho, A. A. (2003). Indexing of powder diffraction patterns by iterative use of singular value decomposition. *Journal of Applied Crystallography*, 36(1), 86–95.

Cohen, A. S. (2003). *Paleolimnology: The History and Evolution of Lake Systems*. Oxford University Press.

Combourieu-Nebout, N., Paterne, M., Turon, J.-L., & Siani, G. (1998). A High-Resolution Record of the Last Deglaciation in the Central Mediterranean Sea: Palaeovegetation and Palaeohydrological Evolution. *Quaternary Science Reviews*, 17(4–5), 303–317.

Combourieu Nebout, N., Turon, J., Zahn, R., Capotondi, L., Londeix, L., & Pahnke, K. (2002). Enhanced aridity and atmospheric high-pressure stability over the western Mediterranean during the North Atlantic cold events of the past 50 k.y. *Geology*, 30(10), 863–866.

Combourieu Nebout, N., Peyron, O., Dormoy, I., Desprat, I., Beaudouin, C., Kotthoff, U., & Marret, F. (2009). Rapid climatic variability in the west Mediterranean during the last 25 000 years from high resolution pollen data. *Climate of the Past*, 5, 503–521.

Comín, F. A., & Alonso, M. (1988). Spanish salt lakes: Their chemistry and biota. *Hydrobiologia*, 158(1), 237–245.

Constable, C., & Korte, M. (2015). 5.09 Centennial- to millennial-scale geomagnetic field variations. In G. Schubert (Ed.), Treatise on Geophysics (pp. 309-341). Elsevier, the Netherlands

Corella, J. P., Moreno, A., Morellón, M., Rull, V., Giralt, S., Rico, M. T., Pézez-Sanz, A, Valero-Garcés, B. L. (2011). Climate and human impact on a meromictic lake during the last 6,000 years (Montcortés Lake, Central Pyrenees, Spain). *Journal of Paleolimnology*, 46(3), 351–367.

Corella, J. P., Stefanova, V., El Anjoumi, A., Rico, E., Giralt, S., Moreno, A., Plato-Montero, A, Valero-Garcés, B. L. (2013). A 2500-year multi-proxy reconstruction of climate change and human activities in northern Spain: The Lake Arreo record. *Palaeogeography, Palaeoclimatology, Palaeoecology,* 386, 555–568.

Cressie, N. A. C. (1991). *Statistics for spatial data. Wiley Series in Probability and Mathematical Statistics*. John Wiley & Sons, 900 pp.

Currás, A., Zamora, L., Reed, J. M., García-Soto, E., Ferrero, S., Armengol, X., Mezquita-Joanes, F.

Marqués, M. A., Riera, S. Julià, R. (2012). Climate change and human impact in central Spain during Roman times: High-resolution multi-proxy analysis of a tufa lake record (Somolinos, 1280m asl). *Catena*, 89(1), 31–53.

Currat, M., Poloni, E. S., & Sanchez-Mazas, A. (2010). Human genetic differentiation across the Strait of Gibraltar. *BMC Evolutionary Biology*, 10(237), 1–18.

Dantín Cereceda, J. (1940). La aridez y el endorreismo en España. El endorreismo betico. *Estudios Geogrificos*, 1, 75–117.

Dantín, J. (1942). El endorreismo aragonés. *Estudios Geográficos*, 8, 505–595.

Davies, S. J., Lamb, H. F., & Roberts, S. J. (2015). *Micro-XRF Studies of Sediment Cores*. Vol. 17, pp. 189–226).

Davis, J. L., Lake, S., & Thompson, R. (2010). Freshwater biodiversity and climate change. In I. Jubb, P. Holper, & W. Cai (Eds.), *Managing Climate Change: Papers from the Greenhouse 2009 Conference* (pp. 73–84). Commonwealth Scientific and Industrial Research Organisation (CSIRO) Publishing, Collingwood, Australia.

Davis, M. B. (1968). Pollen Grains in Lake Sediments: Redeposition Caused by Seasonal Water Circulation. *Science*, 162, 796–799.

Davis, M. B. (1973). Redeposition of pollen grains in lake sediment. Limnology and Oceanography, 18(1), 44–52.

de Castro, M., Martín-Vide, M., & Alonso, S. (2004). The climate of Spain: Past, present and scenarios for the 21st century. In*: Impacts of climatic change in Spain* (pp. 1–62).

de Vicente, I., López, R., Pozo, I., & Green, A. J. (2012). Nutrient and sediment dynamics in a Mediterranean shallow lake in southwest Spain. *Limnetica*, 31(2), 231–250.

deMenocal, P., Ortiz, J., Guilderson, T., Adkins, J., Sarnthein, M., Baker, L., & Yarusinsky, M. (2000). Abrupt onset and termination of the African Humid Period: Rapid climate responses to gradual insolation forcing. *Quaternary Science Reviews*, 19(1–5), 347–361.

Dennell, R., & Roebroeks, W. (2005). An Asian perspective on early human dispersal from Africa. *Nature*, 438(7071), 1099–104.

Denton, G. H., & Karlén, W. (1973). Holocene climatic variations-Their pattern and possible cause. *Quaternary Research*, 3(2), 155–205.

Dewald, A., Heinze, S., Jolie, J., Zilges, A., Dunai, T., Rethemeyer, J., Melles, M. Staubwasser, M. Kuczewski, B. Richter, J. Radtke, U. Von Blanckenburg, F., Klein, M. (2013). Cologne AMS, a dedicated center for accelerator mass spectrometry in Germany. *Nuclear Instruments and Methods in Physics Research, Section B: Beam Interactions with Materials and Atoms*, 294, 18–23.

Díaz-Paniagua, C., & Aragonés, D. (2015). Permanent and temporary ponds in Doñana National Park (SW Spain) are threatened by desiccation. *Limnetica*, 34(2), 407–424.

Dodd, J. R., & Crisp, E. L. (1982). Non-linear variation with salinity of Sr/Ca and Mg/Ca ratios in water and aragonitic bivalve shells and implications for paleosalinity studies. *Palaeogeography, Palaeoclimatology, Palaeoecology*, 38(1–2), 45–56.

Dorado-Valiño, M., Valdeolmillos, A., Ruiz Zapata, M. B., Gil-García, M. J., & Gutiérrez, I. de B. (2002). Climatic changes since the Late-glacial/Holocene transition in La Mancha Plain (South-central Iberian Peninsula, Spain) and their incidence on Las Tablas de Daimiel marshlands. *Quaternaire*, 93–94, 73–84.

Dorman, C. E., Beardsley, R. C., & Limeburner, R. (1995). Winds in the Strait of Gibraltar. *Quarterly Journal of the Royal Meteorological Society*, 121(528), 1903–1921.

Durán Valsero, J. J., García de Domingo, A., & Robledo Ardila, P. (2009). Propuesta de clasificación genético-geológica de humedales. Aplicación a los humedales españoles incluidos en el Convenio de Ramsar. *Bolétin Geológico Y Minero*, 120(3), 335–346.

Eichinger, L. (1983). A contribution to the interpretation of 14C groundwater ages considering the example of a partially confined sandstone aquifer. *Radiocarbon*, 25(2), 347–356.

Eswaran, H., & Zi-Tong, G. (1991). Properties, Genesis, Classification, and Distribution of Soils with Gypsum. In: *SSSA, Special Publication* no. (Vol. 26, pp. 89–119). Soil Sci. Soc. Amer. Madison.

Eugster, H. P., & Hardie, L. A. (1978). Saline Lakes. In E. A. Lerman (Ed.), *Chemistry, Geology, and Physics of Lakes* (pp. 237–293). New York: Springer.

Expósito, A., & Berbel, J. (2017). Agricultural Irrigation Water Use in a Closed Basin and the Impacts on Water Productivity: The Case of the Guadalquivir River Basin (Southern Spain). *Water*, 9(2), 136.

Feely, H. W., & Kulp, J. L. (1957). Origin of Gulf coast salt-dome sulphur deposits. *Bulletin of the American Association of Petroleum Geologists*, 41, 1802–1853.

Fernández-Palacios, J. M. (1990). Lagunas de Cadiz (Medina y Salada). In M. and A. Bernues Sanz (Ed.), *Humedales Espanoles en la Lisa der convenio de Ramsar* (pp. 9–24). Madrid: Ministerio de Agricultura. Pesca y Alimentación, Instituo Nacional para la Conservación de la Naturaleza.

Finlayson, C., Giles Pacheco, F., Rodríguez-Vidal, J., Fa, D. A., Gutierrez López, J. M., Santiago Pérez, A., Finlayson, G, Allue, E, Baena Preysler, J., Cáceres, I., Carrión, J. S. Fernández Jalvo, Y., Gleed-Owen, C. P., Jimenez Espejo, F. J., López, P., López Sáez, J. A., Riquelme Cantal, J.A., Sánchez Marco, A., Giles Guzman, F., Brown, K., Fuentes, N., Valarino, C.A., Villalpando, A., Stringer, C.B., Martinez Ruiz, Francisca Sakamoto, T. (2006). Late survival of Neanderthals at the southernmost extreme of Europe. *Nature*, 443, 850–853.

Finlayson, C., & Carrión, J. S. (2007). Rapid ecological turnover and its impact on Neanderthal and other human populations. *Trends in Ecology and Evolution*, 22(4), 213–222.

Fleming, K., Johnston, P., Zwartz, D., Yokoyama, Y., Lambeck, K., & Chappell, J. (1998). Refining the eustatic sea level curve since the Last Glacial Maximum using far and intermediate field sites. *Earth and Planetary Science Letters*, 163, 327–342.

Fletcher, W. J., Boski, T., & Moura, D. (2007). Palynological evidence for environmental and climatic change in the lower Guadiana valley, Portugal, during the last 13 000 years. *The Holocene*, 17(4), 481–494.

Fletcher, W. J., & Sánchez Goñi, M. F. (2008). Orbital- and sub-orbital-scale climate impacts on vegetation of the western Mediterranean basin over the last 48,000 yr. *Quaternary Research*, 70(3), 451–464.

Fletcher, W. J., Sanchez Goñi, M. F., Peyron, O., & Dormoy, I. (2009). Abrupt climate changes of the last deglaciation detected in a Western Mediterranean forest record. *Climate of the Past*, 6, 245–264.

Fletcher, W. J., & Zielhofer, C. (2013). Fragility of Western Mediterranean landscapes during Holocene Rapid Climate Changes. *Catena*, 103, 16–29.

Florschütz, F., Menéndez Amor, J., & Wijmstra, T. A. (1971). Palynology of a thick quaternary succession in southern Spain. *Palaeogeography, Palaeoclimatology, Palaeoecology*, 10(4), 233–264.

Fontes, J. C., Gasse, F., Callot, Y., Plaziat, J.-C.-, Carbonell, P., Dupeuble, P. A., & Kaczmarska, I. (1985). Freshwater to marine-like environments from Holocene lakes in northern Sahara. *Nature*, 317, 608–610.

Fritz, S. C. (1996). Paleolimnological records of climatic change in North America. *Limnology and Oceanography*, 41(5), 882–889.

Furest, A., & Toja, J. (1984). Reconocimiento limnológico de lagunas andaluzas. In L. *Zonas húmedas en Andalucía* (Ed.), Agencia de Medio Ambiente. Madrid: Monogiafías de la Dirección General de Medio Ambiente.

Gao, X., & Giorgi, F. (2008). Increased aridity in the Mediterranean region under greenhouse gas forcing estimated from high resolution simulations with a regional climate model. *Global and Planetary Change*, 62(3–4), 195–209.

García-Ruiz, J. M. (2010). The effects of land uses on soil erosion in Spain: A review. *Catena*, 81(1), 1–11.

Gasse, F. (2000). Hydrological changes in the African tropics since the Last Glacial Maximum. *Quaternary Science Reviews*, 19(1–5), 189–211.

Gasse, F., Téhet, R., Durand, A., Gibert, E., & Fontes, J.-C. (1990). The arid-humid transition in the Sahara and the Sahel during the last deglaciation. *Nature*, 346, 141–146

Giorgi, F., & Lionello, P. (2008). Climate change projections for the Mediterranean region. *Global and Planetary Change*, 63(2–3), 90–104.

Giralt, S., Burjachs, F., & Julià, R. (1999). Late Glacial to Early Holocene environmental adjustment in the Mediterranean semi-arid zone of the Salines playa-lake (Alacante, Spain). *Journal of Paleolimnology*, 21, 449–460.

Giralt, S., Burjachs, F., Roca, J. R., & Julià, R. (1999). Late Glacial to Early Holocene environmental adjustment in the Mediterranean semi-arid zone of the Salines. *Journal of Paleolimnology*, 21, 449–460.

Giralt, S., & Juliá, R. (2003). Water level reconstruction in closed lakes based on the mineralogical composition. In B. L. Valero-Garcés (Ed.), *Limnogeology in Spain: a tribute to Kerry R. Kelts* (pp. 305–325). Madrid: CSIC.

Gleick, P. H. (1993). *Water in Crisis*. (P. H. Gleick, Ed.). Oxford: Oxford University Press.

González-Sampériz, P., Valero-Garcés, B. L., Moreno, A., Jalut, G., García-Ruiz, J., Martí-Bono, M., Delgado-Huertas, A., Navas, A., Otto, T. C., Dedoubat, J. J. (2006). Climate variability in the Spanish Pyrenees during the last 30,000 yr revealed by the El Portalet sequence. *Quaternary Research*, 66(1), 38–52.

Hammer, Ø., Harper, D. A. T., & Ryan, P. D. (2001). Paleontological statistics software package for education and data analysis. *Palaeontologia Electronica*, 4(1), 9–18.

Hein, L., Metzger, M. J., & Moreno, A. (2009). Potential impacts of climate change on tourism; a case study for Spain. *Current Opinion in Environmental Sustainability*, 1(2), 170–178.

Höbig, N., Mediavilla, R., Gibert, L., Santisteban, J. I., Cendón, D. I., Ibáñez, J., & Reicherter, K. (2016). Palaeohydrological evolution and implications for palaeoclimate since the Late Glacial at Laguna de Fuente de Piedra, southern Spain. *Quaternary International*. 407, 29-46

Höbig, N., Weber, M. E., Kehl, M., Weniger, G.-C., Julià, R., Melles, M., Fülöp, R.H., Vogel., H., Reicherter, K. (2012). Lake Banyoles (northeastern Spain): A Last Glacial to Holocene multi-proxy study with regard to environmental variability and human occupation. *Quaternary International*, 274, 205–218.

Hupy, J. P. (2004). Influence of vegetation cover and crust type on wind-blown sediment in a semi-arid climate. *Journal of Arid Environments*, 58(2), 167–179.

Hurrell, J, W. (1995). Decadal trends in the north atlantic oscillation : regional temperatures and precipitation. *Science*, 269(5224), 676–679.

Ibañez, M. J. (1973). Contribución al estudio del endorreismo de la depresión del Ebro. El foco endorreico al W. y SW. de Alcaniz (Teruel). *Geographica,* XX, 21–32.

Ibañez, M. J. (1975). El endorreismo del sector central de la depresión del Ebro. *Cuadernos Inv. Geogr. Hist*., 35–48.

IGME. (1984). *Mapa Geologico de España*; E. 1:50000 Paterna de Rivera, Segunda Se (Madrid).

IPCC. (2013a). *Annex I: Atlas of Global and Regional Climate Projections. Climate Change 2013: The Physical Science Basis. Contribution of Working Group I to the Fifth Assessment Report of the Intergovernmental Panel on Climate Change*, 1311–1394.

IPCC. (2013b). Summary for policymakers. In T. F. Stocker, D. Qin, G.-K. Plattner, M. Tignor, S. K. Allen, J. Boschung, P. M. Midgley (Eds.), *Climate Change 2013: The Physical Science Basis. Contribution of Working Group I to the Fifth Assessment Report of the Intergovernmental Panel on Climate Change*. Cambridge University Press, Cambridge, United Kingdom and New York, NY, USA.

IPCC. (2014): *Climate Change 2014: Synthesis Report. Contribution of Working Groups I, II and III to the Fifth Assessment Report of the Intergovernmental Panel on Climate Change* [Core Writing Team, R.K. Pachauri and L.A. Meyer (eds.)]. IPCC, Geneva, Switzerland, 151 pp.

Jiménez-Moreno, G., & Anderson, R. S. (2012). Holocene vegetation and climate change recorded in alpine bog sediments from the Borreguiles de la Virgen, Sierra Nevada, southern Spain. *Quaternary Research*, 77(1), 44–53.

Jiménez-Moreno, G., García-Alix, A., Hernández-Corbalán, M. D., Anderson, R. S., & Delgado-Huertas, A. (2013). Vegetation, fire, climate and human disturbance history in the southwestern Mediterranean area during the late Holocene. *Quaternary Research*, 79(2), 110–122.

Jiménez Cisneros, B. E., Oki, T., Arnell, N. W., Benito, G., Cogley, J. G., Döll, P., Jiang, T., Mwakalila, S. S. (2014). Freshwater resources. In C. B. Field, V. R. Barros, D. J. Dokken, K. J. Mach, M. D. Mastrandrea, T. E. Bilir, Chatterjee, M., Ebi, K.L., Estrada, Y.O., Genova, R.C., Girma, B., Kissel, E.S.,Levy, A.N., MacCracken, S., Mastrandrea, P.R. & L.L.White (Eds.), *Climate Change 2014: Impacts, Adaptation, and Vulnerability. Part A: Global and Sectoral Aspects. Contribution of Working Group II to the Fifth Assessment Report of the Intergovernmental Panel on Climate Change* (pp. 229–269). Cambridge University Press, Cambridge, United Kingdom and New York, NY, USA.

Junta de Andalucía. (2003). Lagunas Salada, Chica y Juncosa. *Estado y Calidad de los recursos Naturales, Ecosistemas y Humedales*. 1-10

Kaland, P. E., Krzywinsky, K., & Stabell, B. (1984). Radiocarbon-dating of transitions between marine and lacustrine sediments and their relation to the development of lakes. *Boreas*, 13, 243–258.

Kulp, J. L., Turekian, K., & Boyd, D. W. (1952). Strontium content of limestones and fossils. *Bull. Geol. Soc. Amer.,* 63, 710–716.

Lahr, M. M. (2010). Saharan Corridors and Their Role in the Evolutionary Geography of 'Out of Africa I´. In J. G. Fleagle, J. J. Shea, F. E. Grine, A. L. Baden, & R. E. Leaky (Eds.*), Out of Africa I: The First Hominin Colonization of Eurasia* (pp. 27–46). Springer Netherlands.

Lamb, H., Roberts, N., Leng, M., Barker, P., Benkaddour, A., & Kaars, S. van der. (1999). Lake evolution in a semi-arid montane environment: Responses to catchment change and hydroclimatic variation. *Journal of Paleolimnology*, 21, 325–343.

Lehman, J. T. (1975). Reconstructing the rate of accumulation of lake sediment: The effect of sediment focusing. *Quaternary Research*, 5(4), 541–550.

Lewis, William M., J. (1983). A revised classification of lakes based on mixing. *Canadian Journal of Fisheries and Aquatic Sciences*, 40(10), 1779–1787.

Lindtke, J., Ziegenbalg, S. B., Brunner, B., Rouchy, L. M., Pierre, C., & Peckmann, J. (2011). Authigenesis of native sulphur and dolomite in a lacustrine evaporitic setting (Hellín basin, Late Miocene, SE Spain). *Geological Magazine.* 148(4), 655-669.

Löwemark, L., Chen, H. F., Yang, T. N., Kylander, M., Yu, E. F., Hsu, Y. W., Lee, T. Q., Song, S. R., Jarvis, S. (2011). Normalizing XRF-scanner data: A cautionary note on the interpretation of high-resolution records from organic-rich lakes. *Journal of Asian Earth Sciences*, 40(6), 1250–1256.

Luque, L., Zazo, C., Recio, J. M., Duenas, M. A., Goy, J. L., Lario, J., González-Hernández, F., Dabrio, C. J., González-Delgado, A. (1999). Evolucíon sedimentario de la Laguna de la Janda (Cádiz) durante el Holoceno. *Cuaternario y Geomorfología*, 13(3–4), 43–50.

Luzón, A., Pérez, A., Mayayo, M. J., Soria, A. R., & Sanchez-Goñi, M. F. (2007). Holocene environmental changes in the Gallocanta lacustrine basin, Iberian Range, NE Spain. *The Holocene*, 17(5), 649–663.

MacDonald, G. M., Beukens, R. P., & Kieser, W. E. (1991). Radiocarbon Dating of Limnic Sediments: A Comparative Analysis and Discussion. *Ecology*, 72(3), 1150–1155.

Machel, H. G. (1992). Low-temperature and high-temperature origins of elemental sulfur in diagenetic environments. (G. R. Wessel & B. H. Wimberly, Eds.) *Native sulfur: Developments in Geology and Exploration. Society for Mining, Metallury, and Exploration*, Inc, Littleton, Colorado.

Magny, M., de Beaulieu, J. L., Drescher-Schneider, R., Vannière, B., Walter-Simonnet, A. V., Miras, Y., Millet, L., Bossuet, G., Peyron, O., Brugiapaglia, E., & Leroux, A. (2007). Holocene climate changes in the central Mediterranean as recorded by lake-level fluctuations at Lake Accesa (Tuscany, Italy). *Quaternary Science Reviews*, 26(13–14), 1736–1758.

Marazanof, F. (1967). Ostracodes, cladoceres, hétéropteres et hydracariens nouveaux pour les Marismas du Guadalquivir (Andalousie). *Annales de Limnologie*, 3, 47–64.

Martín-Puertas, C., Valero-Garces, B. L., Mata, M. P., Gonzalez-Samperiz, P., Bao, R., Moreno, A., & Stefanova, V. (2008). Arid and humid phases in southern Spain during the last 4000 years: the Zoñar Lake record, Cordoba. *The Holocene*, 18(6), 907–921

Martín-Puertas, C., Valero-Garcés, B. L., Brauer, A., Mata, M. P., Delgado-Huertas, A., & Dulski, P. (2009). The Iberian–Roman Humid Period (2600–1600 cal yr BP) in the Zoñar Lake varve record (Andalucía, southern Spain). *Quaternary Research*, 71(2), 108–120.

Martín-Puertas, C., Jiménez-Espejo, F., Martínez-Ruiz, F., Nieto-Moreno, V., Rodrigo, M., Mata, M. P., & Valero-Garcés, B. L. (2010). Late Holocene climate variability in the southwestern Mediterranean region: an integrated marine and terrestrial geochemical approach. *Climate of the Past*, 6(6), 807–816.

Martín-Puertas, C., Valero-Garcés, B. L., Mata, M. P., Moreno, A., Giralt, S., Martínez-Ruiz, F., & Jiménez-Espejo, F. (2011). Geochemical processes in a Mediterranean Lake: a high-resolution study of the last 4,000 years in Zoñar Lake, southern Spain. *Journal of Paleolimnology*, 46(3), 405–421.

Martinez-Ruiz, F., Kastner, M., Gallego-Torres, D., Rodrigo-Gámiz, M., Nieto-Moreno, V., & Ortega-Huertas, M. (2015). Paleoclimate and paleoceanography over the past 20,000 yr in the Mediterranean Sea Basins as indicated by sediment elemental proxies. *Quaternary Science Reviews*, 107, 25–46. Martrat, B., Grimalt, J. O., Lopez-Martinez, C., Cacho, I., Sierro, F. J., Flores, J. A., Zahn, R., Canals, M., Curtis, J., & H. Hodell, D. A. (2004). Abrupt temperature changes in the Western Mediterranean over the past 250,000 years. *Science,* 306(5702), 1762–1765.

Martrat, B., Grimalt, J. O., Shackteton, N. J., De Abreu, L., Hutterli, M. A., & Stocker, T. F. (2007). Four climate cycles of recurring deep and surface water destabilizations on the Iberian Margin. *Science*, 317, 502–507.

Martrat, B., Jimenez-Amat, P., Zahn, R., & Grimalt, J. O. (2014). Similarities and dissimilarities between the last two deglaciations and interglaciations in the North Atlantic region. *Quaternary Science Reviews*, 99, 122–134.

Mayewski, P. A., Rohling, E. E., Stager, J. C., Karlén, W., Maasch, K. A., Meeker, L. D., Meyerson, E. A., Gasse, F., van Kreveld, S., Holmgren, K., Lee-Thorp, J., Rosqvist, G., Rack, F., Staubwasser, M., Schneider, R., & Steig, E. J. (2004). Holocene climate variability. *Quaternary Research*, 62(3), 243–255.

Medialdea, T., Somoza, L., Pinheiro, L. M., Fernández-Puga, M. C., Vázquez, J. T., León, R., Ivanov, M. K., Magalhaes, V., Díaz-del-Río, V., & Vegas, R. (2009). Tectonics and mud volcano development in the Gulf of Cádiz. *Marine Geology*, 261(1–4), 48–63.

Meisch, C. (2000). Freshwater Ostracoda of Western and Central Europe. In Schwoerbel, J. & Zwick, P. (eds.). *Akademischer Verlag Spektrum*, Heidelberg),

Mellars, P., & Stringer, C. (Eds.). (1990). *The Human Revolution: Behavioural and Biological Perspectives on the Origins of Modern Humans* (Vol. 2). Edinburgh: University of Edinburgh Press.

Mellars, P. (2004). Neanderthals and the modern human colonization of Europe. *Nature*, 432(7016), 461–5.

Melles, M., Brigham-Grette, J., Minyuk, P. S., Nowaczyk, N. R., Wennrich, V., DeConto, R. M., Anderson, A. M., Andreev, A. A., Coletti, A., Cook, T. L., Haltia-Hovi, E., Kukkonen, M., Lozhkin, A. V., Rosén, P., Tarasov, P., Vogel., H., & Wagner, B. (2012). 2.8 Million Years of Arctic Climate Change from Lake El'gygytgyn, NE Russia. *Science* , 337(6092), 315–320.

Met Office, (1962). Weather in the Mediterranean. In *General Meteorology* (Vol. I, p. 1962). Her Majesty's Stationery Office. London.

Met Office, (2011). Climate: Observations, projections and impacts. *Scientist*, 1–122.

Meyers, P. A. (1997). Organic geochemical proxies of paleoceanographic, paleolimnologic, and paleoclimatic processes. *Organic Geochemistry*, 27(5–6), 213–250.

Meyers, P. A., & Ishiwatari, R. (1993). Lacustrine organic geochemistry—an overview of indicators of organic matter sources and diagenesis in lake sediments. *Organic Geochemistry*, 20(7), 867–900.

Meyers, P. A., & Lallier-Vergès, E. (1999). Lacustrine sedimentary organic matter of Late Quaternary paleoclimates. *Journal of Paleolimnology*, 21(2), 345–372.

Mezquita, F., Roca, J. R., Reed, J. M., & Wansard, G. (2005). Quantifying species-environment relationships in non-marine Ostracoda for ecological and palaeoecological studies: Examples using Iberian data. *Palaeogeography, Palaeoclimatology, Palaeoecology*, 225(1–4), 93–117.

Morales-Molino, C., García-Antón, M., Postigo-Mijarra, J. M., & Morla, C. (2013). Holocene vegetation, fire and climate interactions on the westernmost fringe of the Mediterranean Basin. *Quaternary Science Reviews*, 59, 5–17.

Morellón, M., Valero-Garcés, B., Moreno, A., González-Sampériz, P., Mata, P., Romero, O., Maestro, M., & Navas, A. (2008). Holocene palaeohydrology and climate variability in northeastern Spain: The sedimentary record of Lake Estanya (Pre-Pyrenean range). *Quaternary International*, 181(1), 15–31.

Morellón, M., Valero-Garcés, B., Gonález-Sampéris, P., Vegas-Vilarrúbia, T., Rubio, E., Rieradevall, M., Delgado-Huertas, A., Mata, P., Romero, Ó., Engstrom, D. E., López-Vicente, M., Navas, A., & Soto, J. (2011). Climate changes and human activities recorded in the sediments of Lake Estanya (NE Spain) during the Medieval Warm Period and Little Ice Age. *Journal of Paleolimnology*, 46, 423–452.

Moreno, A., González-Sampériz, P., Morellón, M., Valero-Garcés, B. L., & Fletcher, W. J. (2012). Northern Iberian abrupt climate change dynamics during the last glacial cycle: A view from lacustrine sediments. *Quaternary Science Reviews*, 36, 139–153.

Moreno, A., López-Merino, L., Leira, M., Marco-Barba, J., González-Sampériz, P., Valero-Garcés, B. L., López-Sáez, J. A., Santos, L., Mata, P., & Ito, E. (2011). Revealing the last 13,500 years of environmental history from the multiproxy record of a mountain lake (Lago Enol, northern Iberian Peninsula). *Journal of Paleolimnology*, 46(3), 327–349.

Moreno, A., Pérez, A., Frigola, J., Nieto-Moreno, V., Rodrigo-Gámiz, M., Martrat, B., González-Sampíriz, P., Morellón, M., Martín-Puertas, C., Corella, J. P., Belmonte, Á., Sancho, C., Cacho, I., Herrera, G., Canals, M., Grimalt, J. O., Jiménez-Espejo, F., Martínez-Ruiz, F., Vegas-Vilarrúbia, T., & Valero-Garcés, B. L. (2012). The Medieval Climate Anomaly in the Iberian Peninsula reconstructed from marine and lake records. *Quaternary Science Reviews*, 43, 16–32.

Nambudiri, E. M. V, Teller, J. T., & Last, W. M. (1980). Pre-Quaternary microfossils—A guide to errors in radiocarbon dating. *Geology*, 8(3), 123–126.

Nieto-Moreno, V., Martínez-Ruiz, F., Giralt, S., Jiménez -Espejo, F., Gallego-Torres, D., Rodrigo-Gámiz, M., García -Orellana, J., Ortega-Huertas, M., & de Lange, G.J., 2011. Tracking climate variability in the Western Mediterranean during the Late Holocene: a multiproxy approach. *Climate of the Past*, 7, 1395-1414.

Oliver, M. A., & Webster, R. (1990). Kriging: a method of interpolation for geographical information systems. *International Journal of Geographical Information Systems*, 4(3), 313–332.

Olsen, J., Anderson, N. J., & Knudsen, M. F. (2012). Variability of the North Atlantic Oscillation over the past 5,200 years. *Nature Geoscience*, 5(11), 808–812.

Paéz, M. (1991). Los Humedales endorréios graditanos encuadre geográfico comercal. In Agencia de Medio Ambiente.editor. *Plan Rector de Uso y Gestión de las Reservas Naturales de las Lagunas de Cádiz*, Cádiz: Agencia de Medio Ambiente, 25–46.

Palmquist, R. (1979). Geologic controls on doline characteristics in mantled karst. *Zeitschrift Für Geomorphologie*, Supplement, 90–106.

Pantaléon-Cano, J., Yll, E.-I., Pérez-Obiol, R., & Roure, J. M. (2003). Palynological evidence for vegetational history in semi-arid areas of the western Mediterranean (Almería, Spain). *The Holocene*, 13(1), 109–119.

Pardo, L., 1948. Catálogo de los lagos de Espãnia. *Biología de las aguas continentals*, VI, 522 pp. Ministerio de Agricultura. Madrid.

Peel, M. C., Finlayson, B. L., & McMahon, T. A. (2007). Updated world map of the Köppen-Geiger climate classification. *Hydrology Earth System Science*, 11, 1633–1644.

Pérez-Sanz, A., González-Sampériz, P., Moreno, A., Valero-Garcés, B., Gil-Romera, G., Rieradevall, M., Tarrats, P., Lasheras-Álvarez, L., Morellón, M., Belmonte, A., Sancho, C., Sevilla-Callejo, M., & Navas, A. (2013). Holocene climate variability, vegetation dynamics and fire regime in the central Pyrenees: The Basa de la Mora sequence (NE Spain). *Quaternary Science Reviews*, 73, 149–169.

Pérez, A., Luzón, A., Roc, A. C., Soria, A. R., Mayayo, M. J., & Sánchez, J. A. (2002). Sedimentary facies distribution and genesis of a recent carbonate-rich saline lake: Gallocanta Lake, Iberian Chain, NE Spain. *Sedimentary Geology*, 148(1–2), 185–202.

Plans, P. (1969). Problemas del endorreismo español. *Rev. Real Acad. Ciencias Ex. Fis. Nat.*, 63, 271–309.

Pons, A., & Reille, M. (1988). The Holocene- and Upper Pleistocene pollen record from Padul (Granada, Spain): A new study. *Palaeogeography, Palaeoclimatology, Palaeoecology*, 66(3–4), 243–263.

Porta, J. (1998). Methodologies for the analysis and characterization of gypsum in soils: A review. *Geoderma*, 87(1–2), 31–46.

Puigdefábregas, J., & Mendizabal, T. (1998). Perspectives on desertification: western Mediterranean. *Journal of Arid Environmen*ts, 39(2), 209–224.

R Core Team (2016). R: A language and environment for statistical computing. R Foundation for Statistical Computing, Vienna, Austria.

Ramsey, C. B. (2009). Bayesian Analysis of Radiocarbon Dates. *Radiocarbon*, 51(1), 337–360.

Reed, J. M., Stevenson, A. C., & Juggins, S. (2001). A multi-proxy record of Holocene climatic change in southwestern Spain: the Laguna de Medina, Cádiz. The Holocene, 11(6), 707–719.

Rasouli, H., Scharf, B., Meisch, C. & Aygen, C. (2016). An updated checklist of the Recent non-marine Ostracoda (Crustacea) of Iran, with a redescription of *Eucypris mareotica* (Fischer, 1855). *Zootaxa*, 4154, 273-292.

Reimer, P. J., Bard, E., Bayliss, A., Beck, J. W., Blackwell, P. G., Bronk, C., Caitlin, R., Hai, E. B., & Edwards, R. L. (2013). Intcal13 and marine13 radiocarbon age calibration curves 0 – 50,000 years cal BP. *Radiocarbon*, 55(4), 1869–1887.

Renaut, R. W., & Gierlowski-Kordesch, E. H. (2010). *Lakes*. In R. Dalrymple & N. James (Eds.), Geological Association of Canada, Toronta (Canada), pp. 541–575.

Rethemeyer, J., Fülöp, R. H., Höfle, S., Wacker, L., Heinze, S., Hajdas, I., Patt, U., König, S., Stapper, B., & Dewald, A. (2013). Status report on sample preparation facilities for 14C analysis at the new Cologne AMS center. *Nuclear Instruments and Methods in Physics Research, Section B: Beam Interactions with Materials and Atoms*, 294, 168–172.

Richter, J. (1996). “Out of Africa II” - Die Theorie über die Einwanderung des modernen Menschen nach Europa auf dem archäologischen Prüfstand. *Archäologische Informationen*, 19, 67–73.

Richter, J., Melles, M., & Schäbitz, F. (2012). Temporal and spatial corridors of Homo sapiens sapiens population dynamics during the Late Pleistocene and early Holocene. *Quaternary International*, 274, 1–4.

Roberts, N., Jones, M. D., Benkaddour, a., Eastwood, W. J., Filippi, M. L., Frogley, M. R., Lamb, H. F., Leng, M. J., Reed, J. M., Stein, M., Stevens, L., Valero-Garcés, B., & Zanchetta, G. (2008).

Stable isotope records of Late Quaternary climate and hydrology from Mediterranean lakes: the ISOMED synthesis. *Quaternary Science Reviews*, 27(25–26), 2426–2441.
Roca, J. R., & Julià, R. (1997). Late-glacial and Holocene lacustrine evolution based on ostracod assemblages in Southeastern Spain. *Geobios*, 30(6), 823–830.
Rodó, X., Giralt, S., Burjachs, F., Comín, F. A., Tenorio, R. G., & Julià, R. (2002). High-resolution saline lake sediments as enhanced tools for relating proxy paleolake records to recent climatic data series. *Sedimentary Geology*, 148(1–2), 203–220.
Rodrigo, F. S., Pozo-Vázquez, D., Esteban-Parra, M. J., & Castro-Díez, Y. (2001). A reconstruction of the winter North Atlantic Oscillation index back to A.D. 1501 using documentary data in southern Spain. *Journal of Geophysical Research*, 106(14), 14805–14818.
Rodríguez-Rodríguez, M., Green, A. J., López, R., & Martos-Rosillo, S. (2012). Changes in water level, land use, and hydrological budget in a semi-permanent playa lake, Southwest Spain. *Environmental Monitoring and Assessment*, 184(2), 797–810.
Rodriguez Vidal, J., Gracia, F. J., & Giles, J. (1993). Deformavíones cuaternarias en la terraza fluvial de la Laguna de Madina (Río Guadalete, Jerez de la Frontera). *Revista de La Sociedad Geológica de España*, 6, 47–55.
Rodwell, M. J., & Hoskins, B. J. (1996). Monsoons and the dynamics of deserts. *Quarterly Journal of the Royal Meteorological Society*, 122(534), 1385–1404.
Rodwell, M. J., & Hoskins, B. J. (2001). Subtropical anticyclones and summer monsoons. *Journal of Climate*, 14(15), 3192–3211.
Ron, H., & Levi, S. (2001). When did hominids first leave Africa? New high-resolution paleomagnetic evidence from the Erk-El-Ahmar formation, Israël. *Geology*, 29(10), 887–890.
Rothwell, R. G., & Rack, F. R. (2006). New techniques in sediment core analysis: an introduction. *Geological Society, London, Special Publications*, 267(1), 1–29.
Rudd, J. W. M., Kelly, C. a., & Furutani, A. (1986). The role of sulfate reduction in longterm accumulation of organic and inorganic sulfur in lake sediments. *Limnology and Oceanography*, 31(6), 1281–1291.
Sánchez Goñi, M. F., Eynaud, F., Turon, J. L., & Shackleton, N. J. (1999). High resolution palynological record off the Iberian margin: Direct land-sea correlation for the Last Interglacial complex. Earth and *Planetary Science Letters*, 171(1), 123–137.
Sánchez Goñi, M. F., Cacho, I., Turon, J. L., Guiot, J., Sierro, F. J., Peypouquet, J. P., Grimalt., J. O., & Shackleton, N. J. (2002). Synchroneity between marine and terrestrial responses to millennial scale climatic variability during the last glacial period in the Mediterranean region. *Climate Dynamics*, 19(1), 95–105.
Santisteban, J. I., Mediavilla, R., Celis, A., Castaño, S., & de la Losa, A. (2016). Millennial-scale cycles of aridity as a driver of human occupancy in central Spain? *Quaternary International*, 407, 96–109.
Schneider, H., Höfer, D., Trog, C., & Mäusbacher, R. (2016). Holocene landscape development along the Portuguese Algarve coast – A high resolution palynological approach. *Quaternary International*, 407, 47-63.
Schröder, T., van ´t Hoff, J., Ortiz, J. E., de Torres Pérez-Hidalgo, T. J., López-Sáez, J. A., Melles, M., Holzhausen, A., Wennrich, V., Viehberg, F., & Reicherter, K. (2017). Shallow hypersaline lakes as paleoclimate archives: A case study from the Laguna Salada, Málaga province, southern Spain. Quaternary International (accepted).
Schuck, W., Richter, J., Schäbitz, F., & Melles, M. (2013). *2nd Phase CRC 806 Proposal 2013-1017*. Funding Proposal.
Schütt, B. (1998). Reconstruction of palaeoenvironmental conditions by investigation of Holocene playa sediments in the Ebro Basin, Spain: preliminary results. *Geomorphology*, 23, 273–283.
Shaw, B., Klessig, L., & Mechenich, C. (2002). *Understanding Lake Data*, G3582. Madison (Wisconsin): University of Wisconsin Cooperative Extension.
Sousa, A., & García-Murillo, P. (2003). Changes in the wetlands of Andalusia (Doñana Natural Park, SW Spain) at the end of the Little Ice Age. *Climatic Change*, 58, 193–217.
Sousa, A., García-Barrón, L., Morales, J., & García-Murillo, P. (2006). Post-little ice age warming, and desiccation of the continental wetlands of the aeolian sheet in the Huelva region (SW Spain). *Limnetica*, 25(1–2), 57–70.

Stein, M., Starinsky, A., Katz, A., Goldstein, S. L., Machlus, M., & Schramm, A. (1997). Strontium isotopic, chemical, and sedimentological evidence for the evolution of Lake Lisan and the Dead Sea. *Geochimica et Cosmochimica Acta*, 61(18), 3975–3992.
Stern, R., Alperovitch, N., & Levy, G. J. (1989a). Rapid removal of gypsum by resin prior to particle-size-distribution analysis in soils. *Soil Science*, 148(6), 448–451.
Streit, B. (1995). Evolution des Menschen. *Spektrum der Wissenschaft Verständliche Forschung Heidelberg.*
Sumner, G., Homar, V., & Ramis, C. (2001). Precipitation seasonality in eastern and southern coastal Spain. *International Journal of Climatology*, 21, 219–247.
Swezey, C. (2001). Eolian sediment responses to late Quaternary climate changes: Temporal and spatial patterns in the Sahara. *Palaeogeography, Palaeoclimatology, Palaeoecology*, 167(1–2), 119–155.
Szabolcs, I. (1990). Effects of predicted climatic changes on European soils, with particular regard to salinization. In M. M. Boer & R. S. De Groot (Eds.), Amsterdam: IOS Press. *Landscape Ecological Impact of Climatic Change* (pp. 177–193).
Tarroso, P., Carrión, J., Dorado-Valiño, M., Queiroz, P., Santos, L., Valdeolmillos-Rodríguez, A., Célio Alves, P., Brito, J. C., & Cheddadi, R. (2016). Spatial climate dynamics in the Iberian Peninsula since 15000 yr BP. *Climate of the Past*, 12(5), 1137–1149.
Tello Ripa, B., & López Bermúdez, F. (1988). *Los lagos*. Guía Física de Espana, 4. Madrid: Alianza Editorial.
Torfstein, A., Gavrieli, I., Katz, A., Kolodny, Y., & Stein, M. (2008). Gypsum as a monitor of the paleo-limnological-hydrological conditions in Lake Lisan and the Dead Sea. *Geochimica et Cosmochimica Acta*, 72(10), 2491–2509.
Toucanne, S., Mulder, T., Schönfeld, J., Hanquiez, V., Gonthier, E., Duprat, J., Cremer, M., & Zaragosi, S. (2007). Contourites of the Gulf of Cadiz: A high-resolution record of the paleocirculation of the Mediterranean outflow water during the last 50,000 years. *Palaeogeography, Palaeoclimatology, Palaeoecology*, 246(2–4), 354–366.
Trigo, R. M., Pozo-Váquez, D., Osborn, T., Castro-Diéz, Y., Gámiz-Fortis, S., & Esteban-Parra, M.-J. (2004). North Atlantic Oscillation influence on precipitation, river flow and water recources in the Iberian Peninsula. *International Journal of Climatology*, 24, 925–944.
Urban, N., Ernst, K., & Bernasconi, S. (1999). Addition of sulfur to organic matter during early diagenesis of lake sediments. *Geochimica et Cosmochimica Acta*, 63(6), 837–853.
Valero-Garcés, B. L., Delgado-Huertas, A., Navas, A., Machín, J., González-Sampériz, P., & Kelts, K. (2000). Quaternary palaeohydrological evolution of a playa lake: Salada Mediana, central Ebro Basin, Spain. *Sedimentology*, 47(6), 1135–1156.
Valero-Garcés, B., Moreno, A., Navas, A., Mata, P., Machín, J., Delgado Huertas, A., González Sampériz, P., Schwalb, A., Morellón, M., Cheng, H., & Edwards, R.L. (2008). The Taravilla lake and tufa deposits (Central Iberian Range, Spain) as palaeohydrological and palaeoclimatic indicators. *Palaeogeography, Palaeoclimatology, Palaeoecology*, 259(2-3), 136-156
Valero-Garcés, B., Morellón, M., Moreno, A., Corella, J. P., Martín-Puertas, C., Barreiro, F., Pérez, A., Giralt, S., & Mata-Campo, M. P. (2014). Lacustrine carbonates of Iberian Karst Lakes: Sources, processes and depositional environments. *Sedimentary Geology*, 299, 1–29.
Valero Garcés, B. L., Moreno, A., Navas, A., Mata, P., Machín, J., Delgado Huertas, A., González Sampériz, P., Schwalb, A., Morellón, M., Cheng, H., & Edwards, R. L. (2008). The Taravilla lake and tufa deposits (Central Iberian Range, Spain) as palaeohydrological and palaeoclimatic indicators. *Palaeogeography, Palaeoclimatology, Palaeoecology*, 259(2–3), 136–156.
van ’t Hoff, J., Schröder, T., Held, P., Opitz, S., Wagner, B., Reicherter, K., & Melles, M. (2017). Modern sedimentation processes in Laguna de Medina, southern Spain, derived from lake surface sediment and catchment soil samples. *Journal of Limnology*, 76(1), 103–115.
van der Knaap, W. O., & van Leeuwen, J. F. N. (1995). Holocene vegetation succession and degradation as responses to climatic change and human activity in the Serra de Estrela, *Portugal. Review of Palaeobotany and Palynology*, 89, 153–211.
van Geel, B., Buurman, J., & Waterbolk, H. T. (1996). Archaeological and palaeoecological indications of an abrupt climate change in The Netherlands, and evidence for climatological teleconnections around 2650 BP. *Journal of Quaternary Science*, 11(6), 451–460.

van Geel, B., Raspopov, O. M., Renssen, H., van der Plicht, J., Dergachev, V. A., & Meijer, H. A. J. (1999). The role of solar forcing upon climate change. *Quaternary Science Reviews*, 18(3), 331–338.

Vegas, J., Ruiz-Zapata, B., Ortiz, J. E., Galán, L., Torres, T., García-Cortés, Á., Gil-García, M. J., Perez-Gonzales, A., & Gallardo-Millán, J. L. (2010). Identification of arid phases during the last 50 cal. ka BP from the Fuentillejo maar-lacustrine record (Campo de Calatrava Volcanic Field, Spain). *Journal of Quaternary Science*, 25(7).

Vera, J. A., & Molina, J. M. (1999). La formacion Capas Rojas: Caracterizacíon y genesis. *Estudios Geologicos*, 55, 45–66.

Voelker, A. H. L., & de Abreu, L. (2011). A review of abrupt climate change events in the Northeastern Atlantic Ocean (Iberian Margin): Latitudinal, longitudinal, and vertical gradients. *Geophysical Monograph Series*, 193(1), 15–37.

Voelker, A. H. L., de Abreu, L., Schönfeld, J., Erlenkeuser, H., & Abrantes, F. (2009). Hydrographic conditions along the western Iberian margin during marine isotope stage 2. *Geochemistry, Geophysics, Geosystems*, 10(12), 1–30.

Voelker, A. H. L., Lebreiro, S. M., Schönfeld, J., Cacho, I., Erlenkeuser, H., & Abrantes, F. (2006). Mediterranean outflow strengthening during northern hemisphere coolings: A salt source for the glacial Atlantic? *Earth and Planetary Science Letters*, 245(1–2), 39–55.

Vogel, H., Wessels, M., Albrecht, C., Stich, H. B., & Wagner, B. (2010). Spatial variability of recent sedimentation in Lake Ohrid (Albania/Macedonia). *Biogeosciences*, 7(10), 3333–3342.

von Storch, H., Zorita, E., & Cubasch, U. (1993). Downscaling of global climate change estimates to regional scales: an application to Iberian rainfall in wintertime. *Journal of Climate*, 6(6), 1161-1171.

Walker, M., Johnsen, S., Rasmussen, S. O., Popp, T., Steffensen, Jø.-P., Gibbard, P., Hoek, W., Lowe, J., Andrews, J., Björck, S., Cwynar, L. C., Hughen, K.,Kershaw, P., Kromer, B., Litt, T., Lowe, D. J., Nakagawa, T., Newnham, R., & Schwander, J. (2009). Formal definition and dating of the GSSP (Global Stratotype Section and Point) for the base of the Holocene using the Greenland NGRIP ice core, and selected auxiliary records. *Journal of Quaternary Science*, 24(1), 3–17.

Wanner, H., Beer, J., Bütikhofer, J., Crowley, T. J., Cubasch, U., Flückiger, J., Goosse, H., Grosjean, M., Joos, F., Kaplan, J. O., Küttel, M., Müller, S. A., Prentice, I. C., Solomina, O., Stocker, T. F., Tarasov, P., Wagner, M., & Widmann, M. (2008). Mid- to Late Holocene climate change: an overview. *Quaternary Science Reviews*, 27, 1791–1828.

Wanner, H., Brönnimann, S., Casty, C., Gyalistras, D., Luterbacher, J., Schmutz, C., Stephenson, D. B., & Xoplaki, E. (2001). North Atlantic Oscillation - Concepts and studies. *Surveys in Geophysics*, 22, 321–382.

Weber, M. E. (1997). Quantitative Ableitung sedimentphysikalischer Parameter mit Hilfe eines Multi-Sensor Core Loggers- neue Wege in der Analytik mariner Sedimente. *Zeitschrift Für Angewante Geologie*, 43(3), 144–153.

Wennrich, V., Francke, A., Dehnert, A., Juschus, O., Leipe, T., Vogt, C., Brigham-Grette, J., Minyuk, P. S., Melles, M., & El´gygygytkin Sience Party (2013). Modern sedimentation patterns in Lake El'gygytgyn, NE Russia, derived from surface sediment and inlet streams samples. *Climate of the Past*, 9(1), 135–148.

Wetzel, R. G. (2001). *Limnology: Lake and River Ecosystems*. SanDi: Academic Press.

Williams, W. D. (2002). Environmental threats to salt lakes and the likely status of inland saline ecosystems in 2025. *Environmental Conservation*, 29(2), 154–167.

Wolf, D., & Faust, D. (2015). Western Mediterranean environmental changes: Evidences from fluvial archives. *Quaternary Science Reviews*, 122, 30–50.

Wolf, D., Seim, A., & Faust, D. (2014). Fluvial system response to external forcing and human impact - Late Pleistocene and Holocene fluvial dynamics of the lower Guadalete River in western Andalucía (Spain). *Boreas*, 43(2), 422–449.

Yll, E. I., Pantaléon-Cano, J., & Pérez-Obiol, R. (1994). Análisis polínico de una secuencia holocénica en Roquetas de Mar (Almería). In I. Mateu, M. Dupré, J. Güemes, & M. E. Burgaz (Eds.), *Trabajos de palinología básica y aplicada* (pp. 98–189). Valencia: Universidad de Valencia.

Ziegenbalg, S. B., Brunner, B., Rouchy, J. M., Birgel, D., Pierre, C., Böttcher, M. E., Immenhauser, A., & Peckmann, J. (2010). Formation of secondary carbonates and native sulphur in sulphate-rich Messinian strata, Sicily. *Sedimentary Geology*, 227(1–4), 37–50.

Zielhofer, C., Fletcher, W. J., Mischke, S., de Batist, M., Campbell, J. F. E., Joannin, S., Tjallingii, R., El Hamouti, N., Junginger, A., Stele, A., Bussmann, J., Schneider, B., Lauer, T., Spitzer, K., Strupler, M., Brachert, T., & Mikdad, A. (2016). Atlantic forcing of Western Mediterranean winter rain minima during the last 12,000 years. *Quaternary Science Reviews*, 157, 29–51.

Zilhão, J. (2000). The Ebro Frontier : A Model for the Late Extinction of Iberian Neanderthals. In C. Stringer, R. N. E. Barton, & C. Finlayson (Eds.*), Neanderthals on the edge:150th anniversary conference of the Forbes' Quarry discovery*, Gibraltar (pp. 111–121). Oxford: Oxbow Books.

Erklärung

Ich versichere, dass ich die von mir vorgelegte Dissertation selbstständig angefertigt, die benutzten Quellen und Hilfsmittel vollständig angegeben und die Stellen der Arbeit – einschließlich Tabellen, Karten und Abbildungen-, die anderen Werken im Wortlaut oder dem Sinn nach entnommen sind, in jedem Einzelfall als Entlehnung kenntlich gemacht habe; dass diese Dissertation noch keiner anderen Fakultät oder Universität zur Prüfung vorgelegen hat; dass sie – abgesehen von unten angegebenen Teilpublikationen – noch nicht veröffentlicht worden ist sowie, dass ich eine solche Veröffentlichung vor Abschluss des Promotionsverfahrens nicht vornehmen werde. Die Bestimmungen dieser Promotionsordnung sind mir bekannt. Die von mir vorgelegte Dissertation ist von Prof. Dr. Martin Melles betreut worden.

Nachfolgend genannte Teilpublikationen liegen vor:

(1) van ’t Hoff, J., Schröder, T., Held, P., Opitz, S., Wagner, B., Reicherter, K., and Melles, M. (2017). Modern sedimentation processes in Laguna de Medina, southern Spain, derived from lake surface sediment and catchment soil samples. *Journal of Limnology*, 76(1), 103–115. http://doi.org/10.4081/jlimnol.2016.1499

Köln, den 19. März 2018 ……………………..

Lebenslauf

Persönliche Informationen

Name	Jasmijn van ´t Hoff
Geburtsdatum	26. März 1987
Geburtsort	Leidschendam, Niederlanden
Nationalität	Niederländisch
Adresse	Luisenstraße 36 52070 Aachen, Deutschland
Telefon	+49 (0) 221 470 2534
Handy	+49 (0) 176 417 22 136
E-Mail	jvanthof@uni-koeln.de

Beruflicher Werdegang

seit Jan 2014	Doktorandin, Institut für Geologie und Mineralogie, Arbeitsgruppe Quartärgeologie Prof. Dr. Martin Melles, SFB 806 „Our Way to Europe" Projekt C3 - **Thema der Doktorarbeit:** Climatic and environmental changes in the Upper Pleistocene - Middle Holocene of the Iberian Peninsula
Sep 2011 – Aug 2013	Master Applied Environmental Geoscience, VU University Amsterdam, Niederlanden - **Thema der Masterarbeit:** Millennial scale climate variability in Heinrich layers in the North Atlantic during the last 53.000 years - **Forschungsprojek:** Development of coastal West-Brabant during the Holocene and the influence of the River Scheldt
Sep 2009 – Aug 2011	Bachelor Earth Sciences, VU University Amsterdam, Niederlanden - **Thema der Bachelorarbeit:** Correlation between weathering state of fluvial sediments and the age of the river terraces of the Garonne in France
2008/2009	Grundstudium B. Sc. Climate & Environment, The Hague University of Applied Science, Niederlanden
Sep 2007 – Jan 2008	B. Sc. German Language and Culture, University Leiden, Niederlanden
Sep 2006 – Jan 2007	B. Sc. Forest and Nature Management, Inholland University of Applied Science, Delft, Niederlanden
Sep 2005 – Aug 2006	B. Sc. Earth Sciences, VU University Amsterdam, Niederlanden
1999/2005	Atheneum, Erasmus College Zoetermeer, Niederlanden

Lehre und Betreuung

Aug 2016	GSGS Summer School on Dates and Rates of Change in the Quaternary, Blankenheim, Deutschland Assistentin im Rahmen der praktischen Übungen während des Schwerpunkttages Limnologie
seit 2015	Betreute Bachelorarbeiten: - Raphael Petri: Sedimentation in der Laguna de Medina, Spanien, im Spätquartär - Sebastian Fuhr: Umweltgeschichte der Laguna de Medina, Südspanien – ein geochemischer Ansatz - Sandra Blanke: Korngrößenverteilung in der Sedimentabfolge der Laguna de Medina, Südspanien - Patrick Braun: Umweltgeschichte der Laguna de Fuente de Piedra, Südspanien – ein geochemischer Ansatz - Tim Stanski: Umweltgeschichte der Laguna Salada, Südspanien – ein geochemischer Ansatz - Gabriele Schmidt: Korngrößenanalyse eines Sedimentkerns aus der Laguna de Salada, Cádiz (Spanien)
seit 2014 (Wintersemester)	Assistentin bei der 2. Semester Übungs-Veranstaltung "Verwitterung, Transport und Sedimentation"
Apr 2013	Betreuung der 4. Semester Feldkampagne im Jura, Frankreich
May 2013	Betreuung der 2. Semester Feldkampagne im West-Brabant, Niederlanden
Feb – Apr 2012 + 2013	Lehre in der Physischen Geographie, 1. Semester Climate & Management, The Hague University, Niederlanden
Apr – Mai 2011 + 2012	Studentische Hilfskraft in der Geobotanik mit Feldarbeit (Betreuung), VU University Amsterdam, Niede4landen
Apr – Mai 2011	Lehre in der Sozialen Geographie, 1. Semester Climate & Management, The Hague University, Niederlanden

Sprachen

Niederländisch	Muttersprachler
Englisch	Exzellent
Deutsch	Exzellent

Köln, den 19. März 2018 ……………………..